

การใช้ อีพิกิวเอ พอร์ทัล โดสซิมีทรี ซอฟแวร์และการหาค่าจำกัดของแกมมาเพื่อตรวจสอบการ
วางแผนการรักษาในเทคนิคการฉายรังสีแบบปรับความเข้มรอบตัวผู้ป่วย



นางจิตรชญา สุวรรณรักษา

จุฬาลงกรณ์มหาวิทยาลัย

CHULALONGKORN UNIVERSITY

วิทยานิพนธ์นี้เป็นส่วนหนึ่งของการศึกษาตามหลักสูตรปริญญาวิทยาศาสตรมหาบัณฑิต

สาขาวิชาอายุเวชศาสตร์ ภาควิชารังสีวิทยา

คณะแพทยศาสตร์ จุฬาลงกรณ์มหาวิทยาลัย

ปีการศึกษา 2556


ลิขสิทธิ์ของจุฬาลงกรณ์มหาวิทยาลัย

บทคัดย่อและแฟ้มข้อมูลฉบับเต็มของวิทยานิพนธ์ตั้งแต่ปีการศึกษา 2554 ที่ให้บริการในคลังปัญญาจุฬาฯ (CUIR)

เป็นแฟ้มข้อมูลของนิสิตเจ้าของวิทยานิพนธ์ ที่ส่งผ่านทางบัณฑิตวิทยาลัย

The abstract and full text of theses from the academic year 2011 in Chulalongkorn University Intellectual Repository (CUIR)
are the thesis authors' files submitted through the University Graduate School.

IMPLEMENTATION AND GAMMA PASS LIMIT OF EPIQA PORTAL DOSIMETRY
SOFTWARE FOR VOLUMETRIC MODULATED ARC THERAPY PRE-TREATMENT
VERIFICATION



Mrs. Chitchaya Suwanraksa

จุฬาลงกรณ์มหาวิทยาลัย

CHULALONGKORN UNIVERSITY

A Thesis Submitted in Partial Fulfillment of the Requirements
for the Degree of Master of Science Program in Medical Imaging

Department of Radiology

Faculty of Medicine

Chulalongkorn University

Academic Year 2013

Copyright of Chulalongkorn University

Thesis Title	IMPLEMENTATION AND GAMMA PASS LIMIT OF EPIQA PORTAL DOSIMETRY SOFTWARE FOR VOLUMETRIC MODULATED ARC THERAPY PRE-TREATMENT VERIFICATION
By	Mrs. Chitchaya Suwanraksa
Field of Study	Medical Imaging
Thesis Advisor	Associate Professor Sivalee Suriyapee, M.Eng

Accepted by the Faculty of Medicine, Chulalongkorn University in Partial Fulfillment
of the Requirements for the Master's Degree

.....Dean of the Faculty of Medicine
(Associate Professor Sophon Napathorn, M.D.)

THESIS COMMITTEE

.....Chairman
(Assistant Professor Chonlakiet Khorprasert, M.D.)

.....Thesis Advisor
(Associate Professor Sivalee Suriyapee, M.Eng)

.....External Examiner
(Professor Franco Milano, Ph.D.)

จุฬาลงกรณ์มหาวิทยาลัย
CHULALONGKORN UNIVERSITY

จิตรชญา สุวรรณรักษา : การใช้ อีพีคิวเอ พอร์ทัล โดสซิมิตรี ซอฟต์แวร์และการหาค่าจำกัดของ
แกมมาเพื่อตรวจสอบการวางแผนการรักษาในเทคนิคการฉายรังสีแบบปรับความเข้มรอบตัวผู้ป่วย.
(IMPLEMENTATION AND GAMMA PASS LIMIT OF EPIQA PORTAL DOSIMETRY
SOFTWARE FOR VOLUMETRIC MODULATED ARC THERAPY PRE-TREATMENT
VERIFICATION) อ.ที่ปริกษาวิทยานิพนธ์หลัก: รศ. ศิวลี สุริยาปี, 85 หน้า.

EPIQA เป็น โปรแกรมแปลงภาพ ที่ได้จากเครื่องถ่ายภาพแบบตัวเลข (EPID) ไปเป็นแผนภาพ
รูปแบบการกระจายตัวของปริมาณรังสี โดยใช้ตัวแปลง GLAaS เนื่องจากการติดตั้งใช้งานของอุปกรณ์ประกัน
คุณภาพใหม่ จึงควรพิจารณากำหนดการประเมินผลแผนการรักษาซึ่งใช้ค่าขีดจำกัดค่าร้อยละการผ่านดัชนี
แกมมาขึ้นโดยเฉพาะ วัตถุประสงค์ของการศึกษานี้คือ การกำหนดขีดจำกัดค่าร้อยละการผ่านดัชนีแกมมาของ
EPIQA ซอฟต์แวร์สำหรับการตรวจสอบแผนการรักษาการฉายรังสีแบบปรับความเข้มรอบตัวผู้ป่วย (VMAT)
ก่อนที่จะนำไปใช้ทางคลินิก ได้ดำเนินการสอบเทียบและการกำหนดค่าของ EPIQA ซอฟต์แวร์พร้อมทั้ง
ประเมินผลเพื่อตรวจสอบความถูกต้องของโปรแกรมด้วยการทดสอบพื้นฐาน หลังจากนั้นทำการส่งแผนการ
รักษาด้วยเทคนิค VMAT 43 แผน ไปยังเครื่องถ่ายภาพแบบตัวเลขซึ่งติดตั้งกับเครื่องเร่งอนุภาค (Varian Clinac
iX) ภาพที่ได้สำหรับผู้ป่วยแต่ละรายจะถูกแปลงเป็นการกระจายของปริมาณรังสีในตัวจำลอง (phantom) ด้วย
EPIQA ซอฟต์แวร์ ซึ่งสามารถเทียบกับที่คำนวณจากระบบแผนการรักษา (TPS) โดยใช้เกณฑ์ผ่านแกมมาที่ความ
แตกต่างของปริมาณรังสี 3% และ ระยะห่าง 3 มม. ได้ทำการเปรียบเทียบเครื่องมือใหม่นี้กับ ArcCHECK ซึ่งใช้
อยู่เป็นประจำในคลินิก และ ทำการตรวจสอบแผนการรักษาอีก 70 แผน พร้อมทั้งหาขีดจำกัดแกมมา โดยใช้
สูตร ขีดจำกัดของความเชื่อมั่น (100-ค่าเฉลี่ย)+1.96ค่าเบี่ยงเบนมาตรฐาน ผลการตรวจสอบเทคนิคพื้นฐานใน
แบบเปิดขอบเขตปกติ แบบใช้ลิ้มไดนามิค และ pyramid IMRT พบว่าการกระจายปริมาณรังสีของ EPIQA
ตรงกับ TPS โดยค่าร้อยละการผ่านดัชนีแกมมาของพลังงาน 6 MV อยู่ในช่วง 95.25-99.79 และ 10 MV อยู่
ในช่วง 99.64-100 สำหรับการเปรียบเทียบแผนการรักษาด้วยเทคนิค VMAT 43 แผน ค่าร้อยละการผ่านดัชนี
แกมมา เฉลี่ยใน EPIQA เท่ากับ 99.29 ± 0.63 และใน ArcCHECK เท่ากับ 98.69 ± 1.14 โดยผลค่าร้อยละการ
ผ่านดัชนีแกมมาของ EPIQA ดีกว่า ArcCHECK สำหรับการศึกษานี้ 70 แผนการรักษาด้วยเทคนิค VMAT ได้ค่า
ร้อยละการผ่านดัชนีแกมมา เฉลี่ย 99.29 ± 0.60 ซึ่งผลของการศึกษานี้สอดคล้องกับการศึกษาของคณะอื่นๆที่
แสดงค่าร้อยละการผ่านดัชนีแกมมาเฉลี่ย 97.10 ± 2.4 และ 99.10 ± 0.6 เมื่อนำข้อมูลทั้งหมดมาหาค่าขีดจำกัด
แกมมาโดยคำนวณในแต่ละบริเวณการรักษา สำหรับบริเวณศีรษะเท่ากับ 98.84% บริเวณศีรษะและลำคอ
เท่ากับ 97.66% บริเวณหน้าอกเท่ากับ 98.09% บริเวณกระดูกเชิงกรานเท่ากับ 98.96% และ กรณีการใช้
เทคนิค SRS/SBRT เท่ากับ 97.28% จากการศึกษาครั้งนี้ รายงานผลขีดจำกัดแกมมาสำหรับบริเวณศีรษะ หน้าอก
และ กระดูกเชิงกรานเท่ากับ 98% สำหรับบริเวณศีรษะและลำคอ และ เทคนิค SRS/SBRT เท่ากับ 97% และ
พบว่า EPIQA เป็นเครื่องมือประกันคุณภาพ ที่ใช้งานง่ายและน่าเชื่อถือ ในการตรวจสอบแผนการรักษาด้วย
เทคนิค VMAT โดยให้ผลที่มีประสิทธิภาพทั้งยังเหมาะสมสำหรับจำนวนผู้ป่วยที่เพิ่มขึ้นอย่างรวดเร็ว

ภาควิชา รังสีวิทยา

ลายมือชื่อนิสิต

สาขาวิชา ฉายาเวชศาสตร์

ลายมือชื่อ อ.ที่ปริกษาวิทยานิพนธ์หลัก

ปีการศึกษา 2556

5574116230 : MAJOR MEDICAL IMAGING

KEYWORDS: PATIENT SPECIFIC QA/EPIQA/ EPID/VMAT/PORTAL DOSIMETRY

CHITCHAYA SUWANRAKSA: IMPLEMENTATION AND GAMMA PASS LIMIT OF EPIQA PORTAL DOSIMETRY SOFTWARE FOR VOLUMETRIC MODULATED ARC THERAPY PRE-TREATMENT VERIFICATION. ADVISOR: ASSOC. PROF. SIVALEE SURIYAPEE, M.Eng, 85 pp.

EPIQA is a program converting a dosimetric image acquired by an EPID into a dose map using the GLAaS conversion algorithm. Due to the implementation of the new QA device, the new gamma pass limit which is employed for the evaluation should be determined. The purpose of this study is to determine the gamma pass limit of EPIQA software for volumetric modulated arc therapy pre-treatment verification. The calibration and configuration of EPIQA (EpiDos s.r.o, Bratislava, Slovakia) were performed and evaluated for the accuracy of simple field techniques before the clinical implementation. The VMAT patient plans were recalculated for homogeneous medium in Eclipse treatment planning and delivered to EPID aS1000 equipped with Varian Clinac iX linear accelerator. The raw PV images in air for each patient were converted to dose in homogeneous phantom in EPIQA and compared with Eclipse treatment plans using gamma pass criteria of 3% dose difference and 3 mm distance to agreement. This new tool was compared with ArcCHECK (Sun Nuclear Corporation, Melbourne, FL) which is used routinely in clinic for 43 VMAT plans. The 70 VMAT plans in various organs using EPIQA verification were evaluated to determine the gamma limit using confidence limit of $(100 \text{ mean}) + 1.96\sigma$. For simple techniques in open, wedge fields and pyramid IMRT, EPIQA showed good agreement of dose distribution with TPS. The percent gamma pass ranged from 95.25 to 99.79 and 99.64 to 100 for 6 and 10 MV. For 43 clinical VMAT plans, the average gamma pass were $99.29 \pm 0.63\%$ and $98.69 \pm 1.14\%$ for EPIQA and ArcCHECK, respectively. The result demonstrated slightly better gamma pass of EPIQA than ArcCHECK. For the study of 70 VMAT plans the average gamma pass was $99.29 \pm 0.60\%$, our results agreed with the two previous works which illustrated the average gamma pass of $97.10 \pm 2.4\%$ and $99.10 \pm 0.6\%$. The calculated gamma limits in each region were 98.84%, 97.66%, 98.09%, 98.96% and 97.28% for head, H&N, chest, pelvis and the cases using SRS/SBRT technique, respectively. This study demonstrates the gamma limits of 98% for head, chest, pelvis regions and 97% for head and neck regions and SRS/SBRT techniques. EPIQA portal dosimetry is a simple and reliable quality assurance tool for VMAT dose verification which provides the efficient results and suitable for a fast growing number of patients.

Department: Radiology

Student's Signature

Field of Study: Medical Imaging

Advisor's Signature

Academic Year: 2013

ACKNOWLEDGEMENTS

I would like to express my sincere gratitude and deepest appreciation to Assoc. Prof. Sivalee Suriyapee, Chief Physicist at Division of Radiation Oncology, Department of Radiology, Faculty of Medicine, Chulalongkorn University, advisor, to guidance, invaluable advice, supervision, constructive comments and support for me.

I would like to deeply thank Mr. Sornjarod Oonsiri, M. Sc. His knowledge, ideas, a very great suggestion and assistant for me were vital to the completion of this research.

I would like to thank Mr. Taweap Sanghangtum Ph.D., Miss Chotika Jampanguen M Sc. Mr. Isralsrangkul Na Ayuthaya M.Sc., Mrs. Puntiva Oonsiri M.Sc., Mr. Tanawat Tawonwong M.Sc. and all staff in Division of Radiation Oncology, Department of Radiology, Faculty of Medicine, King Chulalongkorn Memorial Hospital for a very kindness advice.

I would like to thank Associate Professor Anchali Krisanachinda, Ph.D., Division of Nuclear Medicine, Department of Radiology, Faculty of Medicine, Chulalongkorn University and all the lecturers and staff in the Master of Science Program in Medical imaging, Faculty of medicine, Chulalongkorn University for their teaching of knowledge in Medical imaging.

I would like to thank Professor Franco Milano, Ph.D., who was the external examiner of the thesis defense for his help, kind suggestion and comments in this research.

A special thank goes to Faculty of Medicine, Prince of Songkhla University for support me in financial. I am deeply appreciate Asst. Prof. Duangjai Sangtawan, M.D., Mr. Amporn Funzien, M.Sc. and all staff Division of Radiation Oncology, Department of Radiology, Faculty of Medicine, Songklanagarind Hospital, Prince of Songkhla University for their always encourage and take a good care of me.

Finally, I am grateful to my family for a very great encouragement, entirely care and understanding during the entire course of study.

CONTENTS

	Page
THAI ABSTRACT	iv
ENGLISH ABSTRACT	v
ACKNOWLEDGEMENTS	vi
CONTENTS	vii
LIST OF TABLES	X
LIST OF FIGURES	xii
LIST OF ABBREVIATION.....	xvii
CHAPTER I INTRODUCTION.....	1
1.1 Background and Rationale	1
1.2 Research Objectives	4
CHAPTER II LITERATURE REVIEWS	5
2.1 Theories	5
2.1.1 The linear accelerator (Linac).....	5
2.1.2 Volumetric modulated arc therapy (VMAT)	6
2.1.3 Radiotherapy treatment planning	7
2.1.3.1 Inverse treatment planning	8
2.1.4 Patient specific verification (QA)	8
2.1.5 QA devices for VMAT technique.....	10
2.1.5.1 ArcCHECK.....	10
2.1.5.2 Electronic portal imaging device (EPID).....	11
2.1.6 EPIQA software	14
2.1.7 GLAaS algorithm.....	15
2.1.8 Gamma evaluation	17
2.1.9 Gamma pass limit	21
2.2 Review of related literatures.....	22
CHAPTER III RESEARCH METHODOLOGY	25
3.1 Research design.....	25

	Page
3.2 Research design model	25
3.3 Conceptual frameworks	26
3.4 Key words	26
3.5 Research question	26
3.6 Materials	27
3.6.1 Linear accelerator and portal vision	27
3.6.2 EPIQA software	28
3.6.3 ArcCHECK.....	28
3.6.4 Treatment planning system.....	29
3.6.5 Ionization chamber of 0.13 cm ³	29
3.6.6 The Dose-1 Electrometer	30
3.6.7 Water phantom WP 1D.....	30
3.6.8 70 VMAT plans.....	30
3.7 Methods.....	31
3.7.1 Imager calibration	31
3.7.2 Data calibration for 6 and 10 MV	31
3.7.2.1 Primary radiation configuration	31
3.7.2.2 Transmitted radiation configuration.....	32
3.7.2.3 The diagonal profile from TPS configuration beam data	33
3.7.3. Simple field techniques validation	34
3.7.4 Clinical VMAT plans comparison with ArcCHECK	35
3.7.5 Gamma pass limit set up for EPIQA calculation.....	39
3.8 Outcome measurement	39
3.9 Data collection	39
3.10 Data analysis.....	39
3.11 Benefit of the study	39
3.12 Ethical consideration.....	39

	Page
CHAPTER IV RESULTS	40
4.1 EPIQA portal dose validation of simple field technique	40
4.2 Clinical VMAT plans.....	49
4.2.1 Head region.....	49
4.2.2 Head and Neck region.....	53
4.2.3 Chest region	57
4.2.4 Pelvis region.....	62
4.3 The correlation between percent gamma pass and modulation factor (MU/Gy)	67
4.4 Gamma pass limit set up for EPIQA.....	68
CHAPTER V DISCUSSION AND CONCLUSIONS.....	71
5.1 Discussion	71
5.1.1 EPIQA portal dose validation of simple field technique	71
5.1.2 Clinical VMAT plans of EPIQA compared with ArcCHECK.....	72
5.1.3 The correlation between percent gamma pass and modulation factor (MU/Gy).....	74
5.1.4 Gamma pass limit set up for EPIQA.....	75
5.1.5 Comparison to previous works	78
5.1.6 The limitation of this study	79
5.2 Conclusions.....	79
REFERENCES	81
APPENDIX.....	83
VITA.....	85

LIST OF TABLES

	Page
Table 4.1 Percent gamma pass, Mean gamma, SD gamma and Tested points for 6MV with and without apply Gaussian convolution.....	41
Table 4.2 Percent gamma pass, Mean gamma, SD gamma and Tested points for 10 MV with and without apply Gaussian convolution.....	41
Table 4.3 The data analysis for 11 cases in head region by EPIQA	49
Table 4.4 The comparison of percent gamma pass between EPIQA and ArcCHECK in head region	52
Table 4.5 The data analysis for 10 cases in head and neck region by EPIQA	53
Table 4.6 The comparison of percent gamma pass between EPIQA and ArcCHECK in head and neck region.	56
Table 4.7 The data analysis for 13 cases in chest region by EPIQA.....	57
Table 4.8 The comparison of percent gamma pass between EPIQA and ArcCHECK in chest region	60
Table 4.9 The data analysis for 9 cases in pelvis region by EPIQA	62
Table 4.10 The comparison of percent gamma pass between EPIQA and ArcCHECK in pelvis region.....	65
Table 4.11 The percent gamma pass for EPIQA and ArcCHECK in each treatment region.....	66
Table 4.12 The Comparison between percent gamma pass and modulation factor (MU/cGy).....	67
Table 4.13 The Percent gamma pass in each treatment region	69
Table 4.14 The gamma pass limit in each treatment region	70

Table 5.1 The average percent gamma pass using EPID portal dosimetry compared with other studies..... 78

Table 5.2 The gamma pass limit using EPID based dosimetry compared with other studies..... 78



LIST OF FIGURES

	Page
Figure 1.1 VMAT technique planning.....	1
Figure 1.2 (a) EPID and (b) ArcCHECK.....	2
Figure 1.3 Example of planar dose	3
Figure 1.4 Gamma index method.....	3
Figure 2.1 Varian Clinac iX.....	5
Figure 2.2 Treatment planning of VMAT	6
Figure 2.3 Typical workflow in treatment planning.....	7
Figure 2.4 Example of QA devices for VMAT technique.....	9
Figure 2.5 ArcCHECK.....	10
Figure 2.6 VMAT treatment verification planning of ArcCHECK.....	11
Figure 2.7 Varian electronic portal imaging device detector system.....	13
Figure 2.8 EPIQA principle.....	15
Figure 2.9 Ellipsoid that defines the acceptance criterion for the gamma evaluation method.....	18
Figure 2.10 Displayed gamma analysis of EPIQA.....	20
Figure 3.1 Research design model.....	25
Figure 3.2 Conceptual frameworks	26
Figure 3.3 Varian Clinic iX linear accelerator with portal vision.....	27
Figure 3.4 EPIQA software	28
Figure 3.5 ArcCHECK.....	28
Figure 3.6 Eclipse treatment planning: version 8.9.21	29
Figure 3.7 The CC13 ionization chamber.....	29

Figure 3.8 Electrometer	30
Figure 3.9 Water phantom WP 1D.....	30
Figure 3.10 Geometry setup for image calibration	31
Figure 3.11 Primary dose calibration windows	32
Figure 3.12 Transmission dose calibration windows	33
Figure 3.13 The diagonal profile.....	33
Figure 3.14 Work flow for Simple field techniques validation	34
Figure 3.15 Work flow for verifying EPIQA with ArcCHECK	35
Figure 3.16 Work flow for EPIQA verification.....	37
Figure 3.17 Work flow for ArcCHECK verification.....	38
Figure 4.1 The example of EPIQA data for open field size of $2 \times 2 \text{ cm}^2$ 6 MV without convolution compared with TPS in criteria of 3%/3mm.....	43
Figure 4.2 The example of EPIQA data for open field size of $2 \times 2 \text{ cm}^2$ 6 MV with Gaussian convolution 2.5 mm compared with TPS in criteria of 3%/3mm	43
Figure 4.3 The example of EPIQA data for open field size of $2 \times 2 \text{ cm}^2$ 10 MV without convolution compared with TPS in criteria of 3%/3mm.....	44
Figure 4.4 The example of EPIQA data for open field size of $2 \times 2 \text{ cm}^2$ 10 MV with Gaussian convolution 2.5 mm compared with TPS in criteria of 3%/3mm	44
Figure 4.5 The example of EPIQA data for open field size of $10 \times 10 \text{ cm}^2$ 6 MV without convolution compared with TPS in criteria of 3%/3mm.....	45
Figure 4.6 The example of EPIQA data for open field size of $10 \times 10 \text{ cm}^2$ 6 MV with Gaussian convolution 2.5 mm compared with TPS in criteria of 3%/3mm.	45
Figure 4.7 The example of EPIQA data for open field size of $10 \times 10 \text{ cm}^2$ 10 MV without convolution compared with TPS in criteria of 3%/3mm.	46

Figure 4.8 The example of EPIQA data for open field size of $10 \times 10 \text{ cm}^2$ 10 MV with Gaussian convolution 2.5 mm compared with TPS in criteria of 3%/3mm.	46
Figure 4.9 The example of EPIQA data for Pyramid IMRT of 6 MV without convolution compared with TPS in criteria of 3 % /3mm	47
Figure 4.10 The example of EPIQA data for Pyramid IMRT of 6 MV with Gaussian convolution 2.5 mm compared with TPS in criteria of 3%/3mm	47
Figure 4.11 The example of EPIQA data for Pyramid IMRT of 10 MV without convolution compared with TPS in criteria of 3 %/3mm	48
Figure 4.12 The example of EPIQA data for Pyramid IMRT of 10 MV with Gaussian convolution 2.5 mm compared with TPS in criteria of 3 %/3mm	48
Figure 4.13 The examples of EPIQA data for head region compared with TPS in criteria of 3%/3mm (Arc 1)	50
Figure 4.14 The examples of EPIQA data for head region compared with TPS in criteria of 3%/3mm (Arc 2)	51
Figure 4.15 The examples of EPIQA data for head region compared with TPS in criteria of 3%/3mm (Arc 3)	51
Figure 4.16 The comparison of the percent gamma pass between EPIQA and ArcCHECK for VMAT plans in head region.	52
Figure 4.17 The examples of EPIQA data for head and neck region compared with TPS in criteria of 3%/3mm (Arc 1).....	54
Figure 4.18 The examples of EPIQA data for head and neck region compared with TPS in criteria of 3%/3mm (Arc 2).....	55
Figure 4.19 The examples of EPIQA data for head and neck region compared with TPS in criteria of 3%/3mm (Arc3)	55

Figure 4.20 The Comparison of the percent gamma pass between EPIQA and ArcCHECK for VMAT plans in head and neck region	56
Figure 4.21 The examples of EPIQA data for chest region compared with TPS in criteria of 3%/3mm (Arc1).....	58
Figure 4.22 The examples of EPIQA data for chest region compared with TPS in criteria of 3%/3mm (Arc2).....	59
Figure 4.23 The examples of EPIQA data for chest region compared with TPS in criteria of 3%/3mm (Arc3).....	59
Figure 4.24 The Comparison of the percent gamma pass between EPIQA and ArcCHECK for VMAT plans in chest region.....	61
Figure 4.25 The examples of EPIQA data for pelvis region compared with TPS in criteria of 3 %/3mm (Arc 1).....	63
Figure 4.26 The examples of EPIQA data for pelvis region compared with TPS in criteria of 3 %/3mm (Arc 2).....	64
Figure 4.27 The examples of EPIQA data for pelvis region compared with TPS in criteria of 3%/3mm (Arc 3)	64
Figure 4.28 The Comparison of the percent gamma pass between EPIQA and ArcCHECK for VMAT plans in pelvis region.....	65
Figure 4.29 The Comparison of the percent gamma pass for EPIQA and ArcCHECK of VMAT plans in each treatment region.....	66
Figure 5.1 The Screen capture of EPIQA analysis to define the difference between EPID and TPS	74
Figure 5.2 The correlation between percent gamma pass and modulation factor (MU/Gy) in each region.....	74

Figure 5.3 The scatter plot of percent gamma pass in each treatment region..... 75

Figure 5.4 The screen captures for the case of low percent gamma pass (Arc 1) 76

Figure 5.5 The screen captures for the case of low percent gamma pass (Arc 2) 77

Figure 5.6 The screen captures for the case of low percent gamma pass (Arc 3) 77



LIST OF ABBREVIATION

ABBREVIATION	TERMS
γ	Gamma index
σ	Standard deviation
μm	Micrometer
2D	Two Dimension
3%/3mm	3 percentage of dose difference and 3 millimeter
	Distance to agreement
3D	Three Dimension
AAA	Analytical anisotropic algorithm
AAPM	American Association of Physicists in Medicine
aSi	Amorphous silicon
cm	Centimeter
cm^2	Square centimeter
CT	Computed Tomography
D	Dose value
DD	Dose difference
DICOM	Digital Imaging and Communications in Medicine
D_{max}	Depth at dose maximum
DTA	Distance-to-agreement

ABBREVIATION	TERMS
DVH	Dose volume histogram
EPID	Electronic portal imaging device
EwwF	Equivalent Window Width of the Field
GAI	Gamma agreement index
Gy	Gray
H&N	Head and neck
i.e.	id est (That is)
IAS	Image acquisition system
IDU	Image detection unit
IMRT	Intensity modulated radiation therapy
Kg	Kilogram
Linac	Linear accelerator
MeV	Mega electron volt
MLC	Multileaf collimator
mm	Millimeter
MRI	Magnetic resonance imaging
MU	Monitor unit
MV	Megavoltage
OAR	Organ at risk
OF	Output factor

ABBREVIATION	TERMS
PV	Portal vision
QA	Quality assurance
RD	Radiotherapy dose
RI	Radiotherapy image
RP	Radiotherapy plan
RT	Radiotherapy
SBRT	Stereotactic body radiotherapy
SD	Standard deviation
SRS	Stereotactic radiosurgery
SSD	Source surface distance
TFT	Thin film transistor
TG	Task group
TPS	Treatment planning system
VMAT	Volumetric modulated arc therapy

CHAPTER I

INTRODUCTION

1.1 Background and Rationale

The primary goal of radiation therapy is to deliver a prescribed dose to a target volume, while at the same time minimize the damaging effects of radiation to normal tissue. Various techniques are used to achieve this goal, Volumetric modulated arc therapy (VMAT) is a novel treatment technique aiming to deliver highly modulated plans with variable multileaf collimator (MLC) shapes, dose rate and gantry speed during rotation. This rotational therapy delivers prescribed dose in relatively shorter duration and has better dose conformity, uniformity, and normal organ sparing. The treatment plans of VMAT is shown in figure 1.1

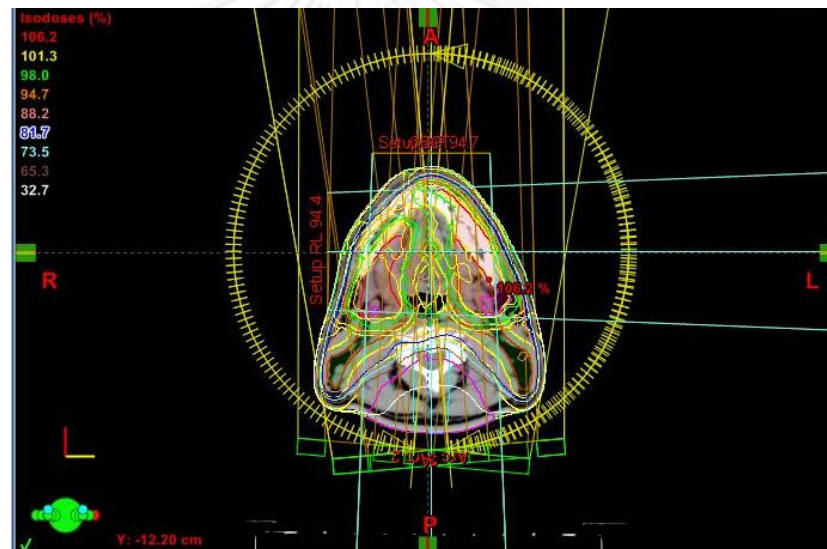


Figure 1.1 VMAT technique planning

The VMAT technique is performed by inverse treatment planning. The optimization in VMAT by minimize a cost function for dose-volume constrains for targets and organs at risk and also optimize leaf positions and dose rate under the constrains from machine capability. However, due to the complexity and uniqueness of the treatment plans, patient specific pre-treatment quality assurance (QA) of all treatment plans to ensure that the correct amount of radiation is being delivered to the correct location are demanded.

Patient-specific QA pre-treatment verification performed by treatment plans are copied onto a phantom geometry in which dosimetric measurements can be taken. The treatment is delivered to measurement device. So the measured doses are compared to calculated doses from treatment planning system (TPS) to analyze the agreement between the measured and the calculated doses.

For the dose measurement device, good spatial resolution, fast response and easy analysis of the measured data are a prerequisite for their application as the tools for dosimetric verification of individual treatment plans [1]. There are many QA devices that may be well suited for rotational measurements have been developed, such as EPID and ArcCHECK which are shown in figure 1.2



(a) EPID



(b) ArcCHECK

Figure 1.2 (a) EPID and (b) ArcCHECK

In present day, the 3D diode array (ArcCHECK: Sun Nuclear, USA) is employed for patient specific QA for VMAT in the radiation oncology division at King Chulalongkorn Memorial Hospital. The ArcCHECK consists of 1386 diode detectors that are arranged in a spiral pattern with a distance between detectors of 1 cm.

Recently, there has been growing interest on using Electronic portal imaging devices (EPIDs) for dosimetry applications [2]. They were originally developed for the purpose of patient setup verification. EPIDs are typically part of the linear accelerator (Linac) structure. It can be positioned automatically without any manual setup in a highly reproducible manner, high data density and high resolution (aSi1000 resolution 0.39mm). However the component of EPID is amorphous silicon detector, high atomic number materials, not water-equivalent [3]. The raw EPID image is not a dose image. Thus, a number of vendors have produced algorithms to either predict calibrated EPID response, or to convert calibrated EPID response into a simulated dose plane, such that EPID images can be used to verify the calculation.

EPIQA (EpiDos s.r.o, Bratislava, Slovakia) is a program converting a dosimetric image acquired by an EPID into a dose map in phantom using the GLAaS conversion algorithm. The dose map could be compared with a reference dose distribution in phantom calculated by Eclipse treatment planning.

The gamma index method is a tool to evaluate dose distribution comparisons between measurement and calculation. Planar dose are shown in figure 1.3.

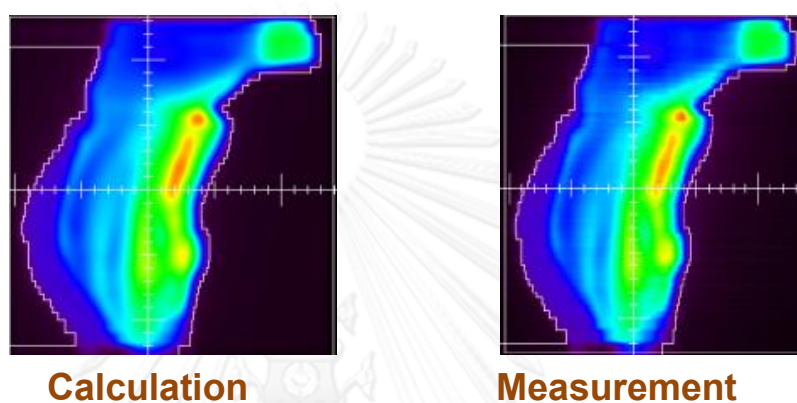


Figure 1.3 Example of planar dose

The criteria for acceptable calculation performance are generally defined as a tolerance of the dose differences and distance-to-agreement (DTA) and a combination of these two parameters to determine the agreement between two dose distributions is the gamma index. Normally the tolerance dose difference is 3% and the tolerance distance to agreement is 3 mm (3%/3mm) [4]. The gamma index method is shown in figure 1.4

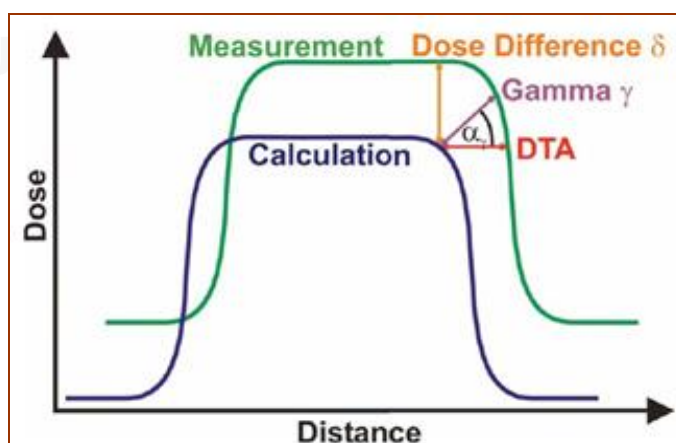


Figure 1.4 Gamma index method

The percentage of measured point compared with the calculation that passed the criteria can be called the percent gamma pass. The gamma pass is represented to the quantitative indicator of the calculation accuracy. The gamma pass limit is an acceptable limit that is an achievable level of dose agreement for a dose deviation. It is clinically acceptable in an accurate, optimal patient treatment or whether it is sufficiently inaccurate that the treatment plan was unsuitable for patient treatment. Normally, the gamma pass limit of 95% for all QA devices is employed [4]. The percent gamma pass depends on several factors, such as the model used in treatment planning, the dose delivery system and the QA devices which have different available options [5].

EPIQA is a newly software and independent with TPS. EPIQA can verify VMAT treatment plans in the rotational method. Due to implement the new QA device, the new gamma pass limit should be set up. The purpose of this work is to perform the commissioning and verifying the EPIQA and then the gamma pass limits are determined for head, head & neck, chest, pelvis regions and SRS/SBRT techniques.

1.2 Research Objectives

To determine the gamma pass limits of EPIQA Software for volumetric modulated arc therapy pre-treatment verification.

CHAPTER II

LITERATURE REVIEWS

2.1 Theories

2.1.1 The linear accelerator (Linac)

A linear accelerator such as the Varian Clinac iX (Varian Medical systems, Palo Alto, CA), which is shown in figure 2.1, accelerates electrons to a high velocity (i.e energy) using radiofrequency waves. The accelerated electrons produce X-rays when they collide with a tungsten target and the resulting photon beam can be used for treatment after additional filtering, collimation and shielding of the beam in the treatment head. Beam shielding is a prerequisite in high dose-high precision radiotherapy in order to obtain dose distributions that conform to the tumor volume while sparing neighboring healthy tissue. Both individual moulded blocks and a multileaf collimator (MLC) can be used for beam shielding. The latter device is located inside the treatment head of a LINAC which can be positioned individually to shape the beam aperture. Furthermore, modern LINACs are usually equipped with an electronic portal imaging device (EPID) which allows imaging of the high energetic MV photon beam. These images can be used not only for patient set-up verification or detection of organ motion but also for dosimetric verification of a treatment which is called portal dosimetry [6].



Figure 2.1 Varian Clinac iX (Varian Medical systems, Palo Alto, CA)

2.1.2 Volumetric modulated arc therapy (VMAT)

VMAT delivers radiation by rotating the gantry of a linac through one or more arcs with the radiation continuously on. As it does so, a number of parameters can be varied. These include: the MLC aperture shape, dose rate, the gantry rotation speed and the MLC orientation. It is undisputed that VMAT can deliver highly conformal dose distributions similar to those created by other forms of IMRT.

VMAT can take advantage of the above mentioned for four available variable parameters, but must do so while respecting the physical constraints of the linac and MLC such as the maximum gantry speed, maximum leaf speed, the MLC orientation constraints and the available subdivisions of fluence output rate. The first and fourth of these are of course linked. Provided that the gantry speed can be varied continuously, it does not require a continuous variation of fluence output rate to obtain a continuous variability of fluence output rate per degree. The minimum fluence output rate and the maximum gantry speed determine the constraining minimum fluence output rate per degree. Where there is a maximum fluence output rate and minimum gantry speed, there will be a constraining maximum fluence output rate per degree [7].

The primary advantage of VMAT over fixed-beam IMRT is that VMAT treatments can be delivered significantly faster. The possible advantages of decreased treatment time include increased patient comfort and compliance, increased patient throughput, and enhanced image guidance. Another advantage of VMAT is the increased monitor unit (MU) efficiency, meaning that fewer MUs are required to deliver the prescribed dose. Both decreased treatment time and increased MU efficiency have been achieved while maintaining target coverage and OAR sparing similar to fixed-beam IMRT. In some cases, VMAT has shown better OAR sparing than fixed-beam IMRT. The main disadvantage of VMAT has been an increased optimization time as compared to fixed-beam IMRT. However, optimization times have decreased, and as techniques develop, this disadvantage will continue to be mitigated[8]. The treatment plan of VMAT is shown in figure 2.2

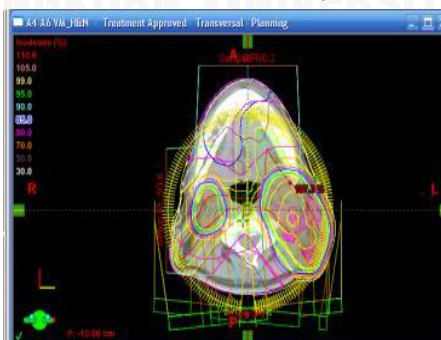


Figure 2.2 Treatment planning of VMAT

2.1.3 Radiotherapy treatment planning

The computerized TPS are used in external beam radiotherapy to generate beam shape and dose distributions with the intent to maximize tumor control and minimize normal tissue complications. Patient anatomy and tumor targets can be represented as 3D models. The medical physicist is responsible for the overall integrity of the computerized TPS to accurately and reliably produce dose distributions and associated calculations for external beam radiotherapy. The simultaneous development of CT, along with the advent of readily accessible computing power, led to the development of CT based computerized treatment planning, providing the ability to view dose distributions directly superimposed upon a patient's axial anatomy. Various computer algorithms are used to model the interactions between the radiation beam and the patient's anatomy to determine the spatial distribution of the radiation dose. Different algorithms are necessary to account for the different types of radiation and computational complexity. With the increase in computational performance available today, improved algorithms are being developed. The entire treatment planning process involves many steps, beginning from beam data acquisition and entry into the computerized TPS, through patient data acquisition, to treatment plan generation and the final transfer of data to the treatment machine[9]. Typical workflow in treatment planning was show in figure 2.3

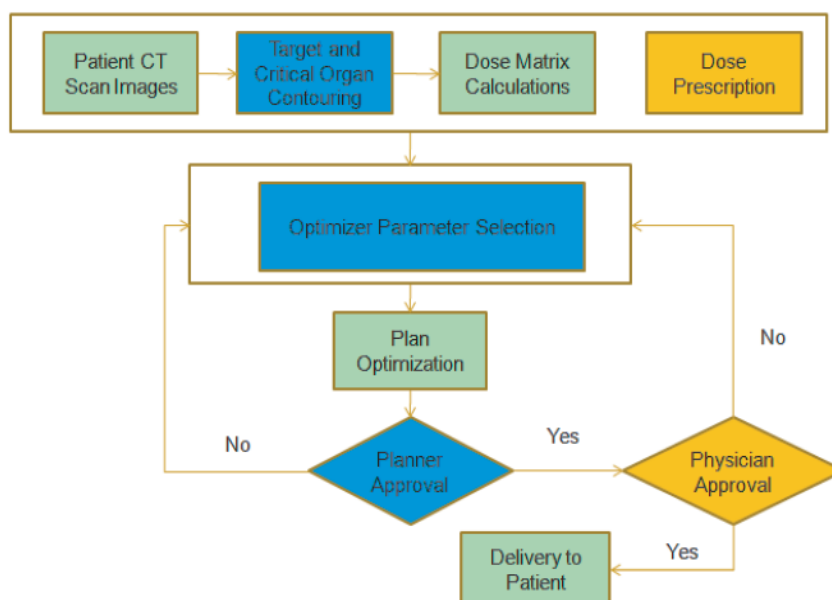


Figure 2.3 Typical workflow in treatment planning

2.1.3.1 Inverse treatment planning

Traditional forward based treatment planning is based on a trial and error approach by experienced professionals. The inverse planning makes use of dose optimization techniques to satisfy the user specified criteria for the dose to the target and critical structures. Dose optimization is possible by making use of DVH based on CT, MRI or other digital imaging techniques. These optimized plans make use of the required dose to the target organ while respecting dose constraint criteria for critical organs.

In VMAT, the objective function is a function of the beamlet weights. The number of beamlets for a given case varies from a few hundred to several thousands. A given objective function can be optimized using many different optimization algorithms such as iterative methods, simulated annealing, filtered back projection, genetic algorithm, maximum likelihood approach and linear programming, etc. For all their complexity, the algorithms to optimize a multidimensional function are routine mathematical procedures. An iterative method is a widely used technique to optimize a multidimensional objective function by starting with an initial approximate solution and generating a sequence of solutions that converge to the optimal solution of the system. In addition to the prescription doses, the current planning system requires the user to pre select the angular variables (gantry, couch, and collimator angles) and the relative importance factors of the involved structures. These variables and parameters constitute an additional multi-dimensional space, which is coupled to the beam profiles in a complicated fashion [10].

2.1.4 Patient specific verification (QA)

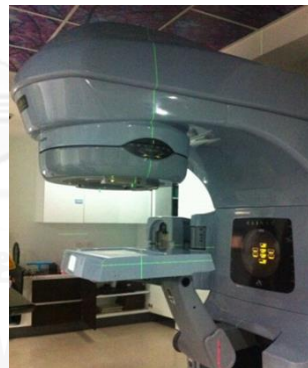
Quality assurance (QA) in radiation therapy is the method used to ensure that the correct amount of radiation is being delivered to the correct location. QA is performed routinely on all parts of the treatment process, from planning to delivery. IMRT treatments are considerably more complex than traditional treatments, and have a greater potential for delivery errors. In addition, IMRT often delivers treatment fields of higher doses that come closer to critical structures. This makes the consequences of misdelivery more pronounced than with traditional radiation therapy. Because of this, IMRT treatments are verified individually prior to being delivered to the patient. This is called patient specific QA. IMRT patient specific QA has several purposes. First, IMRT consists of the addition of many small fields delivered using precise positioning of the MLC, and the treatment planning system may have difficulty accurately modeling this kind of complexity. Patient specific QA ensures that the treatment planning system has accurately calculated the dose for the planned treatment. Second, patient specific QA verifies that the large amounts of treatment data involved has been faithfully transferred from the treatment planning

system to the record and verify system. Third, patient specific QA ensures that the delivery system is capable of delivering the fields as planned. The most accurate QA possible would be performed by taking dosimetric measurements inside of the patient during the treatment delivery. However, this is not a practical method. Instead, treatment plans are typically copied onto a phantom geometry in which dosimetric measurements can be taken. The treatment is delivered to the phantom and measured doses are compared to calculated doses from the treatment planning system. The assumption is made that if the planning system can accurately predict the dose to a phantom, it can also accurately predict the dose to a patient.

Since the introduction of IMRT, pre-treatment measurements have been widely employed as a part of routine patient-specific QA of intensity-modulated treatments. Film dosimetry has gradually been replaced by different types of detector arrays. As VMAT has found its way into clinical practice, so have new detectors and plan verification methods. VMAT plans are often highly modulated and contain many degrees of freedom: the dose rate, gantry speed and MLC positions are all simultaneously variable. The QA of VMAT plans is generally derived from (or similar to) that of IMRT. This includes the use of diode or ionisation chamber arrays, or portal dosimetry systems[8]. Recently, new QA devices that may be well suited for rotational measurements have been developed, such as the ArcCheck (Sun Nuclear) and EPID, they are shown in figure 2.4



(a) ArcCHECK



(b) EPID

Figure 2.4 Example of QA devices for VMAT technique

2.1.5 QA devices for VMAT technique

2.1.5.1 ArcCHECK

ArcCHECK [11] (Sun Nuclear Corp., Melbourne, Florida, USA) is a detector array designed specifically for rotational delivery. ArcCHECK utilizes a unique cylindrical detector geometry that is nearly isotropic regardless of gantry angle. In addition, ArcCHECK utilizes Sun Nuclear SunPoint® diode detectors and appropriate detectors for routine, patient specific QA. ArcCHECK detector is shown in figure 2.5.

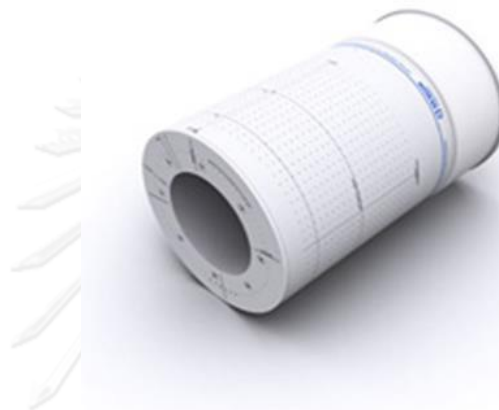


Figure 2.5 ArcCHECK

ArcCHECK phantoms are ideally shaped like a patient. The cylindrical design of ArcCHECK intentionally emulates patient geometry to better match reality. ArcCHECK weighs 16 kg. The number of sensors is 1386 which are arranged in spiral pattern and the distance between detectors is 1cm.

ArcCHECK QA plans are in three dimensions. The DICOM RT Dose and RT plan are imported to measurement device. The dose grid corresponding to detector locations is extracted for comparison to measurement. Verification treatment planning of ArcCHECK is shown in figure 2.6

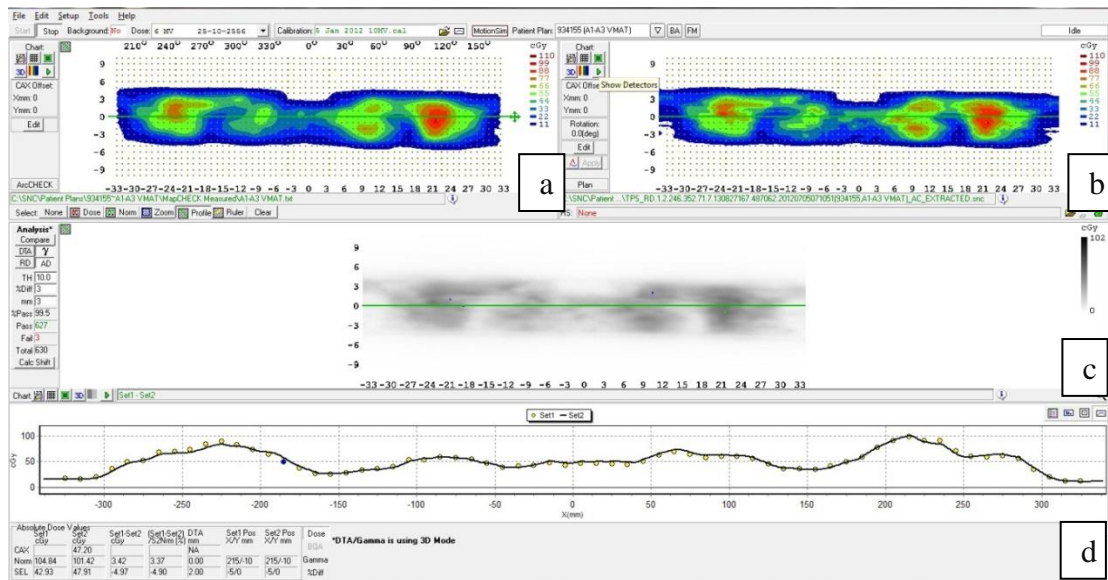


Figure 2.6 VMAT treatment verification planning of ArcCHECK

a) Measured b) Planned c) Gamma index comparison and d) Profiles comparison

2.1.5.2 Electronic portal imaging device (EPID)

Currently, electronic portal imaging devices (EPIDs) [1, 12] are mainly used for patient setup verification during treatment, but several other geometric properties like beam blocking shapes and leaf positions can also be determined. Recent literature indicates an increase in treatment verification with portal imaging and it is an effective means of reducing setup errors. Furthermore, one of the most recent usages of EPIDs is portal dosimetry, which allows the possibility of dosimetric treatment verification.

A. Varian electronic portal imaging device detector system

The Varian aSi1000 is an amorphous silicon flat panel imaging device which is an indirect detection system and comprises three main components.

A.1 Image detection unit (IDU)

It has the shape and size of a standard film cassette and is positioned in the imaging plane using a robotic- controlled R-arm or exact-arm. It is connected by cables to the therapy control area from where image acquisition, processing and display are controlled. EPID (SED) distance is from 95 cm to 180 cm. It has an active imaging area of $40 \times 30 \text{ cm}^2$ (at an SSD of 105 cm). The image matrix is created from an array of 1024×768 pixels. The maximum frame

acquisition rate is 9.574 frames /second, the permitted dose range is 4-25 MV, and the permitted dose rates are 50-600 MU/min.

The detector has four main components. Inside the exterior plastic housing there is a Copper build-up plate, 1 mm in thickness. This is useful in MV imaging to absorb x-ray photons and emit recoil electrons. It also helps to improve the efficiency of the entire imaging system, by partially shielding the downstream components (including the scintillation screen) from scattered radiation. Underneath this plate lies the phosphor screen. In this EPID, it is a Kodak Lanex Fast B scintillating screen, made up of a 0.4mm thick Gadolinium Oxysulfide ($Gd_2O_2S:Tb$) phosphor. This component absorbs the recoil electrons coming from the Copper plate, and transforms them into visible light. Below the phosphor, there is a 1024 x 768 pixel matrix, deposited on a 1 mm glass substrate. This constitutes the sensitive image forming layer of the photodiode system, and it is 1.5 μm thick. Each pixel consists of a Si n-i-p photodiode to integrate the incoming light in charge captures and a thin film transistor (TFT) to act as a three-terminal switch for readout. The final major component is the accessory electronics, which drive the TFT switches and read out the charge captures. The gate driver powers the gate lines during the time that the data lines are feeding the accumulated charge to the read-out electronics. When a voltage is applied to a gate-line, all of the TFTs in that row become transparent and the charge is then transferred to the data lines. Each row is read out in succession, and as one row is read the TFTs in the next row become transparent. External charge sensitive amplifiers capture the charge data. To form one frame of an image, a sequential readout of all of the rows is necessary.

A.2 Image acquisition system (IAS)

The image acquisition system (IAS) contains drivers and acquisition electronics for the image detection unit. The IAS interfaces to the IDU, the linac and the imager controller (the R-Arm or the exact-Arm). It is essentially a digital signal processor that provides frame averaging capabilities and image buffering. It controls and reads the image detector and performs image corrections.

A.3 Acquisition computer control software

The computer control software maintains the interfaces and controls the communication between the IDU and the acquisition unit. Image correction data and acquisition parameters are stored on the hard disk of this computer. The EPID image is the average of acquired frames in the integration mode. Varian electronic portal imaging device detector system is shown in figure 2.7.

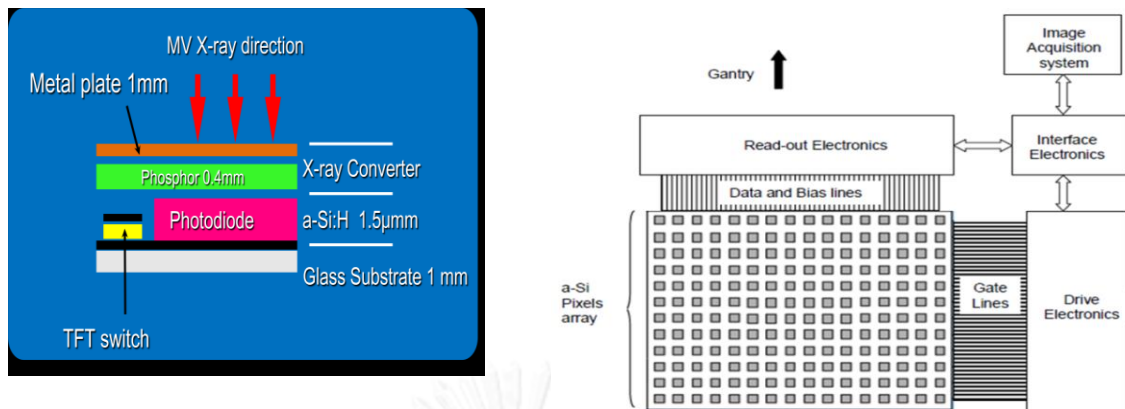


Figure 2.7 Varian electronic portal imaging device detector system

B. Dosimetric characteristics of a-Si electronic portal imaging devices [13, 14]

B.1 Effect of buildup

The EPID signal corresponding to no extra buildup is within 1% of the maximum (at 0.5 cm buildup) due to the inherent buildup provided by the copper plate and other detector components. The profiles for the open fields with and without the 0.5 cm of solid water buildup were also within 1%. The effect of the extra buildup was only evident in a slight blurring of the penumbra. Therefore no extra buildup was utilized in the following measurements. For dosimetric measurements without a patient or scattering material present there is no necessity indicated here for extra buildup at this energy.

B.2 Dose response

The linearity of dose response can be investigated by applying a range of monitor units (MUs) using a fixed field size and evaluating the EPID response per MU for each image. It is always preferable to have a dosimeter that responds linearly with dose. However, some under-response is detected for low MUs (<50 MU).

B.3 Dose rate dependence

Investigate the relation between the dose rate and a-Si EPID response; it is desirable to have a detector system that responds independently of dose rate.

B.4 Reproducibility (temporal stability)

The reproducibility of EPID measurements is investigated by checking the variation in pixel response to the same field in the same conditions over a certain period of time (hours for short term reproducibility and months for long term). All studies have confirmed high temporal stability of a-Si EPIDs which is a very important characteristic for dosimetry purposes.

B.5 Gain ghosting and image lag

Gain ghosting refers to the reduction of detector response (pixel sensitivity) as a result of successive irradiations, which can be attributed to the semiconductor structure of a-Si EPIDs. Image lag is a memory effect and appears when a frame is recorded after an exposure but some charges are still left from an earlier exposure.

B.6 Energy response

Amorphous silicon EPIDs are known to have energy dependent response. They over respond to low energy radiation (below 1 MeV), due to the presence of the phosphor layer which has a high atomic number and therefore has a higher cross section for photoelectric interactions. EPIDs need to be corrected for this effect if used for dosimetry, since radiotherapy beams are poly-energetic and have components in this energy range. In addition, the beam energy may change due to differences in field size, off-axis distance and passage through patient/phantom or MLC.

2.1.6 EPIQA software

EpiqaTM [15] is a program that allows to convert a dosimetric image acquired by an EPID into a dose map and to compare the dose map with a reference dose distribution. It is possible to utilize EPIQA for a verification of static as well as intensity modulated fields, including VMAT fields. The conversion of a dosimetric image into a dose map is only possible if a response of the imager to a beam is known. The EPID's response shows very good linearity, but exhibits rather strong energy dependence, which causes a difference in response to primary and MLC transmitted radiation. EPIQA overcomes this limitation by the calibration process that takes the energy dependence of the detector into account. For the purpose of calibration, a set of integrated images for open and transmission fields of different field sizes are acquired and consequently imported into EPIQA together with the output factor table (measured by a conventional detector such as ionization chamber) to establish basic algorithm configuration data. Based on the knowledge of jaws position and the trajectory of MLC leafs (for an IMRT field), a calibration factor can be determined for every pixel of an EPID by weighting the contribution of primary and transmitted radiation and by applying an interpolation among the data of the calibration dataset. The pixel based calibration relates the readout of a pixel to a dose at the depth of d_{max} in water equivalent homogenous medium. By applying the conversion to all pixels

of the EPID, a planar dose distribution at the d_{\max} in water is obtained. The image-to-dose conversion algorithm (GLAaS) derives calibration factors for EPID's pixels using empirically measured dataset. The obtained dose map is compared against dose distribution calculated by clinically used dose algorithm. It is therefore an independent method of verification of the dose distribution calculated by a treatment planning system and verification of the delivery device performance. EPIQA principle is show in figure 2.8.

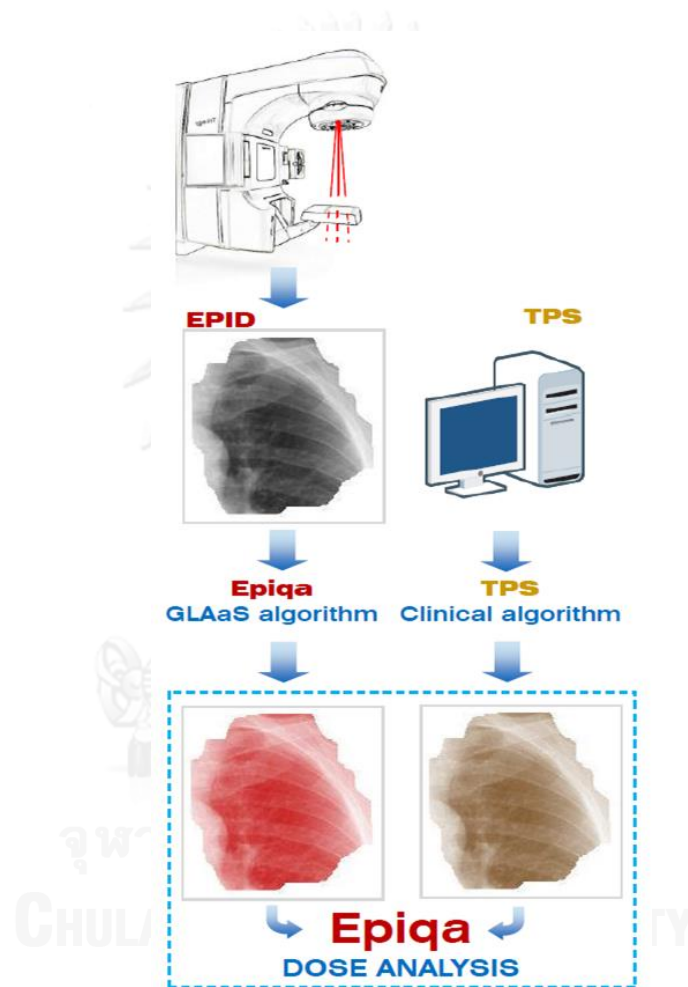


Figure 2.8 EPIQA principle

2.1.7 GLAaS algorithm

The GLAaS algorithm [16] has been used to convert raw images acquired with the portal imager into dose matrices at the depth of the maximum dose d_{\max} . No phantom is used, and radiation field impinges directly onto the detector. This algorithm was originally developed for IMRT pretreatment verification, and here slightly adapted for RapidArc testing. A brief description

of the algorithm follows. For a given beam, the response of the amorphous silicon detectors is linear ($D(\text{Gy}) = m \cdot R + q$). IMRT and RapidArc fields are, however, changing continuously during delivery. GLAaS accounts for those changes in time and position, using different m and q values, and differentiating between primary and transmitted (below the MLC) radiation, on a pixel by pixel basis.

The total dose d_i in the i -th pixel, over the entire field delivery is:

$$d_i = d_{pr,i} + d_{tr,i} = \left(\sum_{s=1}^N m_{pr,s}(E_{wwF}) \cdot r_{i,s} + q_{pr,s} \right) + \left(m_{tr} \cdot \left(R_i - \sum_{s=1}^N r_{i,s} \right) + q_{tr} \right)$$

where: m and q are the slope and the intercept for a field of size E_{wwF} (Equivalent window width Field), r is the reading attributed to the primary radiation for the segment/ control point s , and R is the total PV reading; subscripts p_r refer to primary, t_r to transmitted radiation. The field is considered as a sum of N segments or control points. In the case of single static field or RapidArc, the key elements for GLAaS are the same: knowledge of the MLC shape and of the dose progress at any instant of the delivery. This information is fully stored in the DICOM-RT plans from the treatment planning system. In addition, RapidArc is characterized by variable dose rate during delivery. It was proven in that the detector response is independent on the dose rate; in this view the same calibration parameters set can be used for the whole field, acquired at any (variable) dose rate.

The parameter values computed during the configuration of the GLAaS to analytically obtain the slopes that come from the following empirical algorithm:

$$OF(E_{wwF}) = [x + d \cdot \ln(E_{wwF})]^{-1} \quad (2)$$

Where E_{wwF} is the equivalent field size of each segment

$$m_{pr}(OF) = a \cdot OF + b \quad (3)$$

Where m_{pr} is the slope for primary radiation, and OF is the PV measured output factor as per equation (2).

For transmitted radiation the following relationship is used:

$$m_{tr} = k \cdot m_{pr} \quad (4)$$

GLAaS configuration consists in the determination of a set of empirical parameters: a , b , c , d , k , q_p and q_{tr} .

GLAaS has been configured to convert images acquired without any buildup on the PV cassette into dose at the depth of maximum dose d_{max} (1.5 cm and 3 cm for 6 and 18 MV respectively), at the source-detector distance $SDD = 100$ cm.

The GLAaS algorithm was already tested for verification of fields with high doses, needed when RapidArc fields are concerned, because the full dose is delivered in only one field. This is guaranteed by the way the PV electronics works, averaging the reading per each pixel over a number of frames, and recording the reading values and the number of acquisition frames.

2.1.8 Gamma evaluation [17]

The qualitative evaluation of the treatment planning system calculation is made by superimposing the isodose distributions, directly compare the measured and calculated dose distribution values. Van Dyk et al. described the quality assurance procedures of treatment planning systems and subdivide the dose distribution comparisons into regions of high and low dose gradients, each with a different acceptance criterion. In low gradient regions, the doses are compared directly, with an acceptance tolerance placed on the difference between the measured and calculated doses. A dose-difference distribution can be displayed that identifies the regions where the calculated dose distributions disagree with measurement. In high dose gradient regions (assuming that the spatial extent of the region is sufficiently large), a small spatial error, either in the calculation or the measurement, result in a large dose difference between measurement and calculation. Dose differences in high dose gradient regions may therefore be relatively unimportant, and the concept of a distance-to-agreement (DTA) distribution is used to determine the acceptability of the dose calculation. The DTA is the distance between a measured data point and the nearest point in the calculated dose distribution that exhibits the same dose. The dose-difference and DTA evaluations complement each other when used as determinants of dose distribution calculation quality. A composite analysis uses a pass-fail criterion of both the dose difference and DTA. Each measured point is evaluated to determine if both the dose difference and DTA exceed the selected tolerances (e.g., 3% and 3 mm, respectively). Points that fail both criteria are identified on a composite distribution. Because the composite distribution is a binary distribution, it does not lend itself to a convenient display. Therefore, by convention, the quantity displayed in the composite distribution is the dose difference. While the composite distribution highlights regions of disagreement, the display of the dose difference may accentuate the impression of failure in high dose gradient regions. An additional limitation to this technique is that there is no unique numerical index that enables the

presentation and analysis of a distribution that measures the calculation quality. An extension of the isodose comparison tools is presented that simultaneously incorporates the dose and distance criteria.

It provides a numerical quality index that serves as a measure of disagreement in the regions that fail the acceptance criteria and indicates the calculation quality in regions that pass. The index can be presented in a graphical form to enable a rapid and efficient evaluation of the algorithm criteria are selected, the dose-difference and distance-to-agreement analyses have equivalent significance when determining calculation quality.

The measure of acceptability is the multidimensional distance between the measurement and calculation points in both the dose and the physical distance, scaled as a fraction of the acceptance criteria. In a space composed of dose and spatial coordinates, the acceptance criteria form an ellipsoid surface, the major axis scales of which are determined by individual acceptance criteria and the center of which is located at the measurement point in question.

When the calculated dose distribution surface passes through the ellipsoid, the calculation passes the acceptance test for the measurement point. The minimum radial distance between the measurement point and the calculation points (expressed as a surface in the dose-distance space) is termed the gamma index. The surface representing acceptance criteria is an ellipsoid shown in figure 2.9.

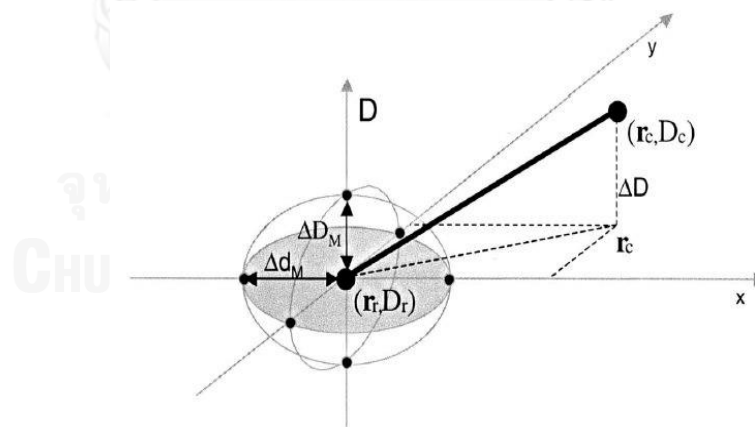


Figure 2.9 Ellipsoid that defines the acceptance criterion for the gamma evaluation method

Acceptance criteria are an ellipsoid defined by:

$$1 = \sqrt{\frac{\Delta r^2}{\Delta d_M^2} + \frac{\Delta D^2}{\Delta D_M^2}}$$

Suppose a reference dose $D_r(r_r)$ at location r_r needs to be compared with a control dose $D_c(r_c)$ at r_c .

The acceptance criteria shall be

$\Delta D_M = D_r(r_r) - D_c(r_c)$ for the dose and

$\Delta d_M = |r_r - r_c|$ for the distance.

For the compared dose to match the reference dose in r_r , it needs to contain at least one point (r_c, D_c) lying within the ellipsoid of acceptance. This means at least one point for which:

$$\gamma_r(r_c, D_c) = \sqrt{\frac{\Delta r^2}{\Delta d_M^2} + \frac{\Delta D^2}{\Delta D_M^2}} \leq 1$$

A quantitative measure of the accuracy of the correspondence is determined by the point with the smallest deviation from the reference point, i.e. the point for which

$\gamma_r(r_c, D_c)$ is minimal. This minimal value is referred to as the quality index $\gamma(r_r)$ of the reference point.

The pass-fail criterion therefore becomes

$\gamma(r_r) \leq 1$, correspondence is within the specified acceptance criteria,

$\gamma(r_r) > 1$, correspondence is not within the specified acceptance criteria

The example of gamma analysis of EPIQA is show in figure 2.10

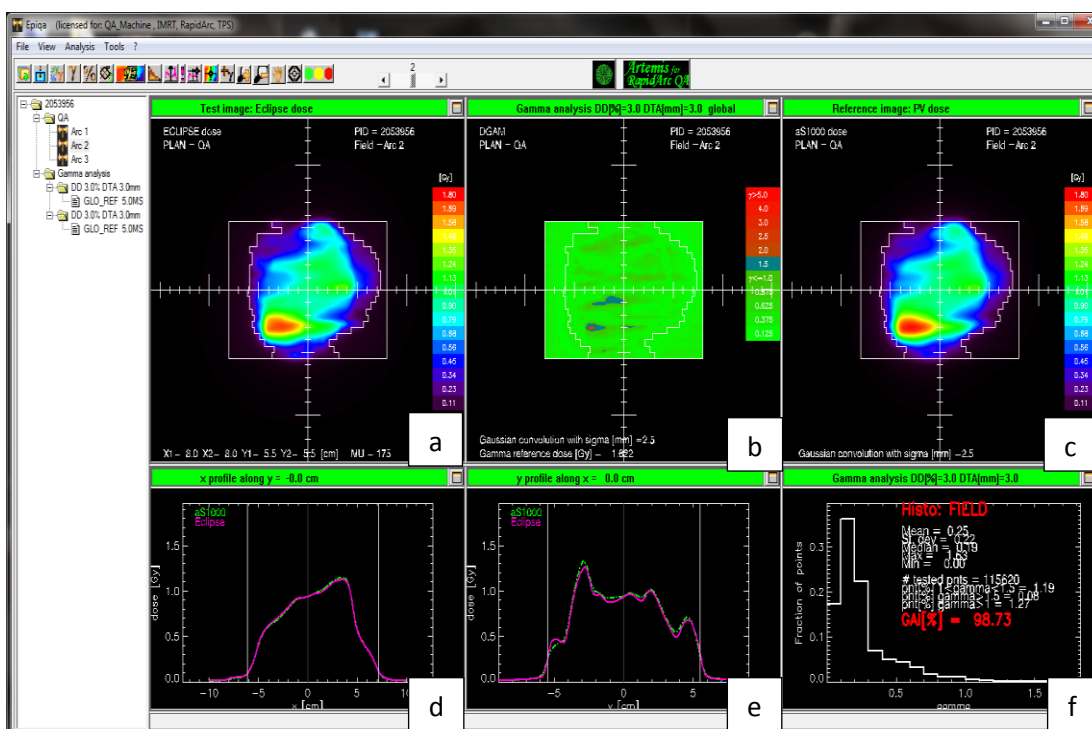


Figure 2.10 Displayed gamma analysis of EPIQA

- a) Dose matrix window, 1st data set(Eclipse dose)
- b) Gamma analysis matrix window
- c) Dose matrix, 2nd data set(Portal vision dose)
- d) Profile display in x direction (left-right) for both dose matrices
- e) Profile display in y direction (feet-head) for both dose matrices
- f) Display of histogram and statistics for the gamma analysis matrix window

2.1.9 Gamma pass limit

Quantitative analysis of patient-specific QA measurements is often used to determine whether the delivered field is appropriate for treating the patient. An important in any QA process is to determine a tolerance or action level. When a QA result falls outside of this tolerance, some appropriate action is taken. The term gamma pass limit is an acceptance levels. In absence of any general consensus on acceptance levels for modulated arc delivery, a threshold to gamma pass = 95% could be applied to define acceptable pre-treatment delivery verifications. For gamma pass in the range between 90 and 95% care should be paid to investigate more in detail potential sources of errors by performing complementary tests (e.g. controlling leaf motion, dose rate or gantry speed performances). Gamma pass should likely be computed with DTA = 3 mm and DD = 3%, since calculation uncertainties from TPS and detector vs. calculation spatial resolution issues would weaken reliability of findings obtained with more stringent parameters [16].

In practice, physicists use commercial tools that have different available options, and so it is difficult to offer definitive guidance regarding acceptance levels for gamma analysis results. The gamma pass depends on several factors, such as the model used in treatment planning, the dose delivery system, the measuring instrument and analysis of extensive institutional QA results. Task Group 119 (TG-119) of the American Association of Physicists in Medicine (AAPM) reported patient specific QA results from a multi-institutional study designed specifically to quantify the degree of agreement that should be expected from patient-specific IMRT QA measurements. They use of the quantity “confidence limit”. The confidence limit is based on the average deviation between measurements and calculations for a number of data points in a comparable situation, and the standard deviation (SD) of the average of the differences. The confidence limit is then defined as the sum of the average deviation and 1.5 SD. The factor 1.5 was based on experience and a useful choice in clinical practice. A multiplicative factor of 1.96 instead of 1.5 has later been proposed for having 5% of the individual points. The gamma pass limit could be calculated using confidence limit of $(100 - \text{mean}) + 1.96\sigma$ [4]

2.2 Review of related literatures

Huang Y. C. et al [18] evaluated EPID performance for VMAT dose verification. First, dosimetric characteristics of EPID were investigated. Then 22 arc fields of 10 patients (6 plans for head and neck and 3 plans for pelvis and 1 plan for esophagus regions.) VMAT dose plans were measured by EPID with the rotational method. GLAaS is an algorithm used to derive absolute dose maps from portal images acquired with EPID. The film system use as a conventional tool for verification showed good agreement both with EPID measurements and treatment planning system (TPS) calculations. From the comparison between films and static EPID measurements, the mean gamma passing rate was $(94.1 \pm 1.5)\%$ with 3%/3mm criteria and the mean gamma passing rate of the comparison between films and TPS calculations was $(97.4 \pm 2.8)\%$. In addition, EPID measurements for VMAT presented good agreement with TPS calculations ($[99.1 \pm 0.6]\%$ with 3 mm/3% criteria). The EPID system performed the robustness of potential error findings in TPS calculations and the delivery system. This study demonstrated that an EPID system can be used as a reliable and efficient quality assurance tool for VMAT dose verification.

Varatharaj C. et al. [19] implemented the newly developed portal dosimetry software using independent dose prediction algorithm EPIDose™ and evaluated this new tool for the pre-treatment IMRT plan quality assurance of Whole Pelvis with Simultaneous Integrated Boost (WP-SIB-IMRT) of prostate cases by comparing with routine two-dimensional (2D) array detector system (MapCHECK™). The 104 split fields using γ -distributions in terms of predefined γ frequency parameters was investigated in this study. The mean γ values were found to be 0.42 (SD: 0.06) and 0.44 (SD: 0.06) for the EPIDose and MapCHECK™, respectively. The average $\gamma\Delta$ for EPIDose and MapCHECK™ were 0.51 (SD: 0.06) and 0.53 (SD: 0.07), respectively. Furthermore, the percentage of points with $\gamma < 1$, $\gamma < 1.5$, and $\gamma > 2$ were 97.4%, 99.3%, and 0.56%, respectively for EPIDose and 96.4%, 99.0% and 0.62% for MapCHECK™. Base on this study results obtained with EPIDose were strong agreement with MapCHECK™, we may conclude that the EPIDose portal dosimetry system has been successfully implemented and validated with our routine 2D array detector.

Urso G. et al [20] proved that EPIQA was reliable and flexible tool for Rapid Arc pre-treatment Quality Assurance. The clinical usage of Epiqa software was presented as a joint experience of two centers, 43 plans from The Istituti Clinici Humanitas (ICH) and 101 plans from the Oncology Institute of Southern Switzerland (IOSI). For each patient, once the VMAT plan was accepted for treatment, the “verification plan” of the original plan with gantry fixed to 0 degree was calculated and then acquisition with the EPIDaS1000 of the original VMAT plan, with NO additional phantom. EPIQA software was based on the GLAaS algorithm for converting raw PV images to dose and comparison between calculated and measured dose matrices was automatic in EPIQA. All patients were treated with 6 MV (except one case with 18 MV at ICH). Gamma agreement index (GAI) represented the percentage of the field area (defined by the jaws) passing the gamma criteria of 3mm distance to agreement and 3% dose difference, relative to the significant maximum dose in the field (arc). ICH center GAI (3mm, 3%) was $97.76 \pm 1.60\%$ and IOSI center was $97.65 \pm 1.23\%$. From the result, Epiqa proved to be a very reliable and flexible tool for RapidArc pre-treatment quality assurance. It was primarily found to be a very reliable and easy to use tool for pre-treatment QA, allowing a fast growth of the number of treated patients, grace to its fast usage.

Krishna Murthy K. [21] validated a locally fabricated phantom of Imatrixx-2D Array by comparing its results with ArcCheck phantom and comparing portal dosimetry measurements with the two phantom studies. Electronic Portal Imaging Devices and Epiqa software were used for portal dosimetry. An Imatrixx-2D array with a locally fabricated phantom and ArcCheck cylindrical phantom were used for phantom studies. Eclipse-TPS with RapidArc treatment planning and portal dose prediction software was used for planar dose calculations. Three verification plans were created for each of the 15 patient plans of various sites, making a total of 45 plans to be delivered on 3 QA systems as above. Fifteen plans each with 2 arcs were delivered on the EPIDs of the Linacs, on Imatrixx-2D array phantom and on ArcCheck cylindrical phantom respectively. The planar dose matrices were analysed using global Gamma Index criteria of 3mm DTA and 3% dose difference. The result showed the maximum deviations of percentage in dose points, in which $\gamma > 1$, are 1.94, 1.89 and 1.5 in Imatrixx phantom, ArcCheck phantom and Portal dosimetry, respectively. Similarly, the mean deviations and SD values are less in portal dosimetry than that of phantom studies. The smaller deviations in portal dosimetry are attributed to closely embedded chambers in the EPID compared to the distance between the detectors

placed in the phantom measurements. After carrying out the comparison of results, the locally fabricated phantom has been validated and accepted for the dosimetric studies. The results revealed that all the three dosimetric QA methods were suitable for the patient-specific QA of RapidArc treatment. This study concluded that, depending on the machine time available, any dosimetric system of these three methods can be used interchangeably for routine patient-specific QA.

Ezzell G. A. et al. [22] produced quantitative confidence limits as baseline expectation values for IMRT commissioning. A set of test cases was developed to assess the overall accuracy of planning and delivery of IMRT treatments. These tests were planned, delivered, measured, and analyzed by nine facilities using a variety of IMRT planning and delivery systems. Each facility had passed the Radiological Physics Center credentialing tests for IMRT. The agreement between the planned and measured doses was determined using ion chamber and film dosimetry. The planar dose distributions used gamma criteria of 3%/3 mm. The mean values and standard deviations were used to develop confidence limits for the test results using the concept confidence limit = $|100 - \text{mean}| + 1.96\sigma$. In this study the overall average was 97.9% with a standard deviation of the average of 2.5%. This corresponds to a confidence limit of 7.0% which means that the percentage of points passing the criteria should exceed 93%. In these study collective results, 94% of the tests fell within the confidence limit.

CHAPTER III
RESEARCH METHODOLOGY

3.1 Research design

This study is an observational descriptive study.

3.2 Research design model

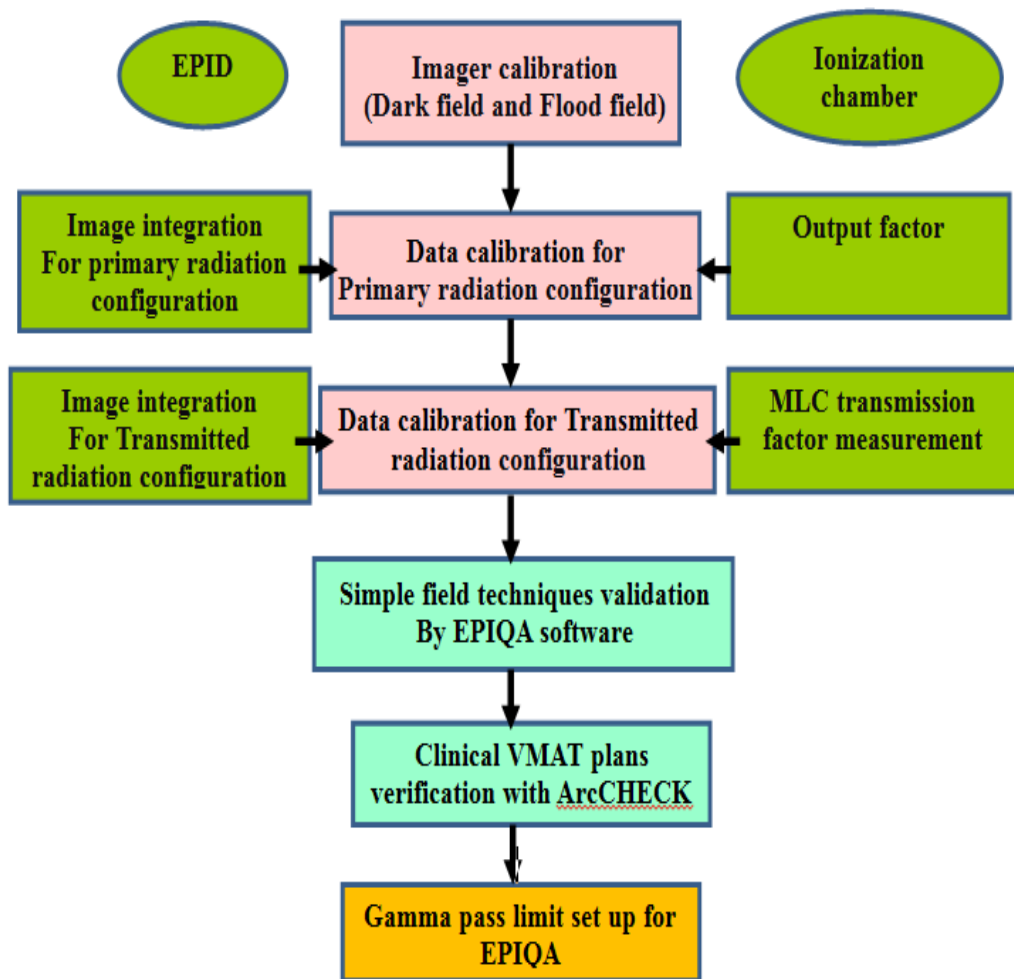


Figure 3.1 Research design model

3.3 Conceptual frameworks

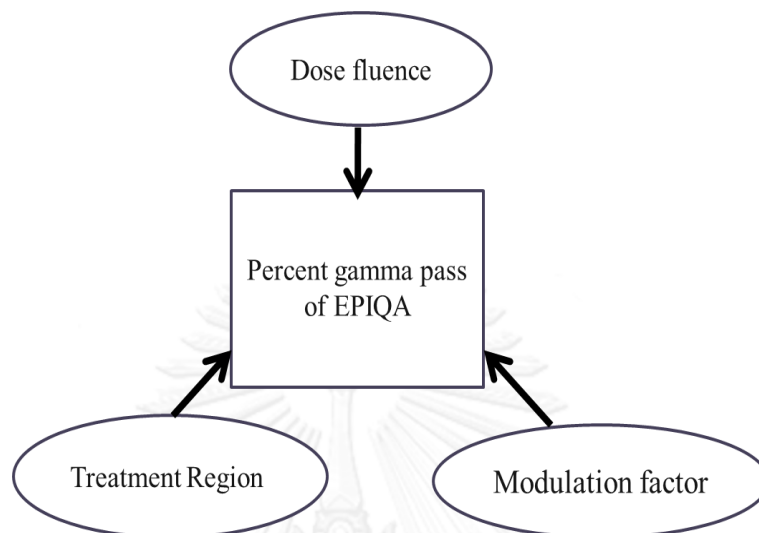


Figure 3.2 Conceptual frameworks

3.4 Key words

- Patient specific QA
- Portal dosimetry
- EPID
- EPIQA
- VMAT

3.5 Research question

What is the gamma pass limit of EPIQA Software for volumetric modulated arc therapy pre-treatment verification?

3.6 Materials

3.6.1 Linear accelerator and portal vision

Varian Clinic iX linear accelerator (Varian Oncology systems, Palo Alto, CA, USA) has dual energy of 6 and 10 MV photon beams and six energy levels of 4, 6, 9, 12, 16 and 20 MeV electron beams. Field sizes can be varied from $0.5 \times 0.5 \text{ cm}^2$ to $40 \times 40 \text{ cm}^2$ at isocenter. Dose rate are ranged from 100-600 monitor units per minute. Multileaf collimator of 120 leave scan move as the dynamic movement. The aS1000 flat-panel EPID Portal Vision has a $40 \times 30 \text{ cm}^2$ detecting surface with a matrix of 1024×768 pixels (0.392 mm pixel pitch). EPID is a part of the linear accelerator. Varian Clinic iX linear accelerator is shown in figure3.3.



CHULALONGKORN UNIVERSITY

Figure 3.3 Varian Clinic iX linear accelerator with portal vision

(Varian Oncology systems, Palo Alto, CA, USA)

3.6.2 EPIQA software

EPIQA is a comprehensive tool for Quality Assurance with Electronic Portal Imaging Devices (EPID). The main core of the package is the conversion algorithm, which converts the readings into absorbed dose at a certain depth using EPID images. EPIQA software is shown in figure3.4



Figure 3.4 EPIQA software (Epidos s.r.o., Bratislava, Slovakia)

3.6.3 ArcCHECK

ArcCHECK Model 1220, which is shown in figure 3.5, is a cylindrical water equivalent phantom with a three dimensional array of 1386 diode detectors, arranged in a spiral pattern, with 10 mm sensor spacing. The center of the phantom is 15 cm diameter. The depth of detector is 2.85 cm which is 3.28 cm water equivalent.

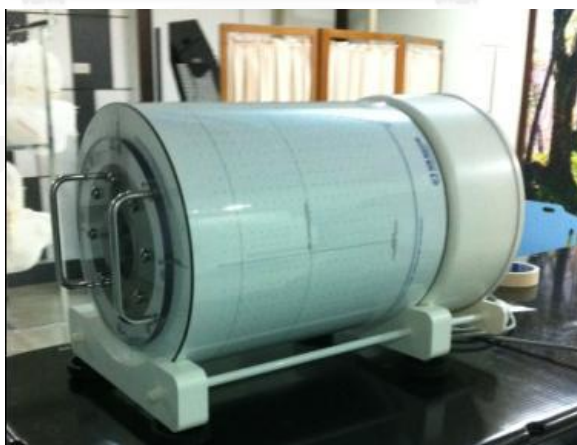


Figure 3.5 ArcCHECK (Sun Nuclear Corp., Melbourne, Florida, USA)

3.6.4 Treatment planning system

The Eclipse treatment planning software (Version 8.9.21, Varian Medical System, Palo Alto, CF, USA) is a comprehensive treatment planning system that simplifies modern radiation therapy planning for all kinds of treatment including 3D conformal, IMRT and VMAT. The conventional technique is planned by forward planning, while IMRT and VMAT are planned by inverse planning using analytical anisotropic algorithm (AAA). The physicists used Eclipse treatment planning software to calculate the dose distribution and verify the best treatment plans for patients. Eclipse treatment planning software version 8.9.21 is shown in figure 3.6.



Figure 3.6 Eclipse treatment planning: version 8.9.21
(Varian Medical System, Palo Alto, CF, and USA.)

3.6.5 Ionization chamber of 0.13 cm³

The absolute and relative dose of photon and electron beams were measured by compact chambers in solid phantoms or in water phantoms. Ionization chamber of 0.13 cm³ is shown in figure 3.7.



Figure 3.7 The CC13 ionization chamber (IBA Dosimetry, Schwarzenbruck, Germany)

3.6.6 The Dose-1 Electrometer

The DOSE-1 is a portable, single channel, high-precision reference class electrometer for measurements of absorbed dose. The device significantly exceeds the recommendations of the IEC 60731. The DOSE-1 Electrometer is shown in figure 3.8.



Figure 3.8 Electrometer (IBA Dosimetry, Schwarzenbruck, Germany)

3.6.7 Water phantom WP 1D

The WP 1D is a 1D stand-alone water phantom for absolute dose measurements according to TG-51 and IAEA TRS-398 dosimetry protocols. Water phantom WP 1D is shown in figure 3.9.



Figure 3.9 Water phantom WP 1D

(IBA Dosimetry, Schwarzenbruck, Germany)

3.6.8 70 VMAT plans from the Division of radiation oncology, Department of Radiology, Faculty of Medicine, Chulalongkorn University.

3.7 Methods

3.7.1 Imager calibration

Firstly, EPID aSi 1000 which was fixed with Varian Clinac iX linear accelerator (Varian Oncology systems, Palo Alto, CA, USA) was set at 100 cm source to detector distance (SDD) (figure 3.10). This configuration relates PV acquisitions performed without adding any build-up material on the top of the PV cassette with doses calculated/measured at D_{max} , where the dose calculation is more reliable. Next, image calibration was performed for 6 and 10 MV photon beams. The highest dose rate considered for clinical used (600 MU/min) was employed to performed data acquisition for calibration so that EPIQA software can be valid up to high dose rate. The dark field and flood field were taken. Dark field image was acquired with no irradiation and represented the electronic noise in the image. Flood field image was delivered by uniform irradiation in the entire area of EPID to correct the gain for each individual pixel.

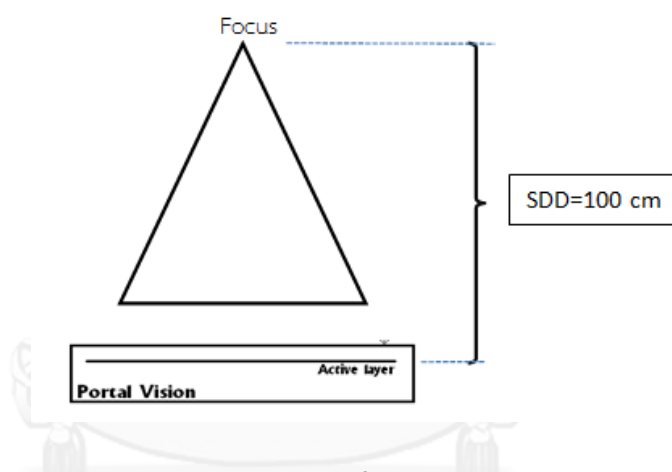


Figure 3.10 Geometry setup for image calibration

3.7.2 Data calibration for 6 and 10 MV

3.7.2.1 Primary radiation configuration

Primary dose calibration window is shown in figure 3.11. The output factors were measured by 0.13 cc ionization chamber (IBA Dosimetry, Schwarzenbruck, Germany) connected with Dose I electrometer (IBA Dosimetry Schwarzenbruck, Germany). The ionization chamber reading at the depth of D_{max} for 3x3, 5x5, 10x10, 12x12, 15x15, 20x20, 25x25 and 30x30 cm² were taken, the output factors were determined (figure 3.11a). The integrated images were required for primary radiation configuration to determine detector response to primary radiation. The images for the same set of open fields: 3x3, 5x5, 10x10, 12x12, 15x15, 20x20, 25x25 and 30x30 cm² were taken. Then the field size factors of image were determined (figure 3.11b). For each field size, three images with 10, 20 and 50 MU were acquired. Then the field size correction factor of image

related to the ionization measurement (Primary dose angular coefficient) was determined by the software (figure 3.11c). It was necessary to acquire the dose calibration factor expressed in terms of MU/Gy for each field size.

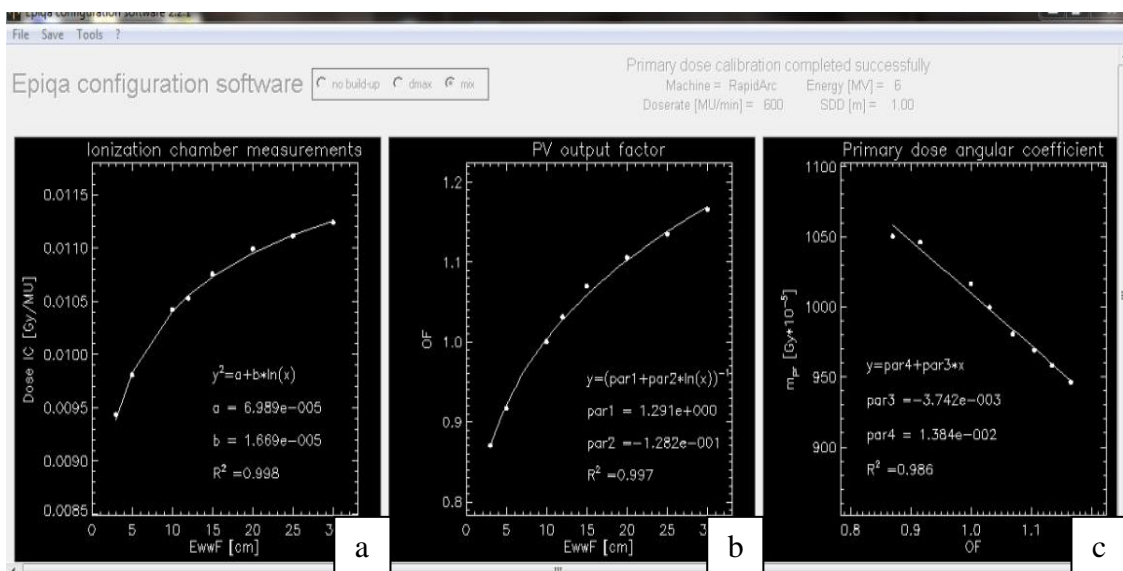


Figure 3.11 Primary dose calibration windows

- Output factor measured by ionization chamber
- Output factor measured by PV
- Primary dose angular coefficient

3.7.2.2 Transmitted radiation configuration

Transmission dose calibration window is shown in figure 3.12. MLC transmission factors were undertaken by measuring the output with 0.13 cc ionization chamber for the open square field (X=10 cm, Y=10 cm) with 100 MU. Follow by the output of the square field (X=10 cm, Y=10 cm) which was close by the multileaf collimator (MLC) irradiated with 100 MU. Then the transmission was calculated (figure 3.12a).

The transmission factors were performed for the image. The integrated images from EPID were acquired for open square field (X=10 cm, Y=10 cm) with 50 MU. Follow by the output of the square field (X=10 cm, Y=10 cm) which was close by the multileaf collimator (MLC) irradiated with 3 different MUs of 50, 100, 200 (figure 3.12b). Then the transmission correction factor related to the ionization measurement (primary dose angular coefficient) was determined by the software (figure 3.12c).

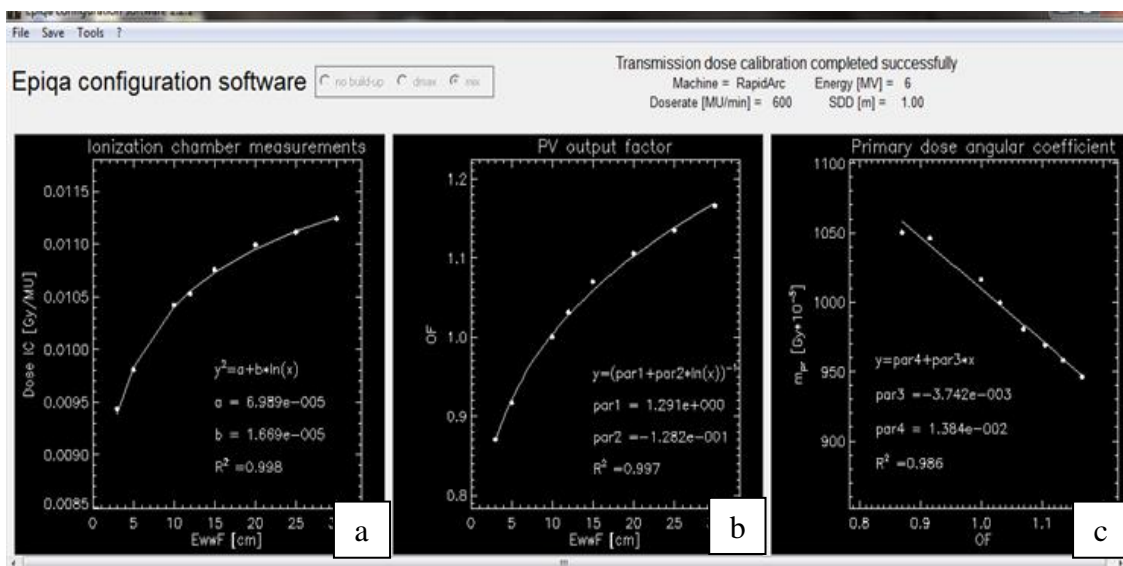


Figure 3.12 Transmission dose calibration windows

- a) Transmission factor measured by Ionization Chamber b) Transmission Factor measured by PV
c) Primary Dose Angular Coefficient

3.7.2.3 The diagonal profile from TPS configuration beam data

The diagonal profiles for $40 \times 40 \text{ cm}^2$ the largest field size in 6 and 10 MV were imported from Eclipse configuration beam data to correct for off axis dose. The diagonal profiles for 6 MV is shown in figure 3.13.

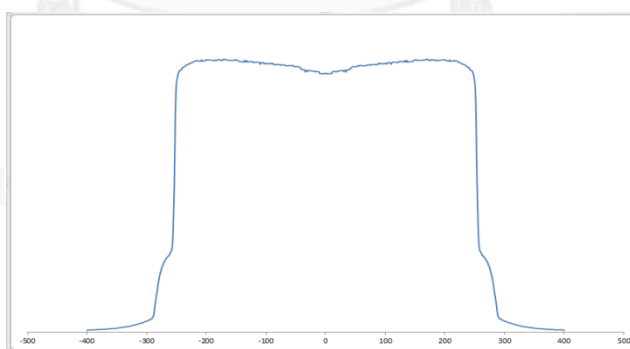


Figure 3.13 The diagonal profile

3.7.3. Simple field techniques validation

After installation and commissioning of EPIQA for dosimetric purpose, the measurements were performed for open field sizes of 2x2, 3x3, 4x4, 5x5, 5x15, 10x10, 20x20 cm², Dynamic wedge 30° with field size of 10x10 cm² and pyramid IMRT field for 6 and 10 MV photon beams. The simple field techniques measurements were aimed to validate the performance of EPIQA software from basic treatment planning. The Work flow for Simple field techniques validation is shown in figure 3.14

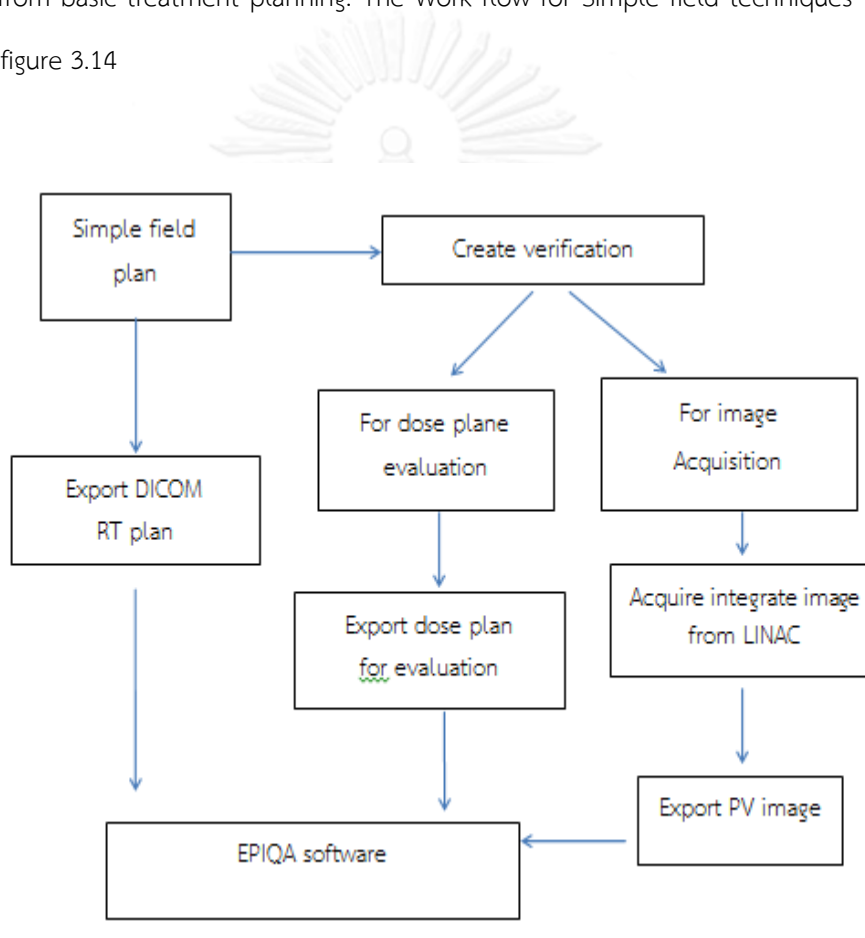


Figure 3.14 Work flow for Simple field techniques validation

3.7.4 Clinical VMAT plans comparison with ArcCHECK

For clinical VMAT plans, Computed tomography (CT) scans of the patient were used to contour target structures and healthy organs by physician. The physicists put the parameters that are required to treatment plan optimization software. VMAT are inverse treatment planning which have the objective function of the beamlet weights. The numbers of beamlet for a given case depend on the tumor size and beamlet size. Many small beamlet of a plan is intensity map. The leaf sequence will generate the intensity map as desired from inverse treatment planning by its software then the software provides the intensity map for TPS [23]. After the plans were approved by the physician, the VMAT plans were transferred to linear accelerator machine for irradiation with ArcCHECK and EPID in the rotational method to verify the intensity map provided by treatment machine. The methods are shown in figure 3.15. For verifying EPIQA with ArcCHECK, the VMAT plans (10 H&N, 11 Head, 13 Chest, 9 Pelvis) 2-5 arcs per plans (145 arc fields) with 6 MV (28 cases) and 10 MV (15 cases) photon beams were selected for this study. For EPID, the images were changed to dose in phantom by EPIQA software. The dose map calculated by EPIQA software was compared with Eclipse treatment planning using gamma criteria of 3 mm distance to agreement and 3% dose difference. This new tool was compared in term of percent gamma pass with ArcCHECK (Sun Nuclear Corporation, Melbourne, FL). ArcCHECK was studied for its properties before clinical use. The clinical was demonstrated excellent performance for VMAT verification [24]. So ArcCHECK is used routinely in our clinic.

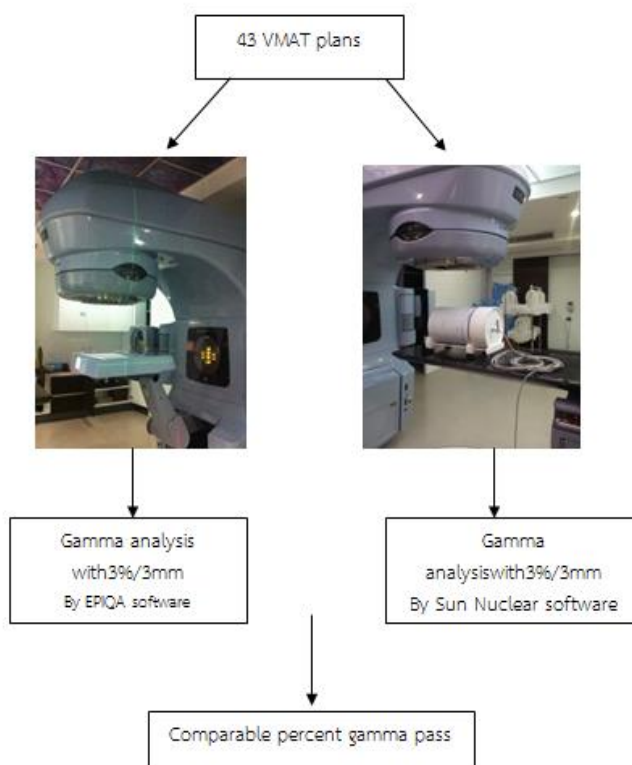


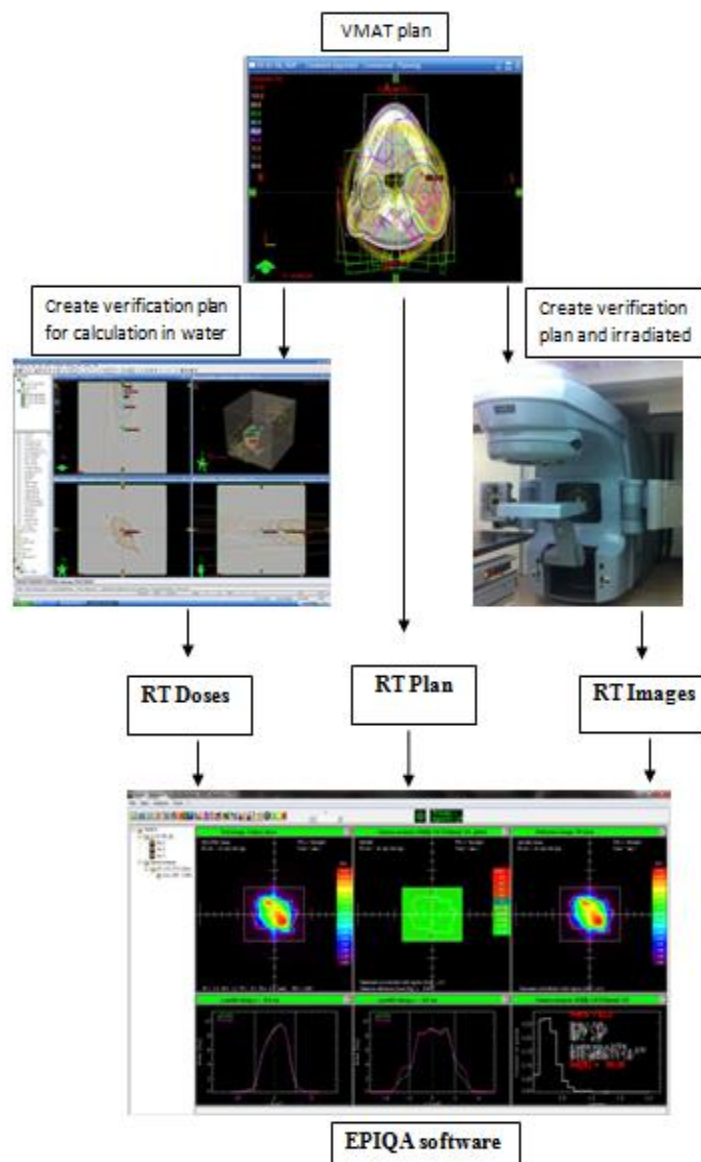
Figure 3.15 Work flow for verifying EPIQA with ArcCHECK

Workflow for clinical VMAT plans verification by EPIQA which is shown in figure 3.16 is described below:

- The VMAT plans that needed to be verified were copied to QA course of patient so that the plans' irradiation will not be counted to clinical irradiation of a patient.
- The VMAT plans were transferred to Linac machine for irradiation with EPID for image acquisition with the same parameters in beam energy, field size, dose rate, MLC movement, monitor units and gantry rotations.
- The verification plan were created for VMAT plans in water phantom for verification with the selecting option to zero for all gantry angles in each field and the dose was calculated at the depth of d_{max} (SSD 98.5 cm.).
- The DICOM files from TPS (RT plan, RT dose, RT image) were exported to EPIQA software
- The results were evaluated

Four files needed to be loaded into EPIQA for evaluated field by field

- 1) Integrated image of a verified field (RT image, RI)
 - 2) Integrated image of a 10x10 field (RT image, RI)
 - 3) RT plan file containing the plan geometry information (RT plan, RP)
 - 4) Reference planar dose distribution for comparison (RT dose, RD)
- Gamma analysis using criteria 3% DD and 3mm DTA.



จุฬาลงกรณ์มหาวิทยาลัย
CHULALONGKORN UNIVERSITY
Figure 3.16 Work flow for EPIQA verification

Work flow for clinical VMAT plans verification by ArcCHECK which is show in figure 3.17 is described below:

- The verification plans were created in ArcCHECK phantom.
- The DICOM files (RT plan, RT dose) were exported to Sun Nuclear software
- The VMAT plans were transferred to Linac machine for irradiation to ArcCHECK with the same parameters in beam energy, field size, dose rate, MLC movement, monitor units and gantry rotations. ArcCHECK measurement devices were placed on the treatment couch at 86.65 cm source to surface distance.
- The results were evaluated
- Gamma analysis Gamma analysis using criteria 3%DD and 3mm DTA

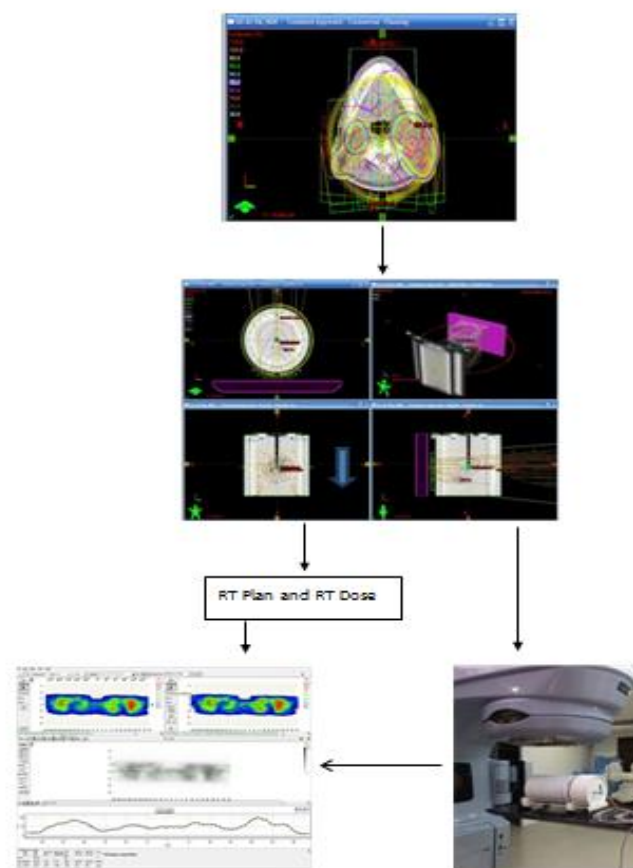


Figure 3.17 Work flow for ArcCHECK verification

3.7.5 Gamma pass limit set up for EPIQA calculation

After validation the performance of EPIQA in clinical VMAT plans in various organs and comparing the result with ArcCHECK then EPIQA was used as a QA device. The 70 VMAT plans (19 H&N, 17 Head, 16 Chest, 12 Pelvis 6 SRS/SBRT) of 228 arc fields, with 6 MV (50 cases) and 10 MV (20 cases) using EPIQA verification were evaluated to determine the gamma pass limit using confidence limit of $(100 - \text{mean}) + 1.96\sigma$. Mean and SD were calculated in term of percent gamma pass of 70 VMAT plan.

3.8 Outcome measurement

- Percent gamma pass for each case

Acquire by comparison dose distribution between EPIQA and TPS.

- Gamma pass limit

Confidence limit = $(100 - \text{mean}) + 1.96\sigma$

Gamma pass limit = $100 - \text{confidence limit}$

3.9 Data collection

After implementation and verification of EPIQA software, EPIQA was evaluated for VMAT pre-treatment verification in term of the percent pass between measured and calculated dose. The percent gamma pass, mean gamma value and SD gamma value were recorded.

3.10 Data analysis

The gamma evaluation of 3% dose difference and 3mm distance to agreement were used between measured and calculated dose.

3.11 Benefit of the study

1. Increasing confidence to use EPID as a QA device.
2. Reducing time workload.
3. The acceptable criteria of EPIQA for patient specific QA.

3.12 Ethical consideration

Although this study used only planning from patient not directly operated to the patient, the proposal was approved by the Ethics Committee of Faculty of Medicine, Chulalongkorn University.

CHAPTER IV

RESULTS

4.1 EPIQA portal dose validation of simple field technique

The EPIQA was evaluated for simple field technique in term of the percent gamma pass between measurement and dose calculation. The gamma evaluation of 3% dose difference and 3 mm distance to agreement were used. The measurement were performed for 6 and 10 MV photon beams in the field sizes of 2x2, 3x3, 4x4, 5x5, 5x15, 10x10, 20x20 cm², Dynamic wedge 30° with field size of 10x10 cm² and pyramid IMRT.

The Gaussian convolution of EPIQA software was undertaken for improving the percent gamma pass before the analysis was performed in EPIQA, measured images was processed by applying a Gaussian convolution. This blurred the EPID images. The degree of blurring was controlled with a Sigma parameter (given in [mm]). In this study, the resolution of EPID image was adjusted to the same as TPS which is 2.5 mm [25].

For 6 MV, the comparison between without (0.39 mm resolution) and with applying Gaussian convolution (2.5 mm resolution) illustrated that the percent gamma pass of EPIQA ranged from 85.87 to 99.66 and 95.25 to 99.79, the mean gamma ranged from 0.33 to 0.60 and 0.32 to 0.56. The SD gamma ranged from 0.18 to 0.36 and 0.19 to 0.32. The number of tested point ranged from 2704 to 262144, respectively, they are shown in table 4.1.

For 10 MV, the comparison between without (0.39 mm resolution) and with applying Gaussian convolution (2.5 mm resolution) illustrated that the percent gamma pass of EPIQA ranged from 62.24 to 97.71 and 99.64 to 100, the mean gamma ranged from 0.26 to 0.88 and 0.18 to 0.44, the SD gamma ranged from 0.25 to 0.46 and 0.17 to 0.25, the number of tested point ranged from 2704 to 262144, respectively, they are shown in table 4.2.

The result for both energies revealed that the percent passing increasing when the resolution of the EPID detector was the same as TPS.

Table 4.1 Percent gamma pass, Mean gamma, SD gamma and Tested points for 6MV with and without apply Gaussian convolution

Field size cm ²	% gamma pass		Mean gamma		SD gamma		Tested points
	0.39 mm	2.5 mm	0.39 mm	2.5 mm	0.39 mm	2.5 mm	
2x2	85.87	98.04	0.60	0.42	0.36	0.32	2704
3x3	95.51	98.42	0.52	0.46	0.27	0.21	6084
4x4	91.06	99.42	0.48	0.37	0.32	0.22	10816
5x5	99.11	98.88	0.55	0.56	0.25	0.19	16384
5x15	99.13	99.38	0.33	0.32	0.24	0.20	49152
10x10	99.42	99.12	0.52	0.45	0.22	0.21	65536
20x20	99.66	99.79	0.34	0.32	0.18	0.22	262144
EDW 30	98.12	95.25	0.46	0.49	0.23	0.24	65536
Pyramid IMRT	94.93	95.57	0.33	0.33	0.32	0.29	196812

Table 4.2 Percent gamma pass, Mean gamma, SD gamma and Tested points for 10 MV with and without apply Gaussian convolution

Field size cm ²	% gamma pass		Mean gamma		SD gamma		Tested point
	0.39 mm	2.5 mm	0.39 mm	2.5 mm	0.39 mm	2.5m m	
2x2	62.24	100.00	0.88	0.36	0.42	0.22	2704
3x3	73.62	99.67	0.70	0.31	0.46	0.23	6084
4x4	87.76	99.72	0.60	0.44	0.43	0.25	10816
5x5	83.87	99.93	0.53	0.26	0.45	0.20	16384
5x15	91.89	99.90	0.46	0.29	0.34	0.19	49152
10x10	96.02	99.92	0.29	0.32	0.30	0.19	65536
20x20	97.71	100.00	0.26	0.22	0.25	0.18	262144
EDW 30	96.80	99.64	0.26	0.18	0.30	0.17	65536
Pyramid IMRT	84.26	99.69	0.62	0.44	0.37	0.20	196812

The example of the comparison of beam profile measured by the measurement devices (EPID) and calculated from Eclipse treatment planning for both 6 and 10 MV photon beams are shown in figure 4.1-4.4 for $2 \times 2 \text{ cm}^2$, 4.5-4.8 for $10 \times 10 \text{ cm}^2$ and 4.9-4.12 for Pyramid IMRT.

The screen capture in figure 4.1-4.12 illustrated the following information:

- a) Dose matrix window, 1st data set(Eclipse dose)
- b) Gamma analysis matrix window
- c) Dose matrix, 2nd data set(Portal vision dose)
- d) Profile display in x direction (left-right) for both dose matrices
- e) Profile display in y direction (feet-head) for both dose matrices
- f) Display of histogram and statistics for the gamma analysis matrix window

For the beam profiles, the measurement data represented in green line and the calculated dose represented in pink line. EPID showed slightly higher response than calculated dose for $2 \times 2 \text{ cm}^2$ and showed slightly lower response than calculated dose for $10 \times 10 \text{ cm}^2$ and Pyramid IMRT. While applying Gaussian convolution, EPID showed good agreement with calculated dose for $2 \times 2 \text{ cm}^2$, $10 \times 10 \text{ cm}^2$ and Pyramid IMRT. They were improved after matching the resolution.

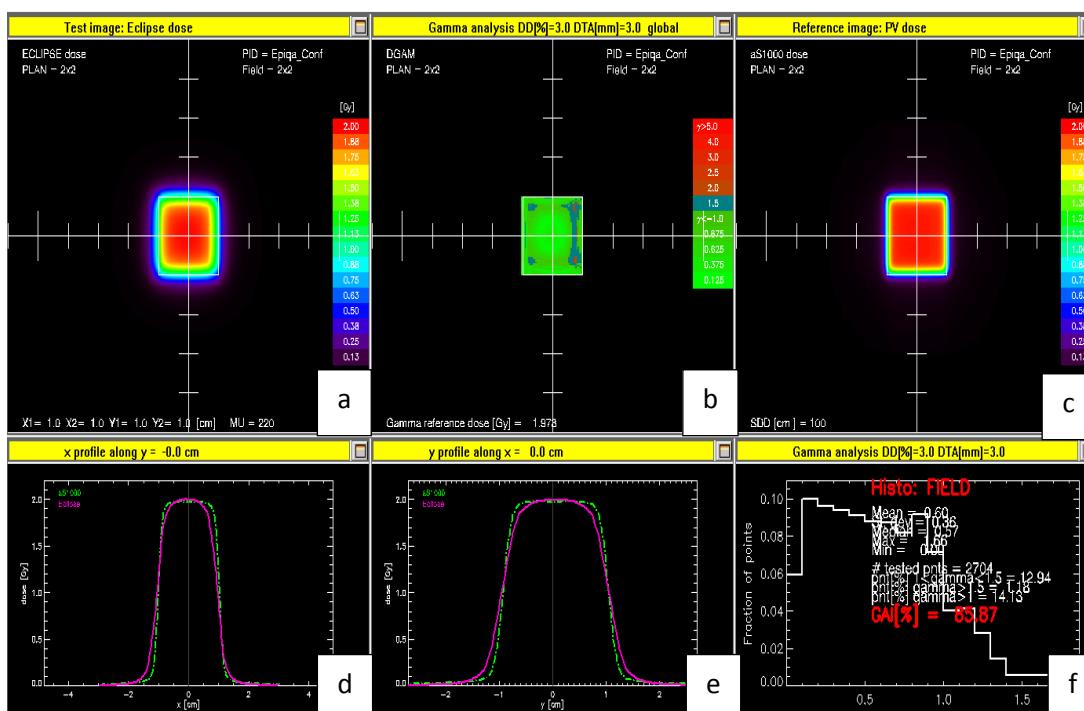


Figure 4.1 The example of EPIQA data for open field size of $2 \times 2 \text{ cm}^2$ 6 MV without convolution compared with TPS in criteria of 3%/3mm.

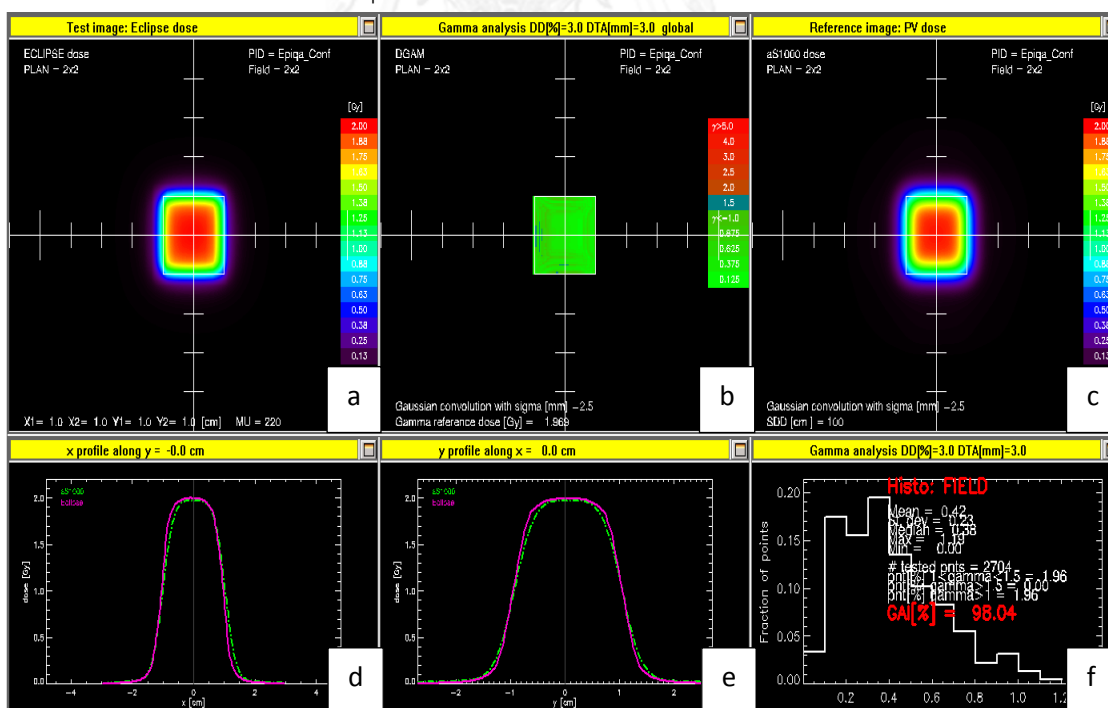


Figure 4.2 The example of EPIQA data for open field size of $2 \times 2 \text{ cm}^2$ 6 MV with Gaussian convolution 2.5 mm compared with TPS in criteria of 3%/3mm

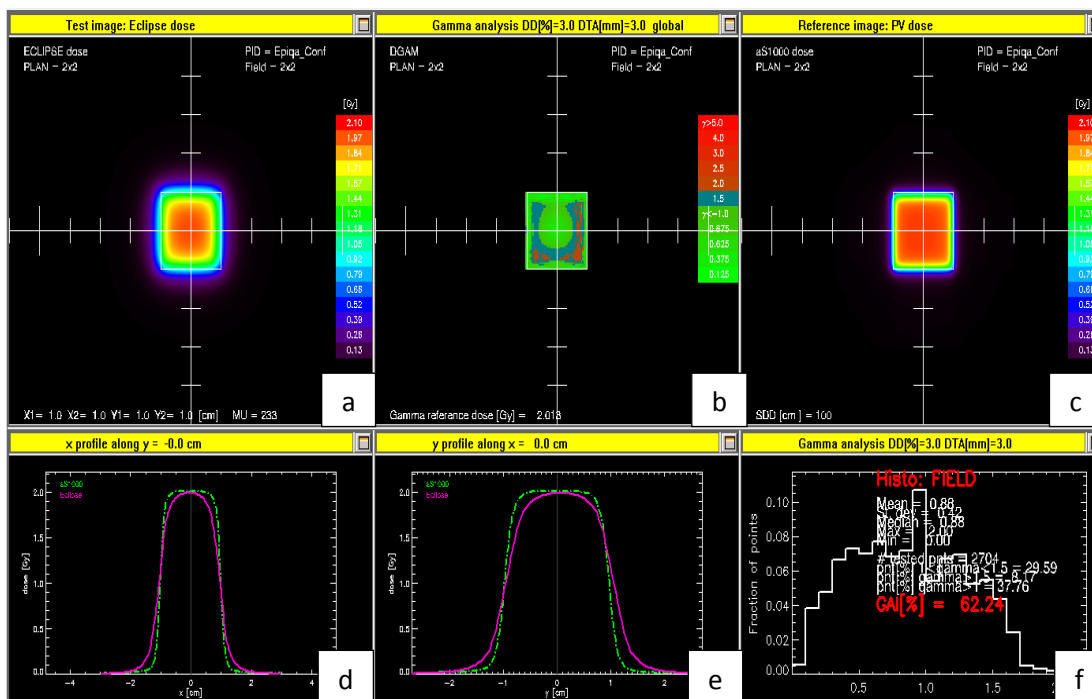


Figure 4.3 The example of EPIQA data for open field size of $2 \times 2 \text{ cm}^2$ 10 MV without convolution compared with TPS in criteria of 3%/3mm

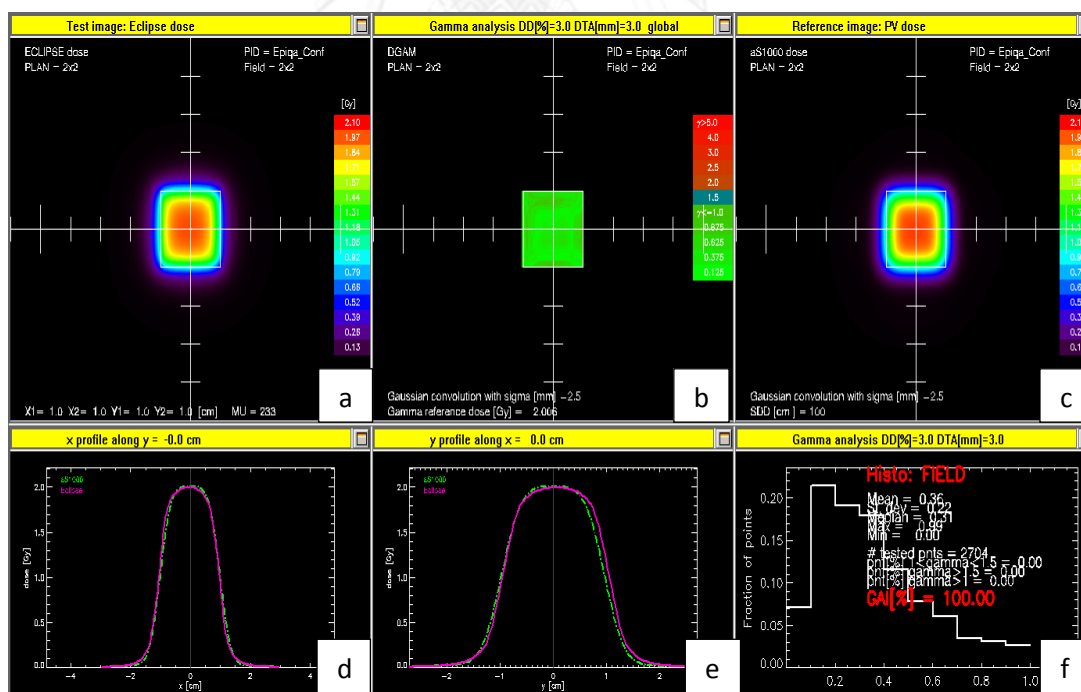


Figure 4.4 The example of EPIQA data for open field size of $2 \times 2 \text{ cm}^2$ 10 MV with Gaussian convolution 2.5 mm compared with TPS in criteria of 3%/3mm

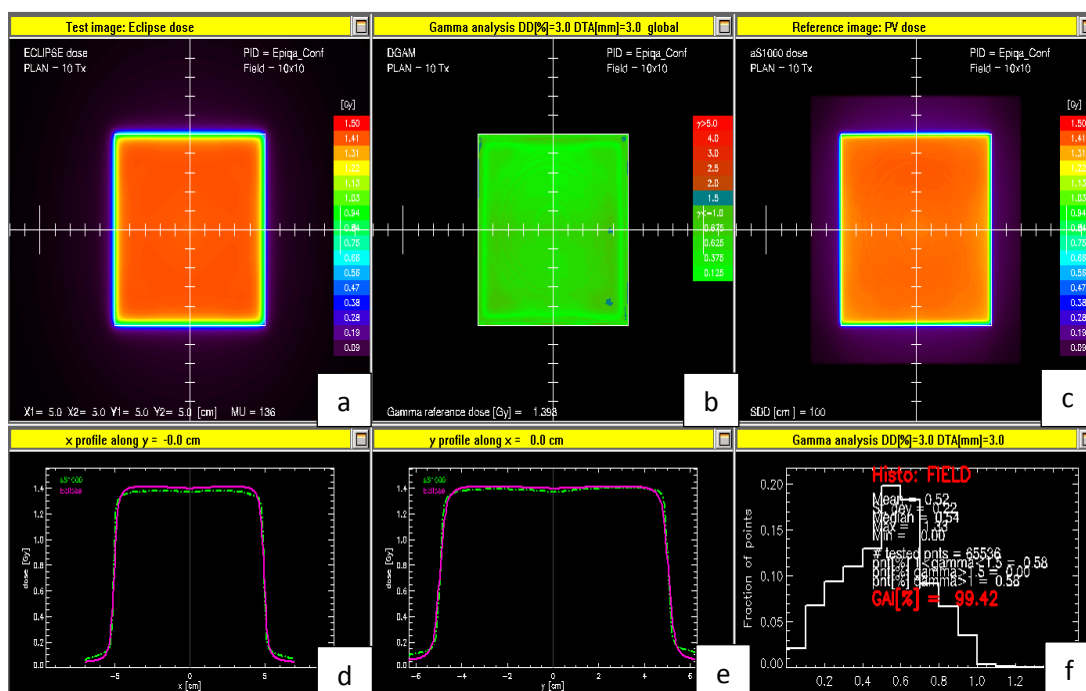


Figure 4.5 The example of EPIQA data for open field size of $10 \times 10 \text{ cm}^2$ 6 MV without convolution compared with TPS in criteria of 3%/3mm.

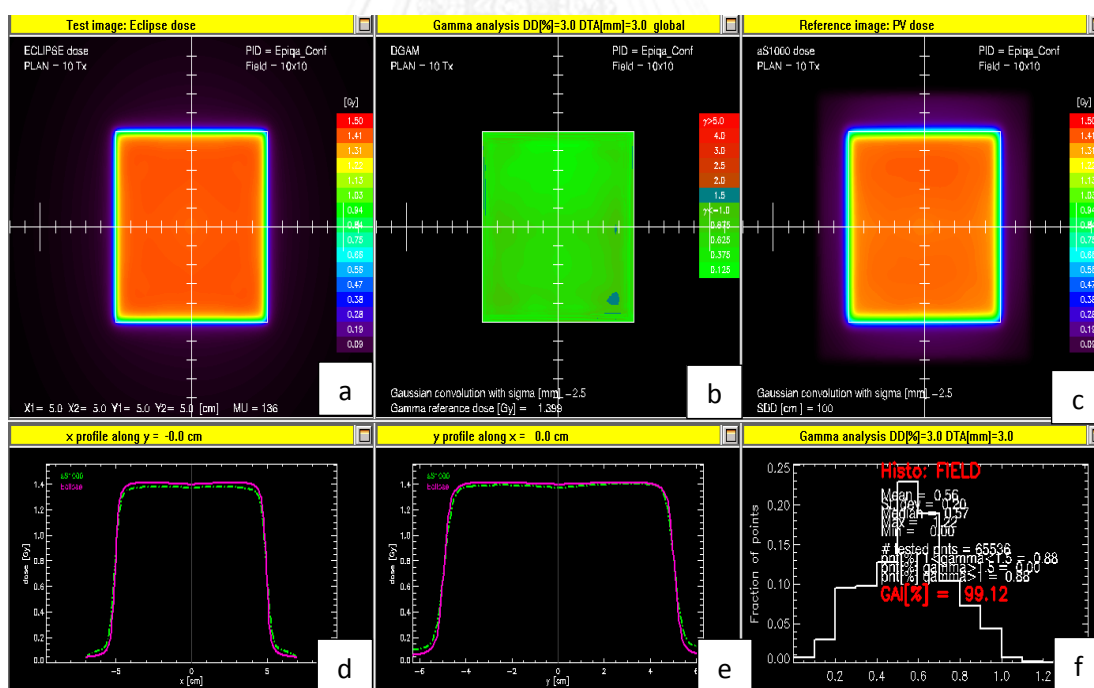


Figure 4.6 The example of EPIQA data for open field size of $10 \times 10 \text{ cm}^2$ 6 MV with Gaussian convolution 2.5 mm compared with TPS in criteria of 3%/3mm.

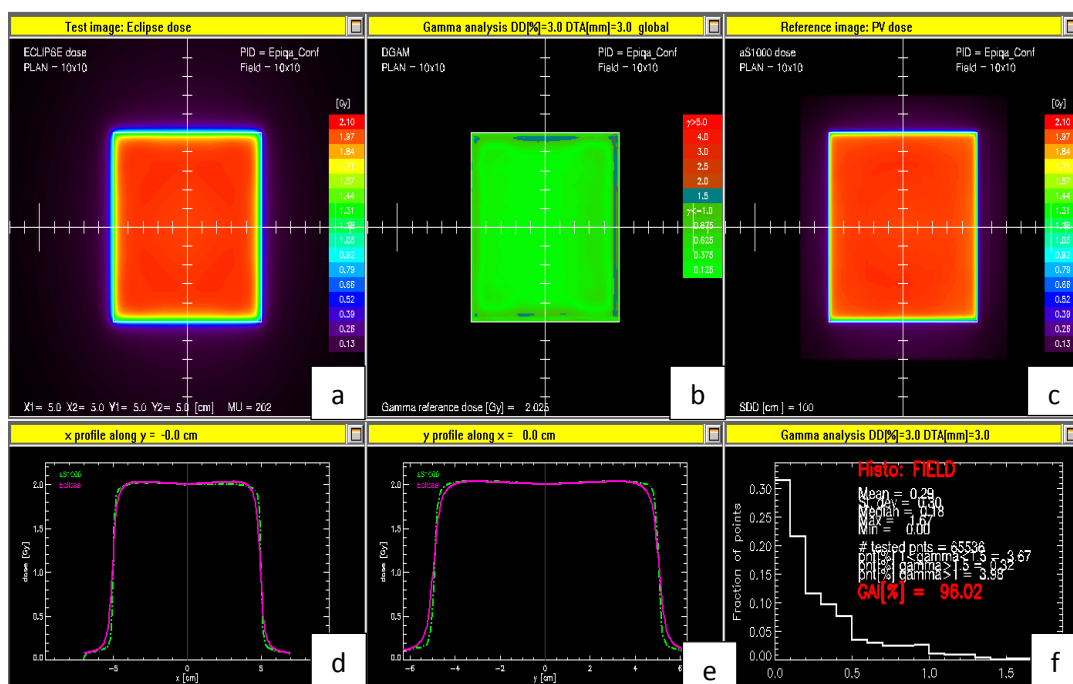


Figure 4.7 The example of EPIQA data for open field size of $10 \times 10 \text{ cm}^2$ 10 MV without convolution compared with TPS in criteria of 3%/3mm.

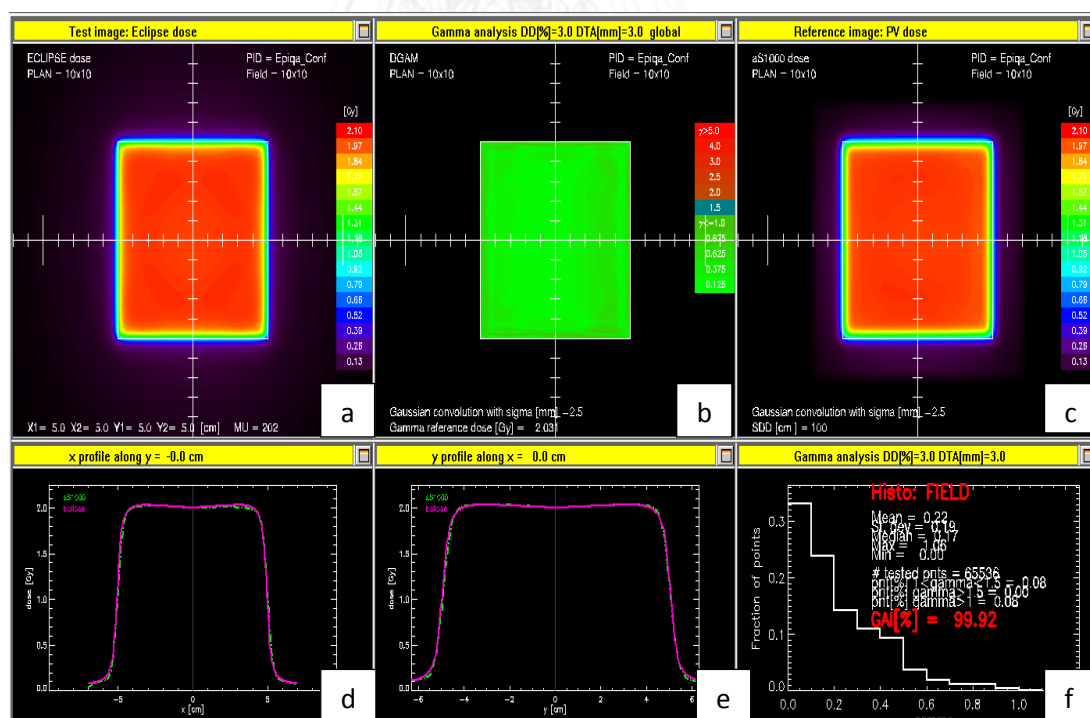


Figure 4.8 The example of EPIQA data for open field size of $10 \times 10 \text{ cm}^2$ 10 MV with Gaussian convolution 2.5 mm compared with TPS in criteria of 3%/3mm.

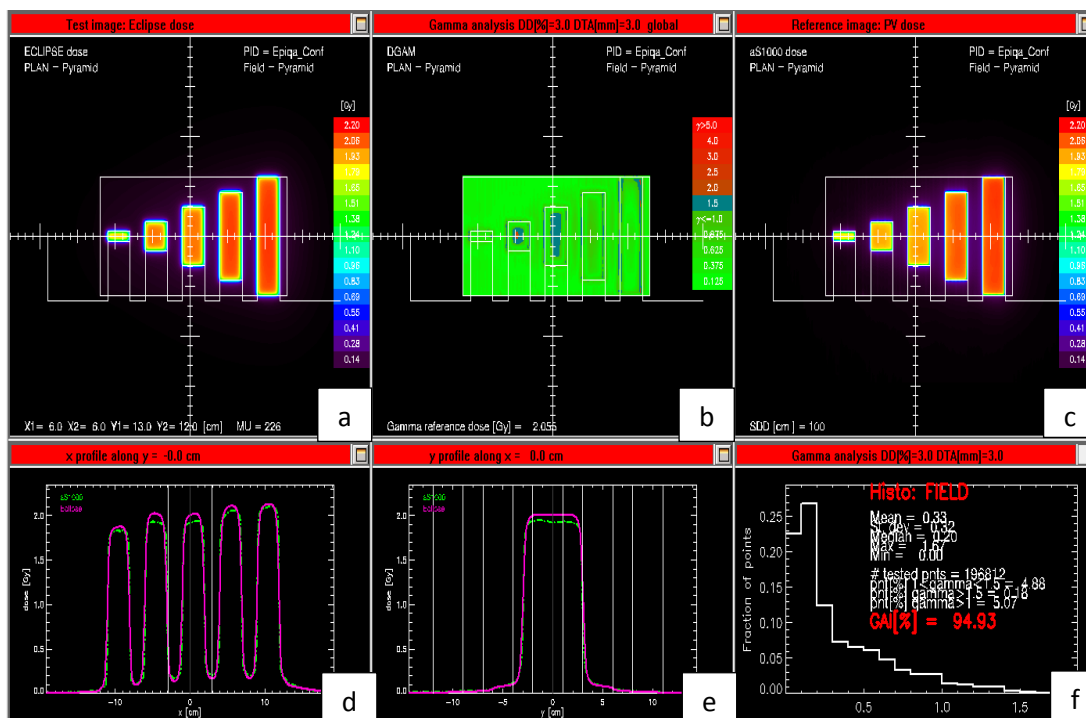


Figure 4.9 The example of EPIQA data for Pyramid IMRT of 6 MV without convolution compared with TPS in criteria of 3%/3mm

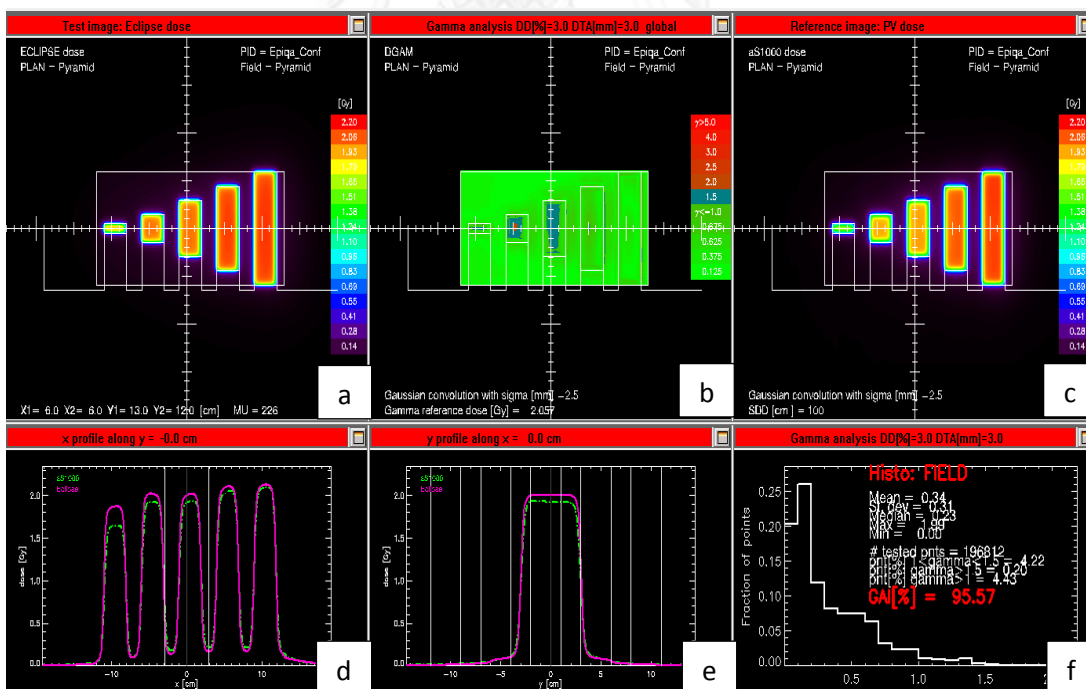


Figure 4.10 The example of EPIQA data for Pyramid IMRT of 6 MV with Gaussian convolution 2.5 mm compared with TPS in criteria of 3%/3mm

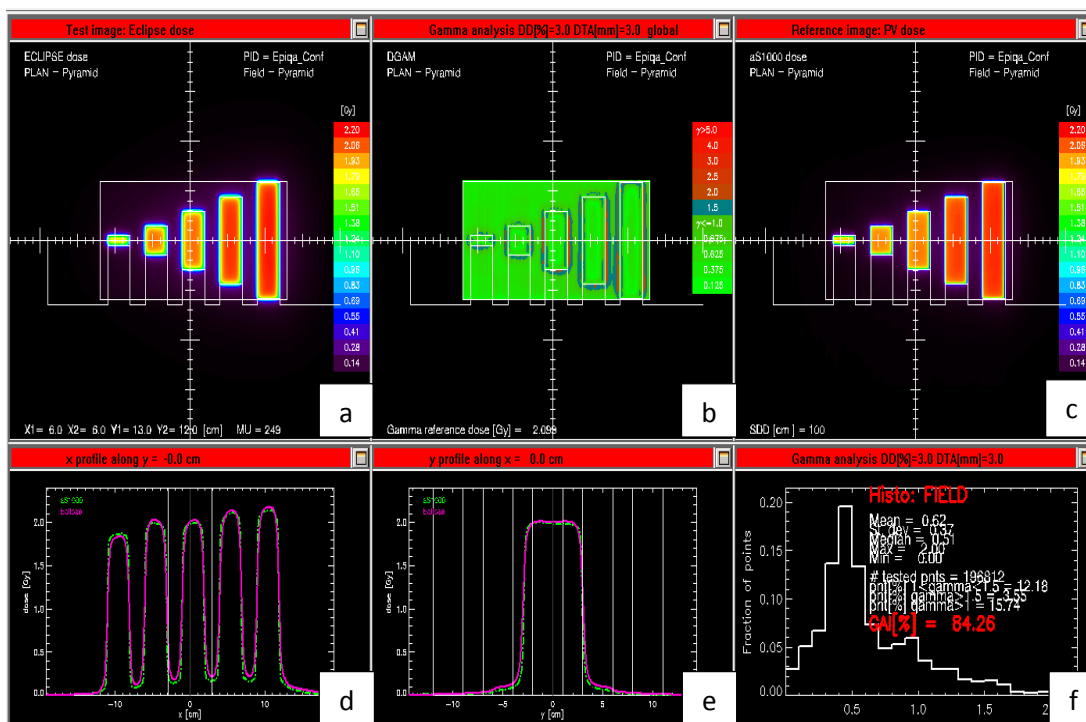


Figure 4.11 The example of EPIQA data for Pyramid IMRT of 10 MV without convolution compared with TPS in criteria of 3%/3mm

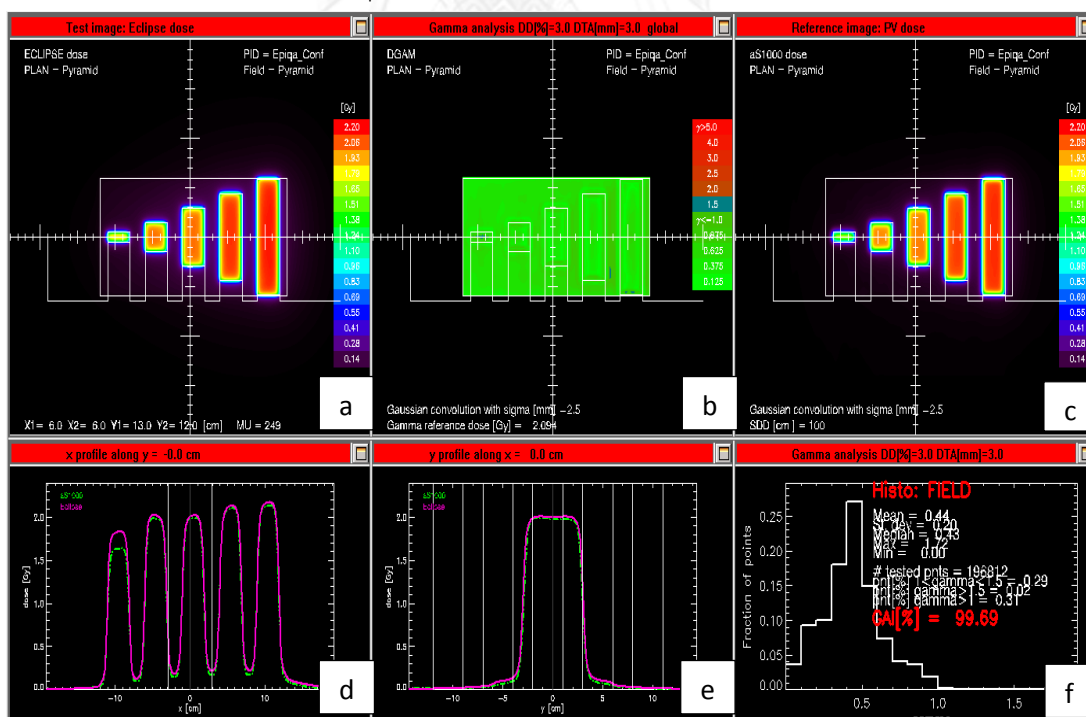


Figure 4.12 The example of EPIQA data for Pyramid IMRT of 10 MV with Gaussian convolution 2.5 mm compared with TPS in criteria of 3%/3mm

4.2 Clinical VMAT plans

After evaluation for the accuracy of the simple techniques in open, wedge fields and pyramid IMRT, the clinical plan were performed. The EPIQA dose was compared with ArcCHECK dose measurements for 43 VMAT plan in term of percent gamma pass in 3%/3mm criteria. The results of percentage passing separated in each treatment site are shown in table 4.4, 4.6, 4.8 and 4.10 for head, head and neck, chest and pelvis, respectively.

4.2.1 Head region

A. EPIQA

Eleven VMAT plans were selected for head region. The analyzed data for 11 cases in head region by EPIQA are shown in table 4.3. The percent gamma pass in EPIQA were evaluated arc by arc and the combined of all measurements were reported. The average percent gamma pass was 99.55 ± 0.36 (98.81 to 100.00 range). The average of mean gamma value was 0.24 ± 0.08 (0.00 to 0.34 range). The tested points were 64964 ± 33663 (10816 to 115620 range).

Table 4.3 The data analysis for 11 cases in head region by EPIQA

No. of cases	Arc1	Arc2	Arc3	Average \pm SD	Mean gamma	Tested points
1	99.72	99.06	98.71	99.16 \pm 0.51	0.27	115620
2	99.74	99.89	99.02	99.55 \pm 0.47	0.27	47380
3	98.89	99.93	97.60	98.81 \pm 1.17	0.27	55683
4	99.95	99.96	100	99.97 \pm 0.03	0.24	27720
5	99.86	99.23	99.56	99.55 \pm 0.32	0.25	72192
6	100.00	100.00	100.00	100.00 \pm 0.00	0.00	55808
7	99.92	99.9	99.92	99.91 \pm 0.01	0.23	41400
8	99.93	99.47	99.89	99.76 \pm 0.25	0.34	109906
9	99.59	99.99	99.04	99.54 \pm 0.48	0.26	98560
10	99.8	99.3	98.87	99.32 \pm 0.47	0.27	79524
11	99.08	99.9	99.71	99.53 \pm 0.43	0.26	10816
Average \pm SD				99.55 \pm 0.36	0.24 \pm 0.08	64964 \pm 33663

The screen captures for VMAT treatment plan in head region using EPIQA software are shown in figure 4.13, 4.14 and 4.15.

The screen capture in figure 4.13, 4.14 and 4.15 illustrated the following information:

- Eclipse treatment planning dose calculation
- Gamma analysis matrix window
- Portal vision dose measurement
- Profile display in x direction (left-right) for both dose matrices
- Profile display in y direction (feet-head) for both dose matrices
- Display of histogram and statistics for the gamma analysis matrix window

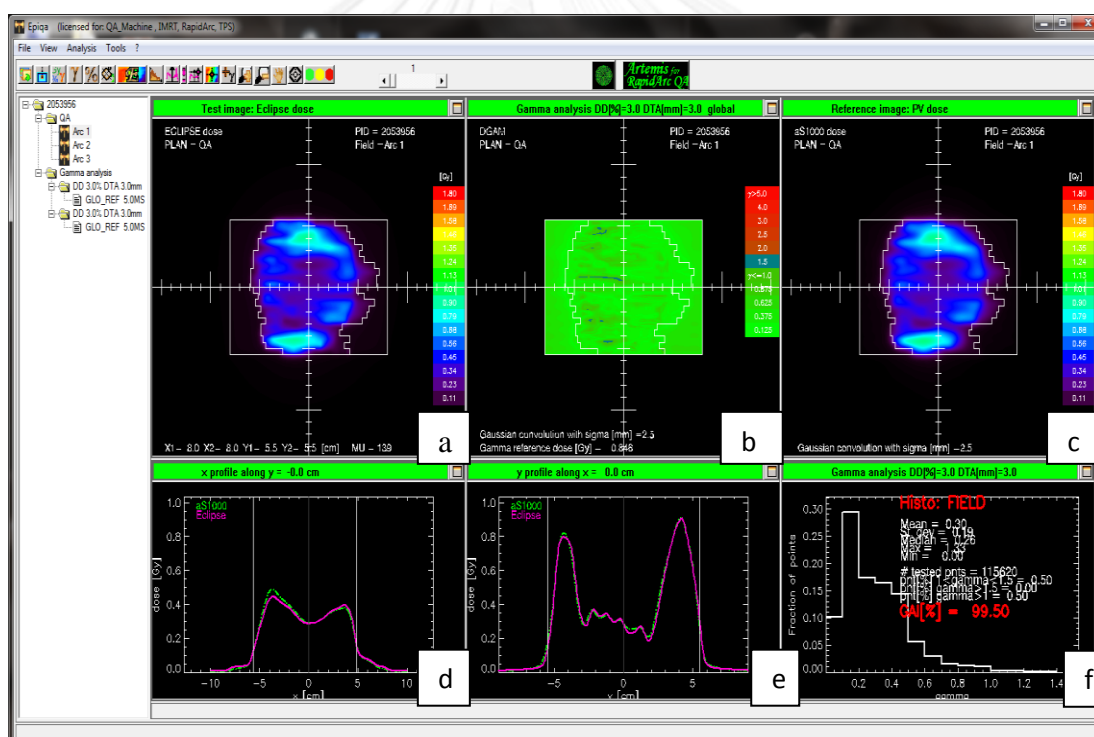


Figure 4.13 The examples of EPIQA data for head region compared with TPS in criteria of 3%/3mm (Arc 1)

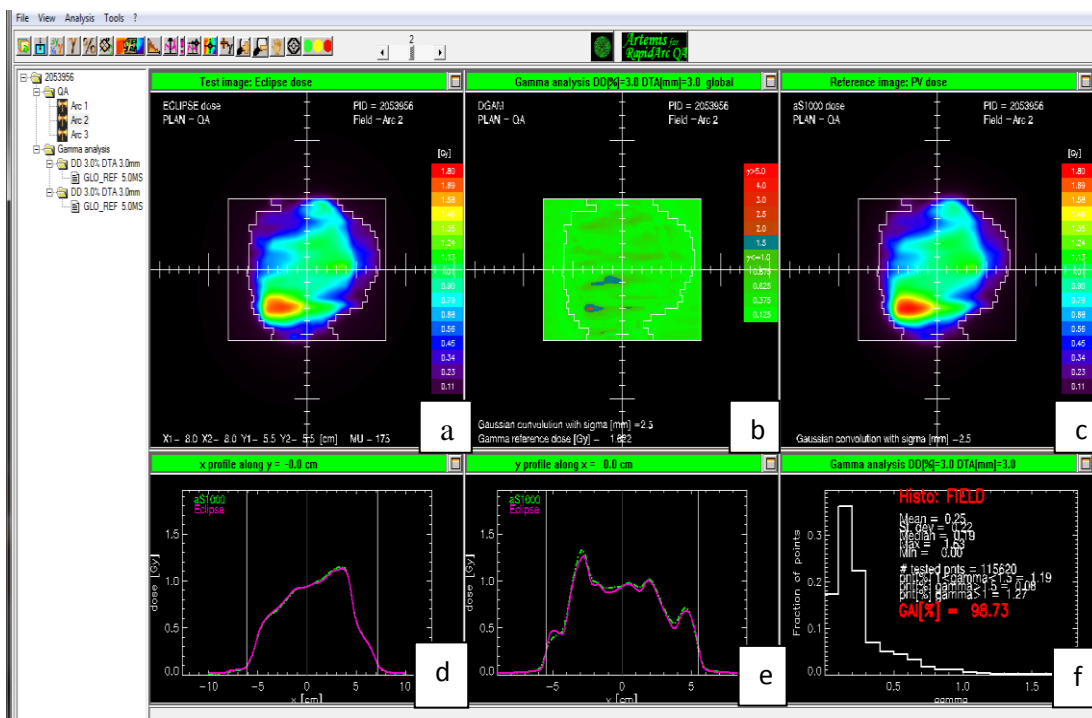


Figure 4.14 The examples of EPIQA data for head region compared with TPS in criteria of 3%/3mm (Arc 2)

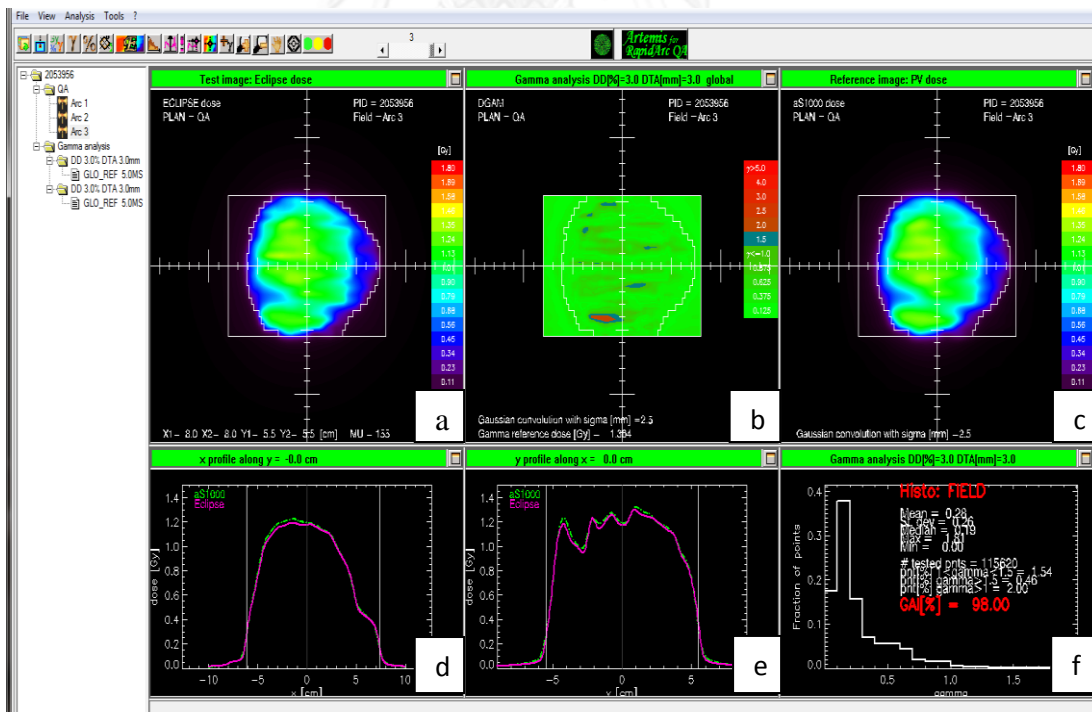


Figure 4.15 The examples of EPIQA data for head region compared with TPS in criteria of 3%/3mm (Arc 3)

B. EPIQA Comparison with ArcCHECK

The average percentage passing were 99.55 ± 0.36 (98.81 to 100 range) and 99.08 ± 0.67 (97.9 to 100 range) for EPIQA and ArcCHECK, respectively, they are shown in table 4.4 The bar graph illustrated the comparison of percent gamma pass between EPIQA and ArcCHECK is shown in figure 4.16.

Table 4.4 The comparison of percent gamma pass between EPIQA and ArcCHECK in head region

No. of cases	Percent gamma pass	
	EPIQA	ArcCHECK
1	99.16	99.50
2	99.55	98.50
3	98.81	98.90
4	99.97	97.90
5	99.55	100.00
6	100.00	99.30
7	99.91	99.00
8	99.76	99.50
9	99.54	99.00
10	99.32	98.30
11	99.53	100.00
Average \pm SD	99.55 ± 0.36	99.08 ± 0.67

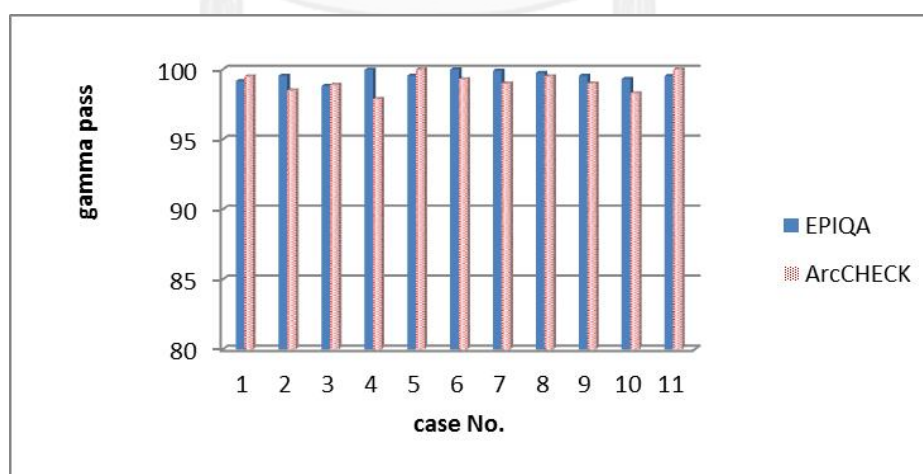


Figure 4.16 The comparison of the percent gamma pass between EPIQA and ArcCHECK for VMAT plans in head region.

4.2.2 Head and Neck region

A. EPIQA

Ten VMAT plans were selected for head and neck region. The analyzed data for 10 cases in head and neck region by EPIQA are shown in table 4.5. The percent gamma pass in EPIQA were evaluated arc by arc and the combined of all measurements were reported. The average percent gamma pass was 98.92 ± 0.93 (96.51 to 99.80 range). The average of mean gamma value was 0.30 ± 0.03 (0.25 to 0.35 range). The tested points were 182670 ± 63344 (27720 to 240470 range)

Table 4.5 The data analysis for 10 cases in head and neck region by EPIQA

No. of cases	Arc1	Arc2	Arc3	Arc4	Average \pm SD	Mean gamma	Tested points
1	99.10	98.69	98.87	-	98.89 ± 0.21	0.35	188600
2	99.81	98.83	97.62	-	98.75 ± 1.10	0.30	225500
3	99.92	99.85	99.66	99.77	99.80 ± 0.11	0.28	204180
4	98.16	99.83	99.38	-	99.12 ± 0.86	0.28	27720
5	97.44	97.11	94.97	-	96.51 ± 1.34	0.33	240470
6	99.18	99.40	99.59	-	99.39 ± 0.21	0.30	220170
7	99.79	97.37	98.84	-	98.67 ± 1.22	0.29	193930
8	99.61	99.82	99.70	-	99.71 ± 0.11	0.25	121464
9	99.17	98.66	99.08	-	98.97 ± 0.27	0.29	188600
10	99.42	99.81	98.93	-	99.39 ± 0.44	0.28	216070
Average \pm SD					98.92 ± 0.93	0.30 ± 0.03	182670 ± 63344

The screen captures for VMAT treatment plan in head and neck region using EPIQA software are shown in figure 4.17, 4.18 and 4.19.

The screen capture in figure 4.17, 4.18 and 4.19 illustrated the following information:

- Eclipse treatment planning dose calculation
- Gamma analysis matrix window
- Portal vision dose measurement
- Profile display in x direction (left-right) for both dose matrices
- Profile display in y direction (feet-head) for both dose matrices
- Display of histogram and statistics for the gamma analysis matrix window

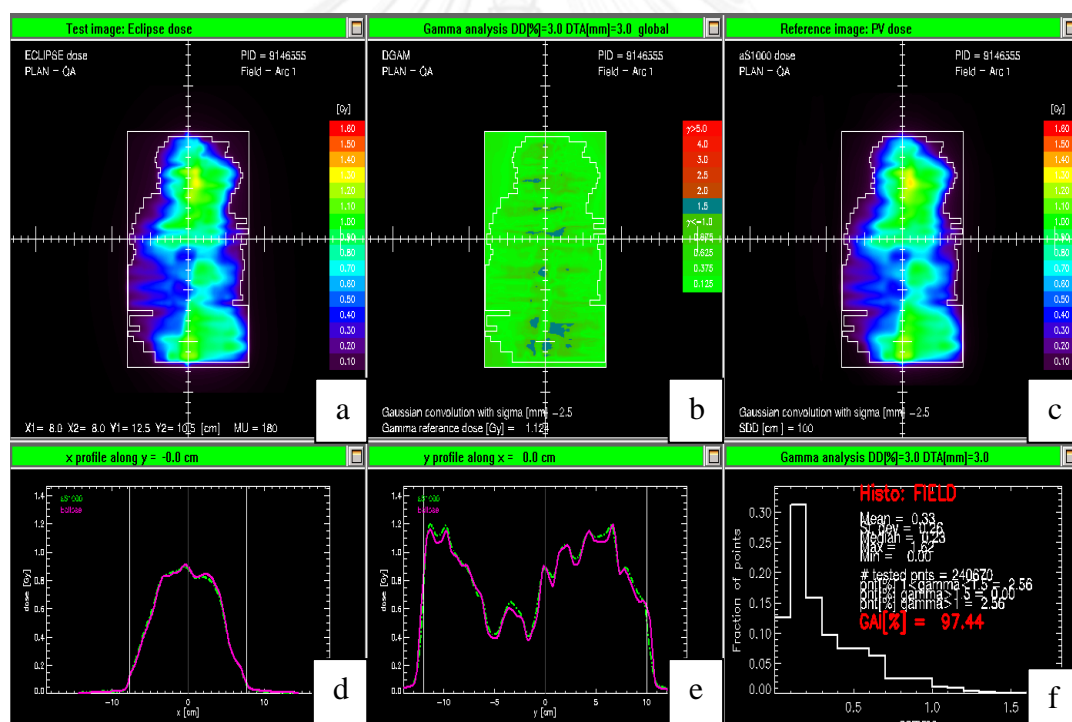


Figure 4.17 The examples of EPIQA data for head and neck region compared with TPS in criteria of 3%/3mm (Arc 1)

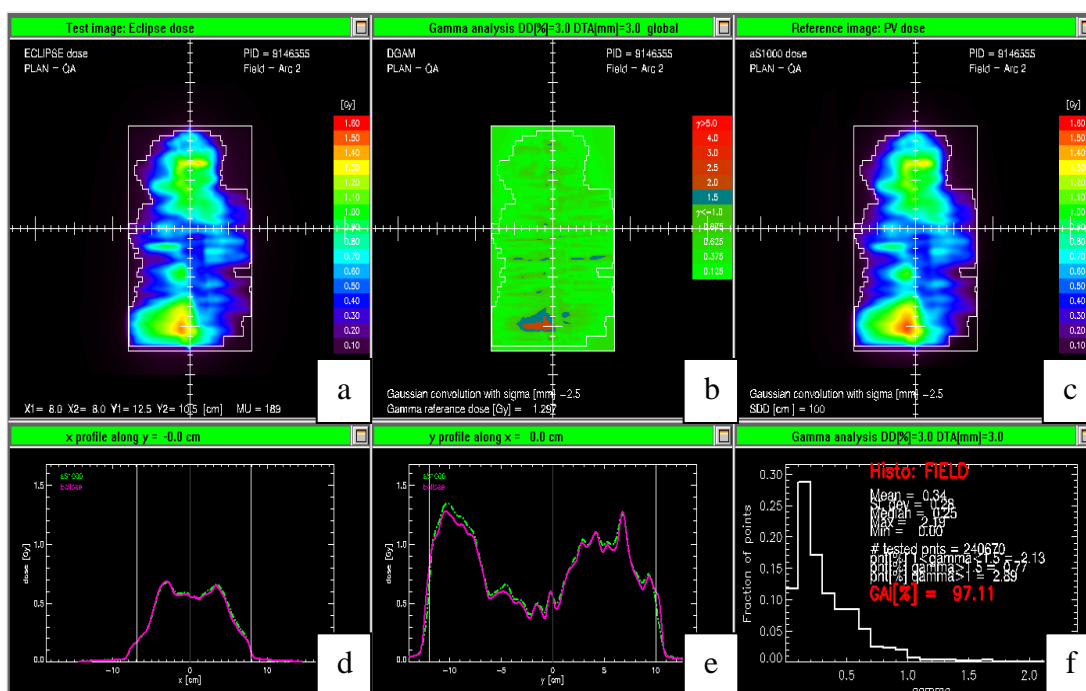


Figure 4.18 The examples of EPIQA data for head and neck region compared with TPS in criteria of 3%/3mm (Arc 2)

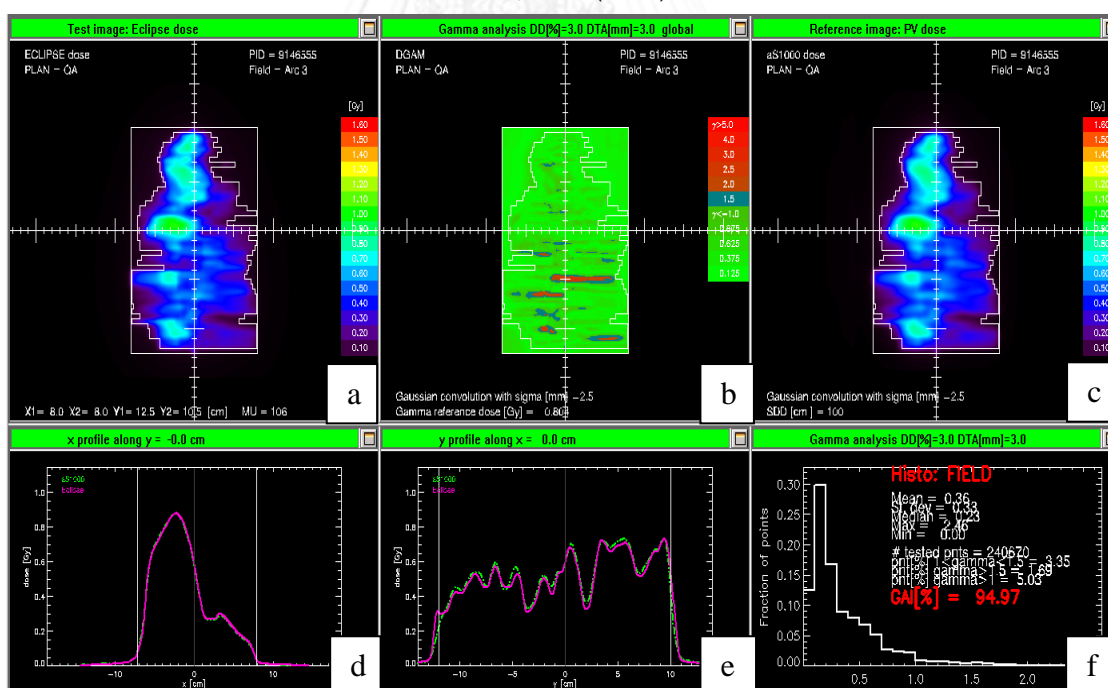


Figure 4.19 The examples of EPIQA data for head and neck region compared with TPS in criteria of 3%/3mm (Arc 3)

B. EPIQA Comparison with ArcCHECK

The average percentage passing were 98.92 ± 0.93 (96.51 to 99.80 range) and 98.25 ± 1.98 (93.30 to 100 range) for EPIQA and ArcCHECK, respectively, they are shown in table 4.6. The bar graph illustrated the comparison of percent gamma pass between EPIQA and ArcCHECK is shown in figure 4.20.

Table 4.6 The comparison of percent gamma pass between EPIQA and ArcCHECK in head and neck region.

No. of cases	Percent gamma pass	
	EPIQA	ArcCHECK
1	98.89	99.70
2	98.75	97.80
3	99.80	99.50
4	99.12	99.10
5	96.51	98.40
6	99.39	93.30
7	98.67	98.20
8	99.71	97.00
9	98.97	99.50
10	99.39	100.00
Average \pm SD	98.92 ± 0.93	98.25 ± 1.98

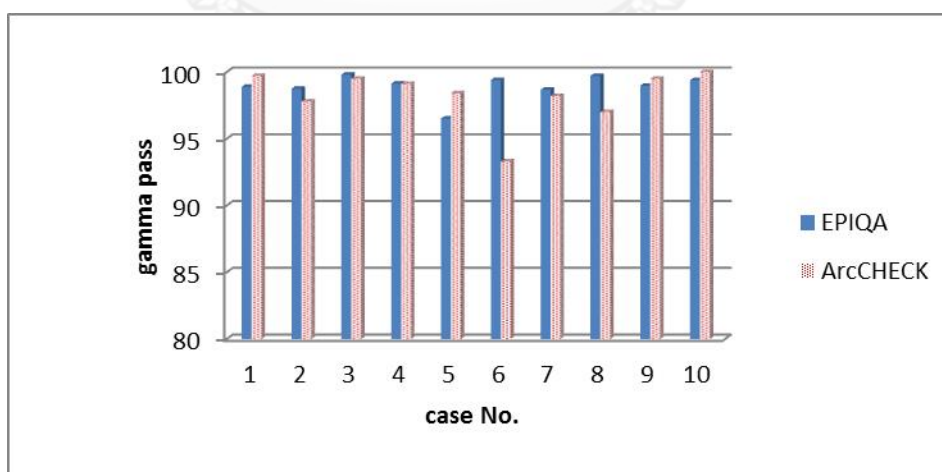


Figure 4.20 The Comparison of the percent gamma pass between EPIQA and ArcCHECK for VMAT plans in head and neck region

4.2.3 Chest region

A. EPIQA

Thirteen VMAT plans were selected for chest region. The analyzed data for 13 cases in chest region by EPIQA are shown in table 4.7. The percent gamma pass in EPIQA were evaluated arc by arc and the combined of all measurements were reported. The average percent gamma pass was 99.20 ± 0.55 (97.97 to 99.96 range). The average of mean gamma value was 0.31 ± 0.05 (0.21 to 0.40 range). The tested points were 121952 ± 65253 (52736 to 251330 range).

Table 4.7 The data analysis for 13 cases in chest region by EPIQA

No. of cases	Arc1	Arc2	Arc3	Arc4	Arc5	Average \pm SD	Mean gamma	Tested points
1	99.65	98.86	99.14	-	-	99.22 ± 0.40	0.31	251330
2	99.68	99.32	99.11	-	-	99.37 ± 0.29	0.30	125870
3	99.71	97.75	97.23	97.20	-	97.97 ± 1.16	0.30	171648
4	99.55	99.85	98.87	-	-	99.42 ± 0.50	0.25	109440
5	99.91	99.61	99.38	-	-	99.63 ± 0.27	0.30	135040
6	99.62	99.3	-	-	-	99.46 ± 0.23	0.37	82340
7	99.58	99.78	98.34	96.54	-	98.56 ± 1.49	0.36	209510
8	99.99	99.90	100.00	-	-	99.96 ± 0.06	0.21	23716
9	98.74	98.09	98.18	98.87	-	98.47 ± 0.39	0.40	152110
10	99.53	99.45	98.96	99.67	99.34	99.39 ± 0.27	0.32	60972
11	99.74	99.50	97.90	-	-	99.05 ± 1.00	0.25	68676
12	99.76	99.22	99.80	-	-	99.59 ± 0.32	0.29	52736
13	99.54	99.77	99.33	-	-	99.54 ± 0.22	0.36	141988
Average \pm SD						99.20 ± 0.55	0.31 ± 0.05	121952 ± 65253

The screen captures for VMAT treatment plan in chest region using EPIQA software are shown in figure 4.21, 4.22 and 4.23.

The screen capture in figure 4.21, 4.22 and 4.23 illustrated the following information:

- Eclipse treatment planning dose calculation
- Gamma analysis matrix window
- Portal vision dose measurement
- Profile display in x direction (left-right) for both dose matrices
- Profile display in y direction (feet-head) for both dose matrices
- Display of histogram and statistics for the gamma analysis matrix window

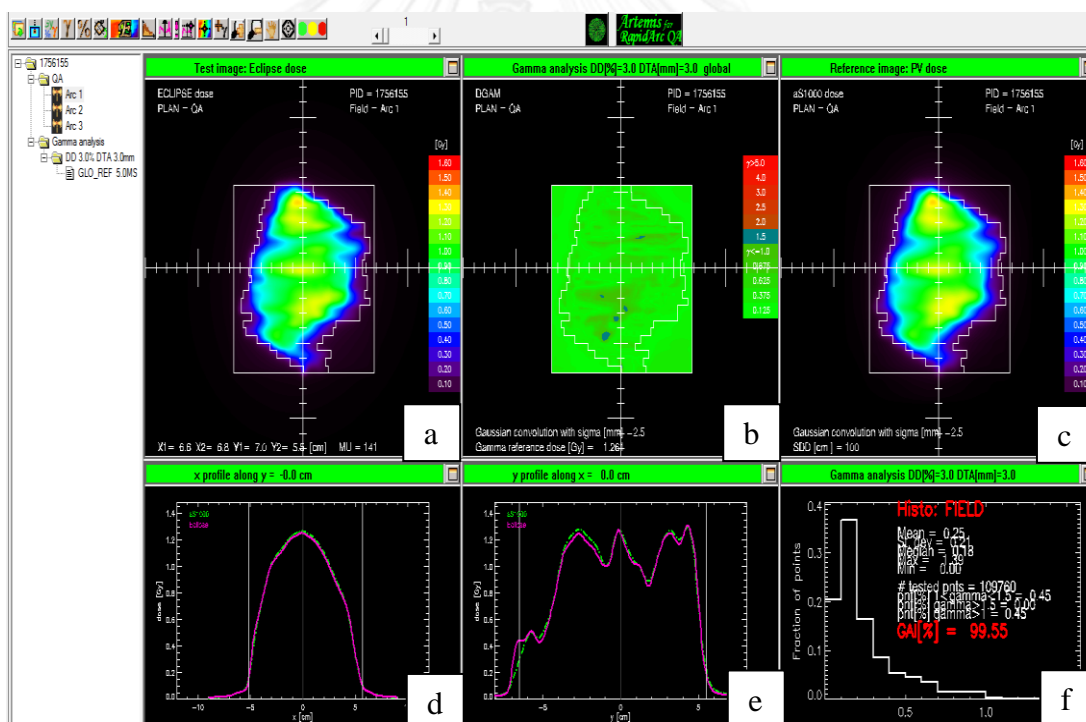


Figure 4.21 The examples of EPIQA data for chest region compared with TPS in criteria of 3%/3mm (Arc1)

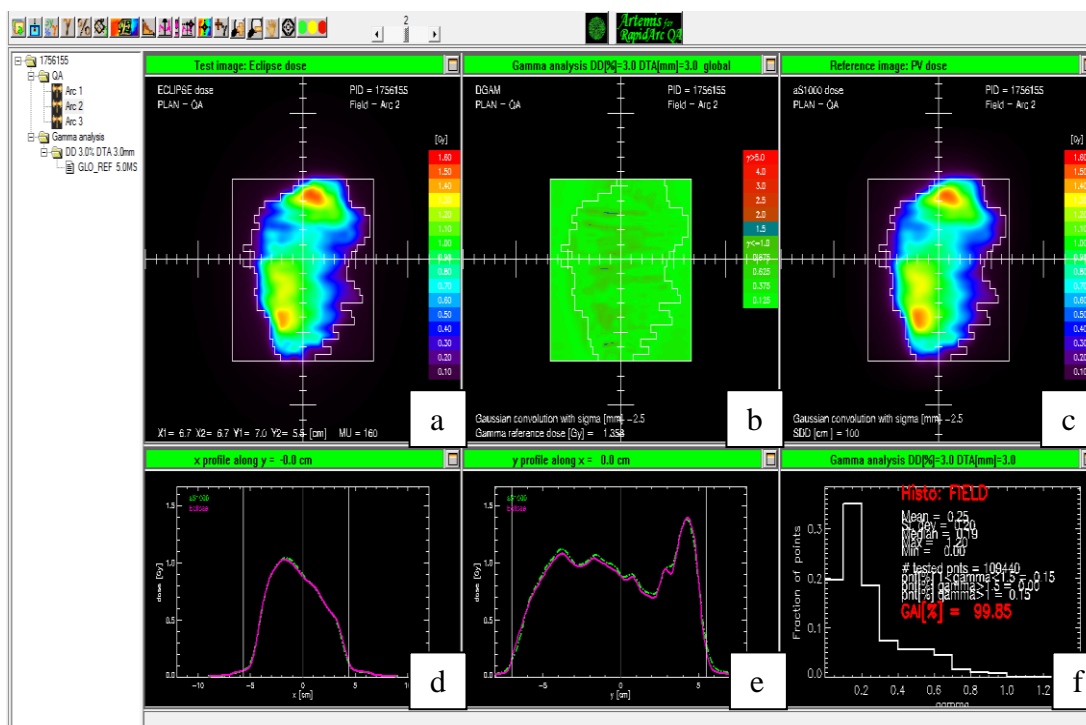


Figure 4.22 The examples of EPIQA data for chest region compared with TPS in criteria of 3%/3mm (Arc2)

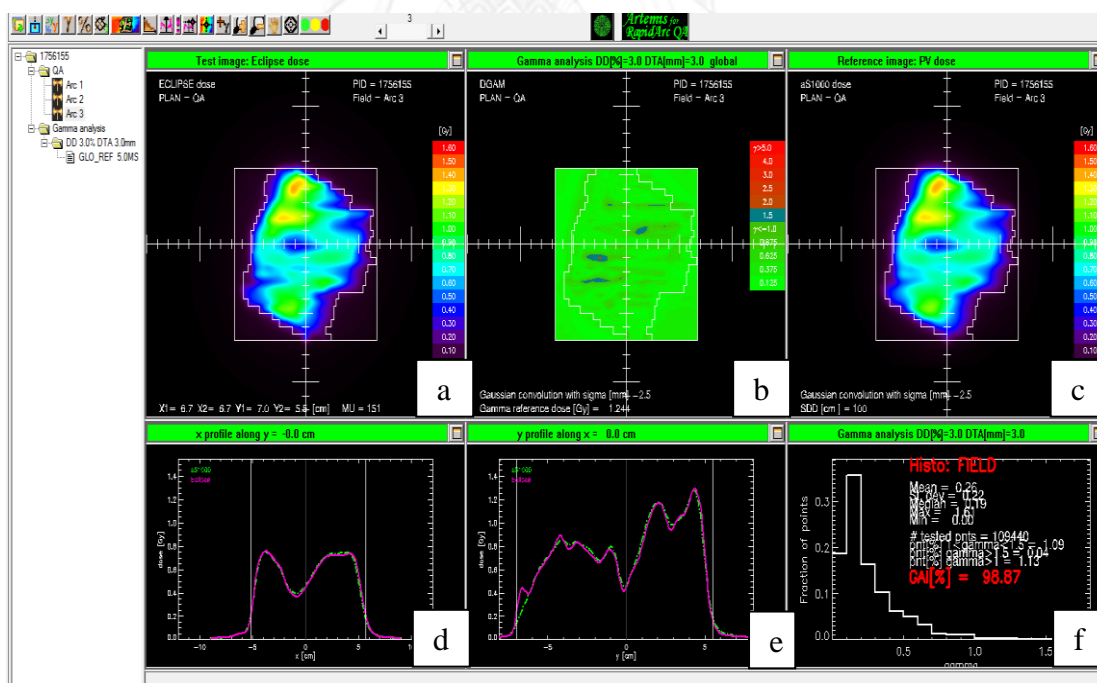


Figure 4.23 The examples of EPIQA data for chest region compared with TPS in criteria of 3%/3mm (Arc3)

B. EPIQA Comparison with ArcCHECK

The average percentage passing were 99.20 ± 0.55 (97.97 to 99.96 range) and 98.61 ± 0.81 (97.30 to 99.80 range) for EPIQA and ArcCHECK, respectively, they are shown in table 4.8. The bar graph illustrated the comparison of percent gamma pass between EPIQA and ArcCHECK is shown in figure 4.24

Table 4.8 The comparison of percent gamma pass between EPIQA and ArcCHECK in chest region

No. of cases	Percent gamma pass	
	EPIQA	ArcCHECK
1	99.22	99.60
2	99.37	98.10
3	97.97	97.90
4	99.42	99.10
5	99.63	99.40
6	99.46	99.80
7	98.56	99.40
8	99.96	97.60
9	98.47	98.90
10	99.39	98.40
11	99.05	97.30
12	99.59	98.40
13	99.54	98.00
Average \pm SD	99.20 ± 0.55	98.61 ± 0.81

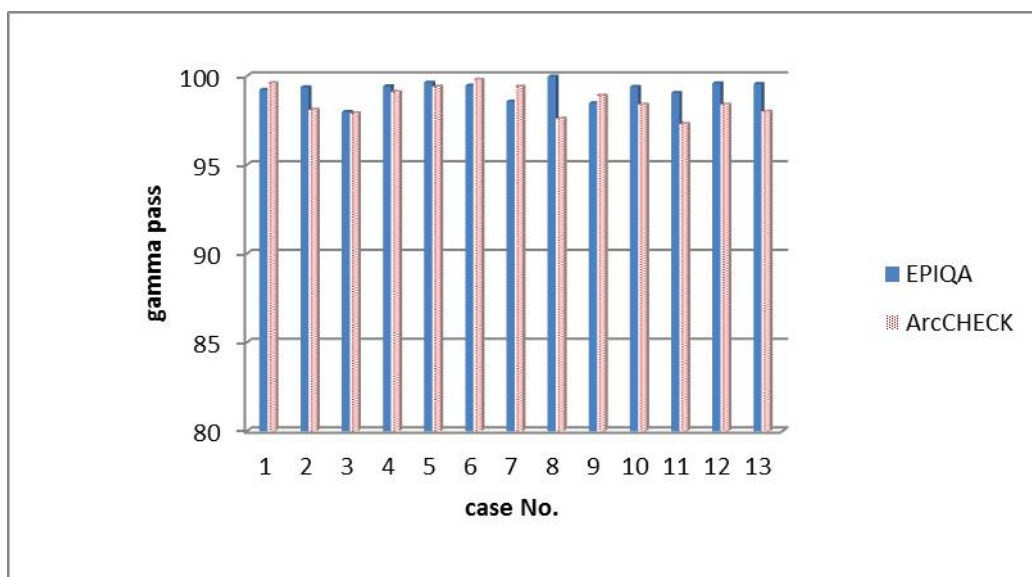


Figure 4.24 The Comparison of the percent gamma pass between EPIQA and ArcCHECK for VMAT plans in chest region

4.2.4 Pelvis region

A. EPIQA

Nine VMAT plans were selected for pelvis region. The analyzed data for 9 cases in pelvis region by EPIQA are shown in table 4.9. The percent gamma pass in EPIQA were evaluated arc by arc and the combined of all measurements were reported. The average percent gamma pass was 99.54 ± 0.37 (98.86 to 99.96 range). The average of mean gamma value was 0.31 ± 0.02 (0.29 to 0.35 range). The tested points were 123655 ± 68877 (60494 to 241080 range)

Table 4.9 The data analysis for 9 cases in pelvis region by EPIQA

No. of cases	Arc1	Arc2	Arc3	Average \pm SD	Mean gamma	Tested points
1	99.81	99.94	-	99.88 \pm 0.09	0.29	60494
2	99.50	99.65	99.19	99.44 \pm 0.23	0.31	118272
3	99.65	99.38	99.16	99.40 \pm 0.25	0.35	78848
4	100.00	100.00	99.89	99.96 \pm 0.06	0.31	100956
5	99.96	99.59	99.76	99.77 \pm 0.19	0.29	78950
6	99.84	97.97	98.77	98.86 \pm 0.94	0.30	241080
7	99.07	99.65	99.65	99.45 \pm 0.33	0.32	82955
8	99.81	98.99	99.25	99.35 \pm 0.42	0.31	241080
9	99.72	99.67	99.72	99.70 \pm 0.03	0.32	110264
Average \pm SD				99.54 \pm 0.37	0.31 \pm 0.02	123655 \pm 68877

The screen captures for VMAT treatment plan in pelvis region using EPIQA software are shown in figure 4.25, 4.26 and 4.27

The screen capture in figure 4.25, 4.26 and 4.27 illustrated the following information:

- Eclipse treatment planning dose calculation
- Gamma analysis matrix window
- Portal vision dose measurement
- Profile display in x direction (left-right) for both dose matrices
- Profile display in y direction (feet-head) for both dose matrices
- Display of histogram and statistics for the gamma analysis matrix window

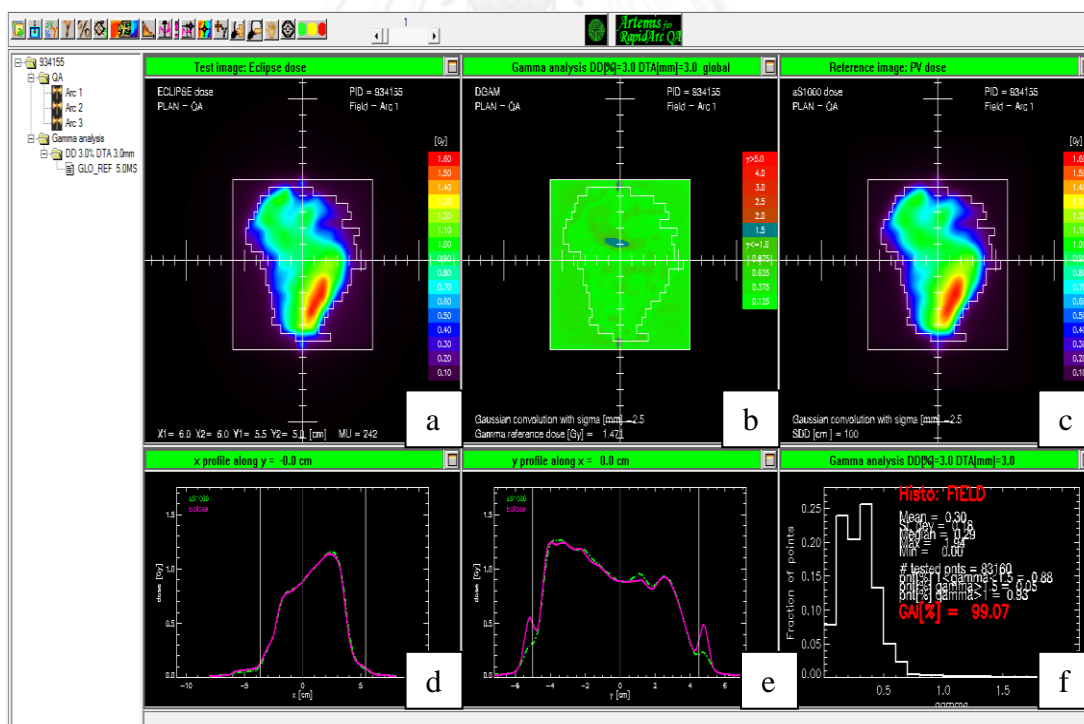


Figure 4.25 The examples of EPIQA data for pelvis region compared with TPS in criteria of 3%/3mm (Arc 1)

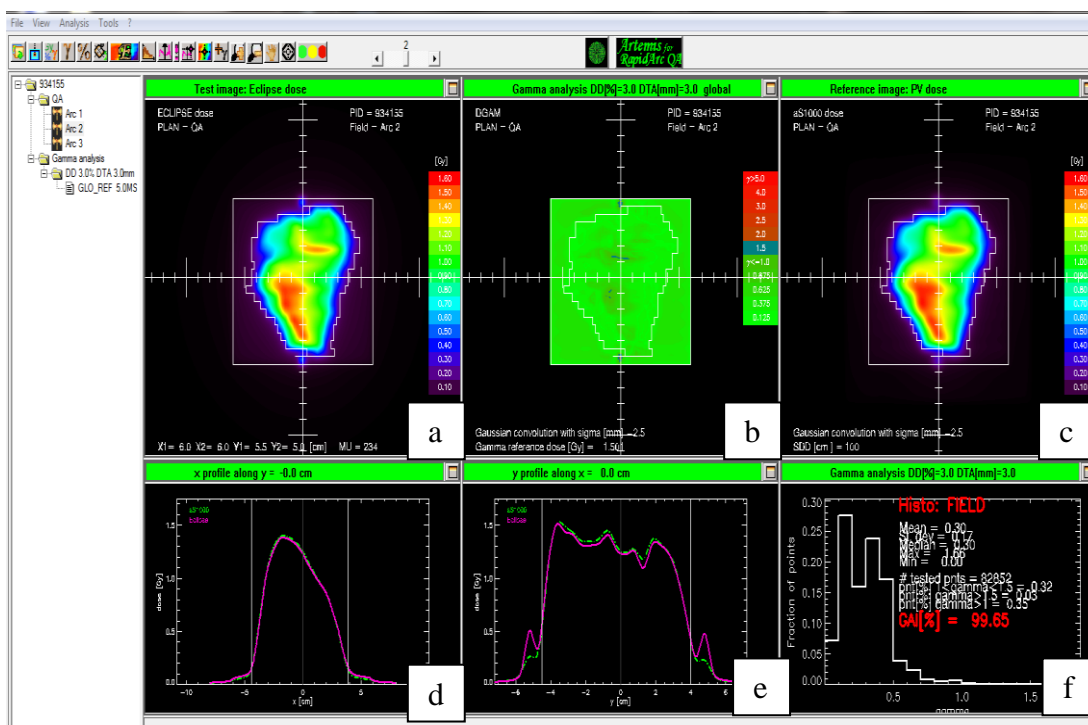


Figure 4.26 The examples of EPIQA data for pelvis region compared with TPS in criteria of 3%/3mm (Arc 2)

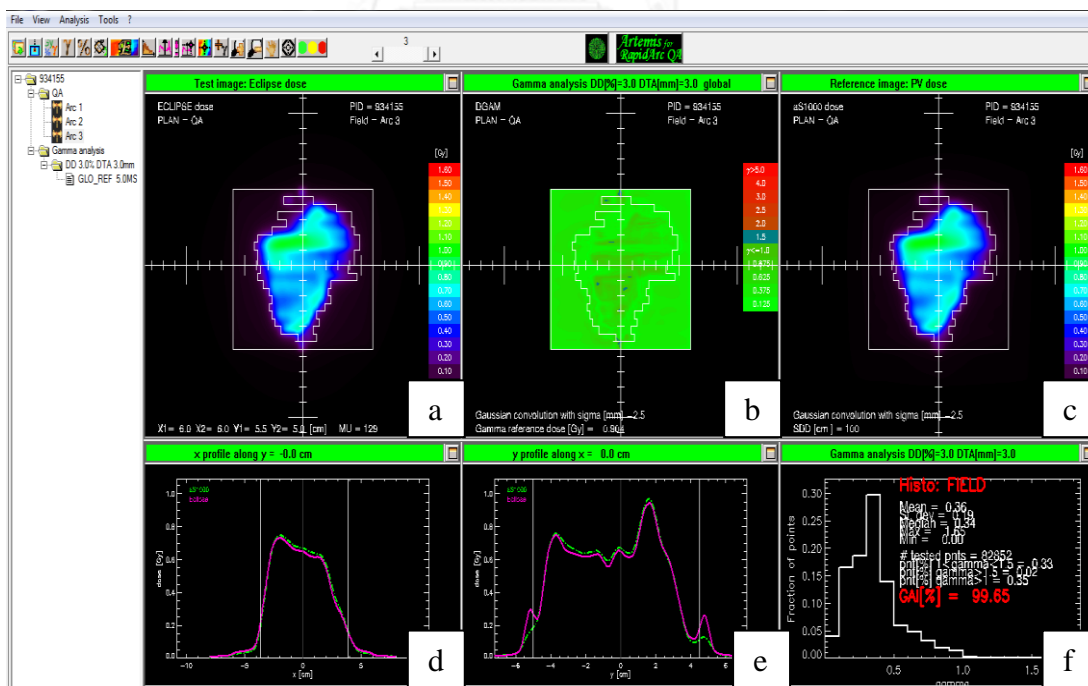


Figure 4.27 The examples of EPIQA data for pelvis region compared with TPS in criteria of 3%/3mm (Arc 3)

B. EPIQA Comparison with ArcCHECK

The average percentage passing were 99.54 ± 0.37 (98.86 to 99.96 ranged) and 98.81 ± 0.64 (97.90 to 99.70 ranged) for EPIQA and ArcCHECK, respectively, they are shown in table 4.10. The bar graph illustrated the comparison of percent gamma pass between EPIQA and ArcCHECK is shown in figure 4.28

Table 4.10 The comparison of percent gamma pass between EPIQA and ArcCHECK in pelvis region

No. of cases	Percent gamma pass	
	EPIQA	ArcCHECK
1	99.88	98.50
2	99.45	97.90
3	99.40	98.60
4	99.96	99.70
5	99.77	98.10
6	98.86	98.60
7	99.46	99.50
8	99.35	98.90
9	99.70	99.50
Average \pm SD	99.54 ± 0.37	98.81 ± 0.64

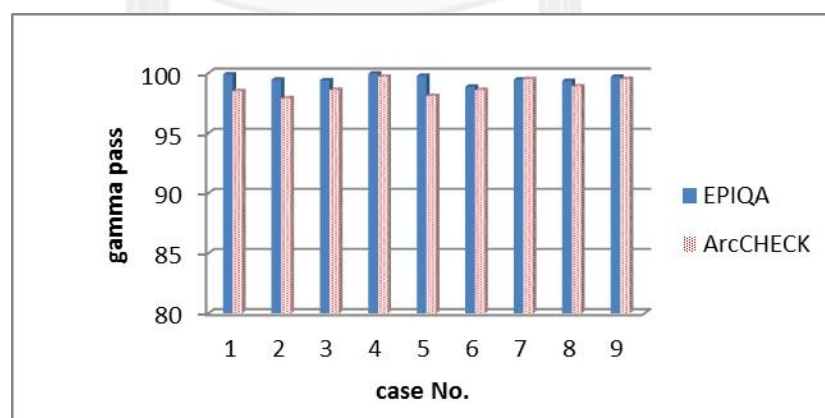


Figure 4.28 The Comparison of the percent gamma pass between EPIQA and ArcCHECK for VMAT plans in pelvis region

In conclusion for 43 VMAT plans, EPIQA and ArcCHECK demonstrated the average percent gamma pass with criteria 3%/3 mm of 99.29 ± 0.63 (96.51 to 100 range) and 98.69 ± 1.14 (93.3 to 100 range), respectively, the details are shown in table 4.11 and figure 4.29.

Table 4.11 The percent gamma pass for EPIQA and ArcCHECK in each treatment region

Treatment regions	EPIQA	ArcCHECK
Head	99.55 ± 0.36	99.08 ± 0.67
H&N	98.92 ± 0.93	98.25 ± 1.98
Chest	99.20 ± 0.55	98.61 ± 0.81
Pelvis	99.54 ± 0.37	98.81 ± 0.64
Total	99.29 ± 0.63	98.69 ± 1.14

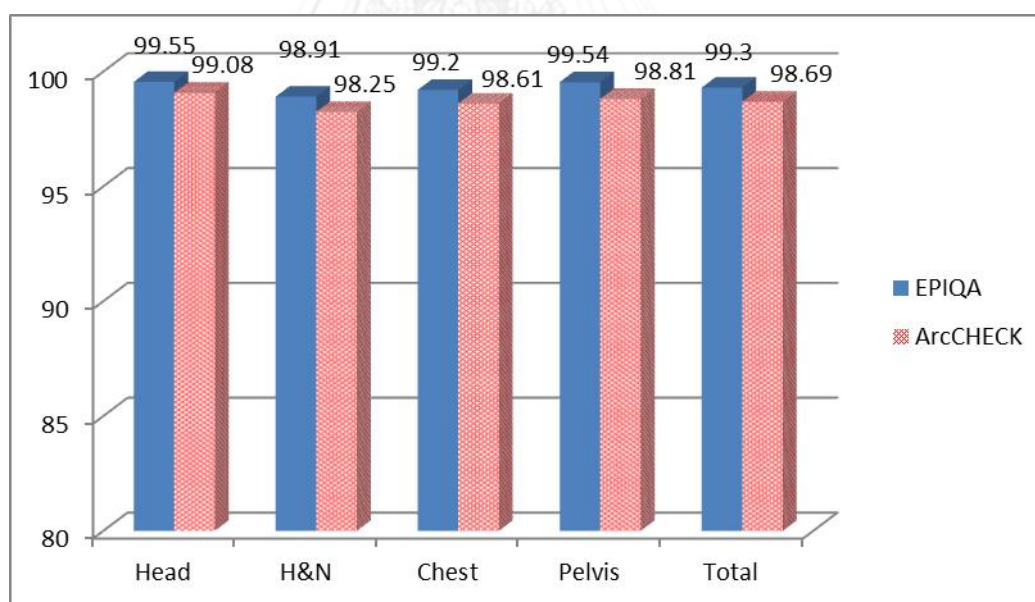


Figure 4.29 The Comparison of the percent gamma pass for EPIQA and ArcCHECK of VMAT plans in each treatment region

4.3 The correlation between percent gamma pass and modulation factor (MU/Gy)

The modulation factor is defined as number of MU delivered by Gy. The average of modulation factor were 2.54 ± 0.33 (2.02 to 3.03 range), 2.83 ± 0.53 (2.24 to 3.96 range), 2.70 ± 0.47 (2.06 to 3.52) and 2.83 ± 0.24 (2.34 to 3.62) for head, head and neck, chest and pelvis, respectively which are shown in table 4.12.

Table 4.12 The Comparison between percent gamma pass and modulation factor (MU/cGy)

No. of cases	Head		H&N		Chest		Pelvis	
	Percent Gamma pass	Modulation factor	Percent Gamma pass	Modulation factor	Percent Gamma pass	Modulation factor	Percent Gamma pass	Modulation factor
1	99.16	2.46	98.89	3.03	99.22	2.76	99.88	3.62
2	99.55	2.85	98.75	2.35	99.37	2.99	99.45	2.50
3	98.81	2.29	99.80	3.09	97.97	2.76	99.40	2.93
4	99.97	2.41	99.12	3.96	99.42	2.26	99.96	2.65
5	99.55	2.92	96.51	2.24	99.63	2.11	99.77	2.99
6	100.00	2.90	99.39	2.94	99.46	2.06	98.86	2.34
7	99.91	2.37	98.67	2.35	98.56	2.36	99.46	3.03
8	99.76	2.02	99.71	2.56	99.96	3.33	99.35	2.71
9	99.54	2.34	98.97	3.22	98.47	3.06	99.70	2.70
10	99.32	2.30	99.39	2.58	99.39	2.51	-	-
11	99.53	3.03	-	-	99.05	3.10	-	-
12	-	-	-	-	99.59	3.52	-	-
13	-	-	-	-	99.55	2.31	-	-
Average ±SD	99.55 ±0.36	2.54 ±0.33	98.92 ±0.93	2.83 ±0.53	99.20 ±0.55	2.70 ±0.47	99.54 ±0.37	2.83 ±0.24

4.4 Gamma pass limit set up for EPIQA

After 43 VMAT plans evaluation with ArcCHECK, the data were corrected for 70 VMAT plans in various treatment sites including the cases using stereotactic radio surgery (SRS) or stereotactic body radiation therapy (SBRT) technique.

For 70 VMAT plans (228 arcs) using EPIQA as a QA device, the average percentage passing was 99.29 ± 0.60 (96.51 to 100 range) while separating in each region 99.56 ± 0.37 (98.78 to 100.00 range), 99.08 ± 0.73 (96.51 to 99.80 range), 99.13 ± 0.53 (97.97 to 99.96 range), 99.55 ± 0.30 (98.86 to 99.96 range), 99.07 ± 0.91 (97.94 to 100.0 range) for head, H&N, chest, pelvis and SRS/SBRT respectively, they are shown in table 4.13.

The 70 VMAT plans were evaluated to determine the gamma limit using confidence limit of $(100 - \text{mean}) + 1.96\sigma$.

The calculated gamma pass limit of 98.12% was observed, while separating each region the gamma pass limit were 98.84%, 97.66%, 98.09%, 98.96% and 97.28% for head, H&N, chest, pelvis and SRS/SBRT respectively, the details are shown in table 4.14.

Table 4.13 The Percent gamma pass in each treatment region

No. of cases	Percent gamma pass in each Treatment Region				
	Head	H&N	Chest	Pelvis	SRS/SBRT
1	99.16	98.89	99.22	99.88	100.0
2	99.55	98.75	99.37	99.45	98.99
3	98.81	99.80	97.97	99.40	99.89
4	99.97	99.12	99.42	99.96	97.94
5	99.55	96.51	99.63	99.77	99.57
6	100.00	99.39	99.46	98.86	98.02
7	99.91	98.67	98.56	99.46	-
8	99.76	99.71	99.96	99.35	-
9	99.54	98.97	98.47	99.70	-
10	99.32	99.39	99.39	99.80	-
11	99.53	98.67	99.05	99.59	-
12	99.51	99.33	99.59	99.41	-
13	99.61	99.60	99.55	-	-
14	98.78	99.76	98.43	-	-
15	99.80	99.13	99.10	-	-
16	99.83	98.71	99.01	-	-
17	99.89	99.63	-	-	-
18	-	99.30	-	-	-
19	-	99.35	-	-	-
Average±SD	99.56±0.37	99.08±0.73	99.13±0.53	99.55±0.30	99.07±0.91

Table 4.14 The gamma pass limit in each treatment region

Treatment site	No of cases	Mean (%)	SD (%)	Confidence limit	Gamma pass limit (%)
Head	17	99.56	0.37	1.16	98.84
H&N	19	99.08	0.73	2.34	97.66
Chest	16	99.13	0.53	1.91	98.09
Pelvis	12	99.55	0.30	1.04	98.96
SRS/SBRT	6	99.07	0.91	2.72	97.28
Total	70	99.29	0.60	1.88	98.12

CHAPTER V

DISCUSSION AND CONCLUSIONS

5.1 Discussion

5.1.1 EPIQA portal dose validation of simple field technique

In this study, basic measurements for simple techniques in different field sizes for open, wedge fields and pyramid IMRT are performed to validate EPIQA software with the treatment planning. The dose calculated by Eclipse treatment planning is agreed with the measurement within the tolerance limit according to IAEA 430 recommendation for open, wedge fields and pyramid IMRT. The measurement is performed during treatment planning commissioning.

The EPIQA software has an option called Gaussian convolution to improve the evaluation results. Gaussian convolution makes the resolution of measured image (the aS1000 even has 1024 x 512 pixel) down to the level of the same calculated image. This clearly improves the agreement so the results show good agreement with TPS in both 6 and 10 MV. The percent gamma pass range from 95.25 to 99.79 and 99.64 to 100 for 6 and 10 MV, respectively. The mean gamma are also improved, all of field sizes show the values of less than 0.5. according to Stock M et al. [26] recommendation. The mean gamma range from 0.32 to 0.56 and 0.18 to 0.44 for 6 and 10 MV, respectively.

The screens captures in simple field technique for 6 MV, 2x2 cm² field size without and with Gaussian convolution are illustrated in figure 4.1 and 4.2, respectively. For 10 MV, 2x2 cm² field size without and with Gaussian convolution are illustrated in figure 4.3 and 4.4, respectively. For 6 MV, 10x10 cm² field size without and with Gaussian convolution are illustrated in figure 4.5 and 4.6, respectively. For 10 MV, 10x10 cm² field size without and with Gaussian convolution are illustrated in figure 4.7 and 4.8, respectively. The screen captures show the dose difference between calculation and measurement at the edge of the field without convolution, correspond with the gamma value that is more than one (blue and red color) at the edge of field. They represent the areas that don't pass the criteria at the high gradient area, so the profile of dose distribution of EPID is sharper than TPS at the edge of field and more pronounce for 10 MV. In small field size, the ratio of failed points to passed points is too high, so they effect to the low gamma pass. While they are less effect in the larger field sizes, the high gamma pass is obtained. When the convolution is applied, the percent gamma pass is improved.

The screen captures in Pyramid IMRT for 6 MV without and with Gaussian convolution are illustrated in figure 4.9 and 4.10, respectively. The 10 MV Pyramid IMRT without and with

Gaussian convolution are illustrated in figure 4.11 and 4.12, respectively. For gamma analysis matrix window without Gaussian convolution, the difference between 6 and 10 MV is observed. For 6 MV, the areas that don't pass the criteria are at the center of field, but the overall percent gamma pass is 94.93. For 10 MV, the areas that don't pass the criteria are at the edge of field; this may be attribute to the effect of high dose gradient. When the convolution is applied, the percent gamma pass are improved from 84.26 to 99.69%.

The percent gamma pass for 10 MV is lower than 6 MV for all of field sizes because the water equivalent depth is 1.5 cm so electronic equilibrium isn't occurred for 10 MV. Due to the presence of high-Z materials, a-Si EPIDs exhibited an over-response for low energy photons. The sensitivity of an a-Si EPID is field-size and depth dependent.

In this study, we observe that the degree of Gaussian blurring also depends on the calculation grid setting so the suitable resolution for QA device should be the same as resolution of TPS to make the high percent gamma pass. The Gaussian convolution is employed in this work.

5.1.2 Clinical VMAT plans of EPIQA compared with ArcCHECK

The 43 VMAT plans for various organs are performed by EPIQA comparing with ArcCHECK in term of percent gamma pass using the criteria of 3% dose difference and 3 mm DTA.

For EPIQA, the percent gamma pass are 99.55 ± 0.36 , 98.92 ± 0.93 , 99.20 ± 0.55 and 99.54 ± 0.37 for head, H&N, chest, and pelvis, respectively. The tested points are largest in H&N and lowest in head region. The percent gamma pass values show slightly difference in head, chest and pelvis with lowest in H&N region. The plans in H&N region are complicated with high dose gradient so the percent gamma pass and the standard deviation are dependent on plan complexity. The mean gamma in each treatment site using EPIQA are 0.24 ± 0.08 , 0.30 ± 0.03 , 0.31 ± 0.05 and 0.31 ± 0.02 for head, H&N, chest and pelvis, respectively which are in the acceptable criteria of mean gamma less than 0.5 (Stock M et al.) [26], so the verification in VMAT plans in EPIQA confirm the reliable in patient specific QA.

For ArcCHECK, the percent gamma pass are 99.08 ± 0.67 , 98.25 ± 1.98 , 98.61 ± 0.81 and 98.81 ± 0.64 for head, H&N, chest, and pelvis, respectively. The percent gamma pass show the close value in head chest and pelvis regions, the highest value is in head region and lowest in H&N which are similar to the result from EPIQA.

For 43 VMAT plans, EPIQA and ArcCHECK demonstrate the average percent gamma pass of 99.29 ± 0.63 and 98.69 ± 1.14 , respectively. Most of the percent gamma pass of EPIQA in all treatment sites are slightly higher than ArcCHECK. The results show similar to previous study by Krishna Murthy [21]: 98.53 ± 0.25 for ArcCHECK and 98.88 ± 0.22 for EPIQA.

The reasons for the difference of percent gamma pass are resolution of detector, directional dependence and also accuracy of the QA devices setup during the treatment delivery.

For the difference of resolution, EPID detector contains 1024x768 pixels with 0.392 mm pixel pitch. The resolution of EPIQA software can be adjusted to be the same as TPS (AAA 2.5 mm) in contrast to the ArcCHECK which has only 1386 diodes with 1 cm spacing. The tolerance of distance to agreement (3mm) is smaller than detector spacing of ArcCHECK so it needs to interpolate measured data between diodes. While the resolution of EPIQA software is the same as treatment plan so it reduces effect in high dose gradient.

For directional dependence, the beam is perpendicular direction to the EPID detector so no error from this factor. In contrast, some detectors of ArcCHECK don't perpendicular to the beam resulting in directional dependent.

For the accuracy of the QA devices setup during the treatment delivery, EPID can be setup automatically which can exclude human error. The uncertainty position of ArcCHECK from human error may cause higher SD than EPIQA.

Furthermore the difference in percent gamma pass may be due to the difference in their dose reconstruction methods. The Portal dosimetry uses transmission, while ArcCHECK uses reconstruction from entry and exit dose.

Figure 4.16 and 4.28 illustrate the percent gamma pass in head and pelvis region, most of the cases show more percent gamma pass by EPIQA than ArcCHECK. Figure 4.20 and 4.24 show the percent gamma pass in H&N and chest region in the same trend of more percent gamma pass by EPIQA than ArcCHECK but the percent gamma pass is distributed for EPIQA and ArcCHECK in H&N and chest region cases. The percent gamma pass in ArcCHECK and EPIQA are affected by treatment sites.

Although the percent gamma pass of all cases are in the tolerance (95%), the profiles in the areas that don't pass the criteria ($\gamma > 1$) can be investigated. Figure 5.1 illustrates the profiles between EPID and TPS which is different and EPID obtains more dose than TPS.

The screen capture in figure 5.1 illustrates the following information:

- a) Eclipse treatment planning dose calculation
- b) Gamma analysis matrix window
- c) Portal vision dose measurement
- d) Profile display in x direction (left-right) for both dose matrices
- e) Profile display in y direction (feet-head) for both dose matrices
- f) Display of histogram and statistics for the gamma analysis matrix window

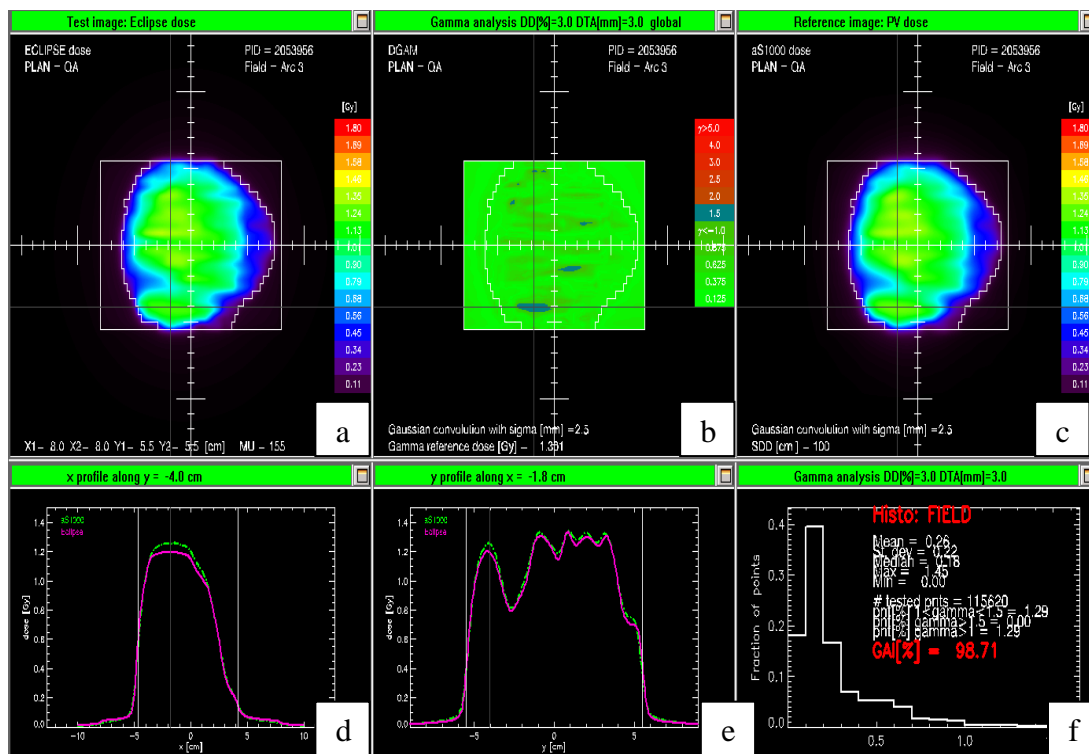


Figure 5.1 The Screen capture of EPIQA analysis to define the difference between EPID and TPS

5.1.3 The correlation between percent gamma pass and modulation factor (MU/Gy)

This study is aimed to observe the relationship between percent gamma pass and modulation factor, they should be low percent gamma pass at high modulation factor but the result shows poor correlation, it is illustrated in figure 5.2.

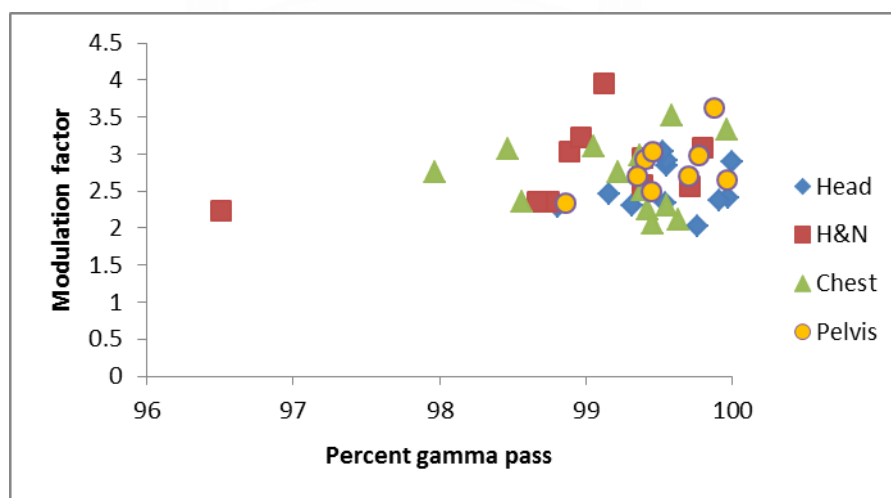


Figure 5.2 The correlation between percent gamma pass and modulation factor (MU/Gy) in each region. Blue dot (head), red dot (H&N), green (chest), orange (pelvis)

5.1.4 Gamma pass limit set up for EPIQA

Normally the gamma pass limit at 95% for all QA devices is employed in the clinic. However the gamma pass depends on several factors, such as the model used in treatment planning, the dose delivery system, QA devices and also institute QA experience. Due to implementation of the new QA device, the new gamma pass limit should be set up.

The 70 VMAT plans are evaluated to determine the gamma limit using confidence limit of $(100 - \text{mean}) + 1.96\sigma$. The calculated gamma pass limit of 98.12% while separating each region are 98.84%, 97.66%, 98.09%, 98.96% and 97.28% for head, H&N, chest, pelvis and SRS/SBRT respectively.

The limitation of 70 VMAT plans is 98% (98.12 % from results). This limit is close to the limitation in each region (98.84%, 98.09% and 98.96% for head, chest and pelvis, respectively), but slightly difference in H&N and SRS/SBRT (97.66% and 97.28%). So the limitation of gamma pass as 98% for head, chest and pelvis region and 97% for H&N and SRS/SBRT are recommended. However the gamma pass limit in each region should be investigated more for large sample size.

Base on this study, 17 cases in head region using the limit at 98% illustrate that all of the cases pass in these criteria. For 19 cases in H&N region with 97% limit, it demonstrates only one case that is fail (96.51%), it is shown in figure 5.4, 5.5 and 5.6. For 16 cases in chest region with 98%, all of the cases pass these criteria. For 12 cases of pelvis region which is 98% limit, all of the cases pass these criteria and for 6 cases of SRS/SBRT which is 97% limit, all of the cases pass, they are shown in scatter plot graph in figure 5.3. If the cases exceed these criteria, that plan is delayed until the source of error is identified. After that the action limit at 95% is used.

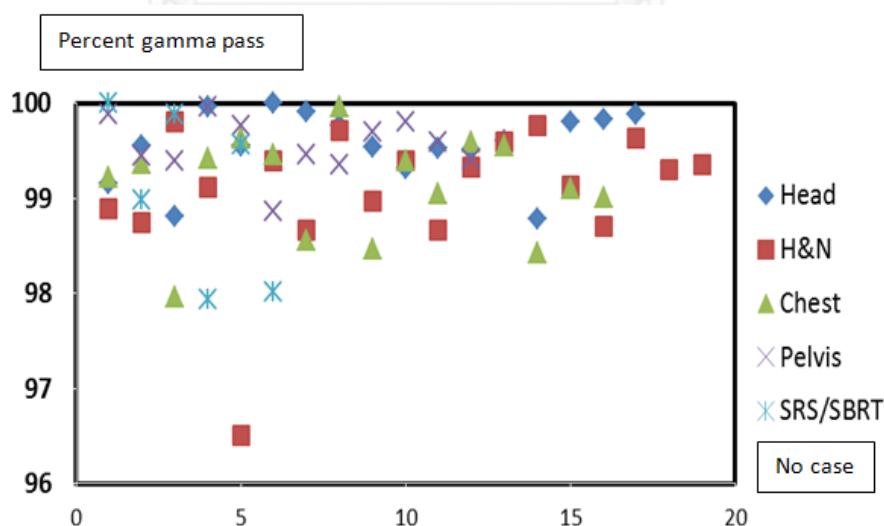


Figure 5.3 The scatter plot of percent gamma pass in each treatment region

The example of case doesn't pass the limit is shown in figure 5.4, 5.5 and 5.6

The screen captures in figure 5.4, 5.5 and 5.6 illustrate the following information:

- Eclipse treatment planning dose calculation
- Gamma analysis matrix window
- Portal vision dose measurement
- Profile display in x direction (left-right) for both dose matrices
- Profile display in y direction (feet-head) for both dose matrices
- Display of histogram and statistics for the gamma analysis matrix window

The main effect for low percent gamma pass of this case is the complicate plan because tumor is very close to organ at risk.

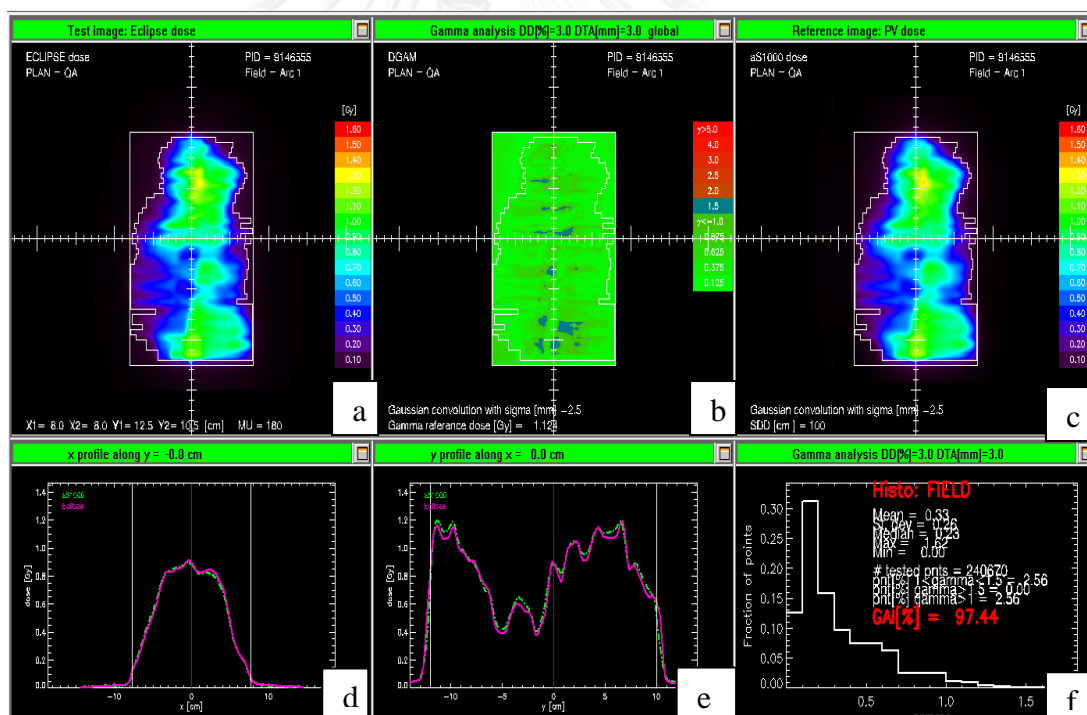


Figure 5.4 The screen captures for the case of low percent gamma pass (Arc 1)

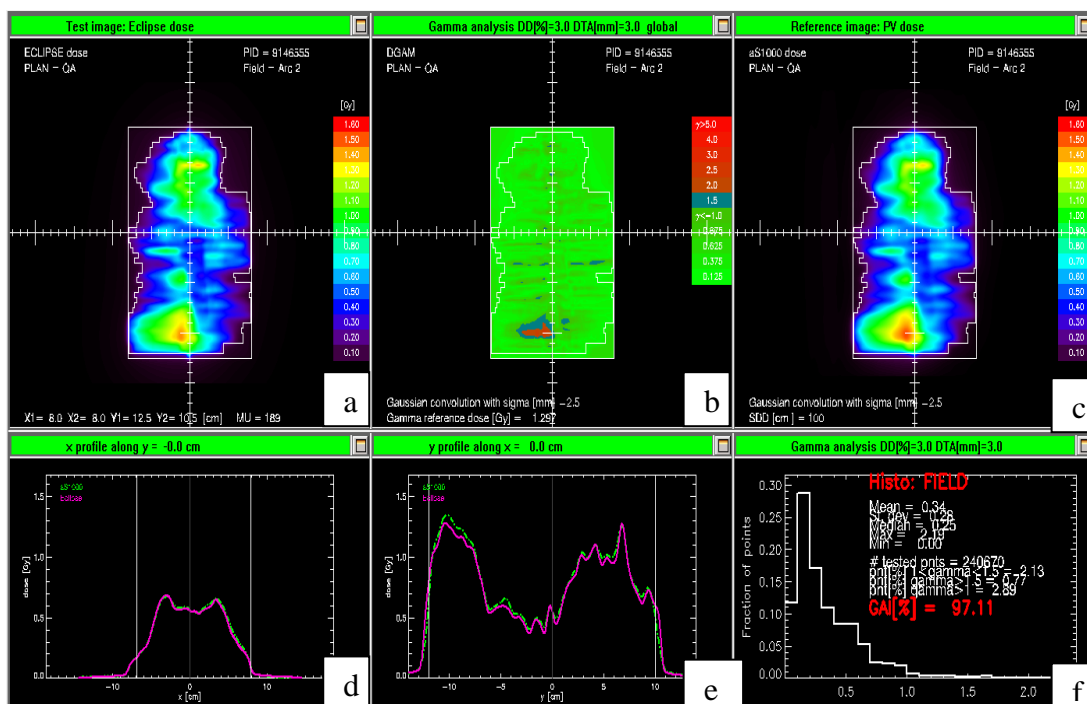


Figure 5.5 The screen captures for the case of low percent gamma pass (Arc 2)

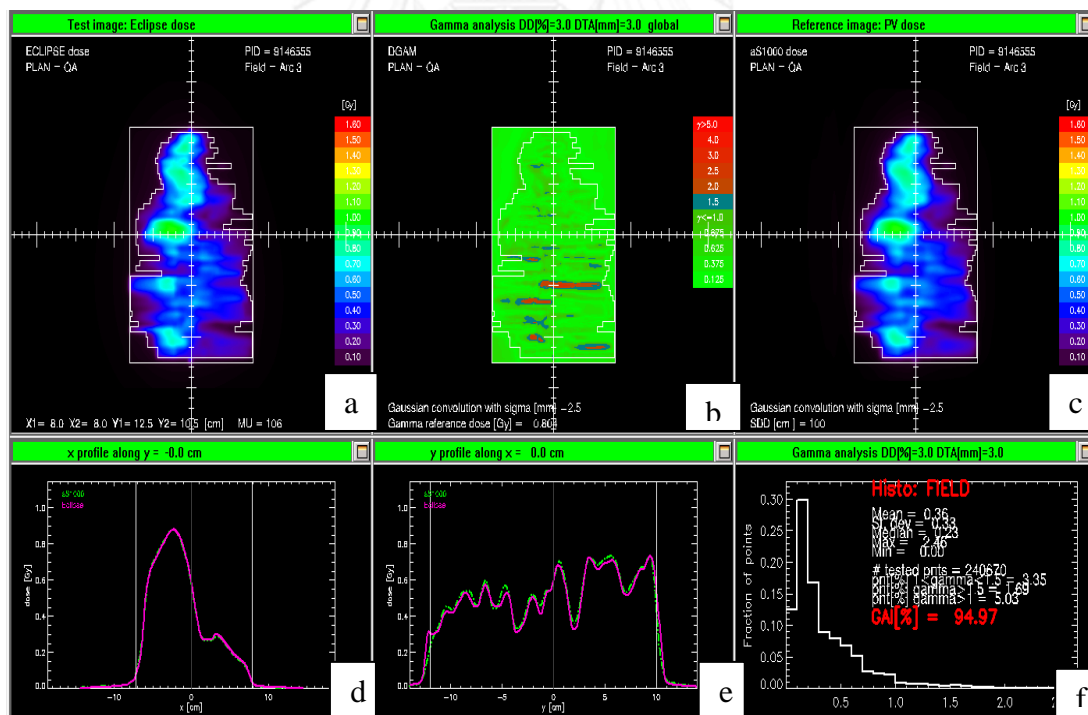


Figure 5.6 The screen captures for the case of low percent gamma pass (Arc 3)

Then the patient specific QA for 70 VMAT plans using EPIQA verification are passed and can delivery to treat patient.

5.1.5 Comparison to previous works

The average percent gamma pass using EPID portal dosimetry compared with other studies is shown in table 5.1

Table 5.1 The average percent gamma pass using EPID portal dosimetry compared with other studies

	The average percentage passing
Yen-Cho Huang et al[18]	99.10±0.60%
A FOGLIATA et al[27]	97.10±2.40%
This study	99.29±0.60%

Yen-Cho Huang et al [18] evaluated EPID performance for VMAT dose verification. EPID measurements for VMAT presented good agreement with TPS calculations 99.1±0.6% with 3%/3mm criteria. A FOGLIATA et al [27] analyzed quality assurance data from five centers to assess the reliability of RapidArc radiotherapy delivery in terms of machine and dosimetric performance using electronic portal imaging device measurements. The average percent gamma pass of clinical fields was 97.10±2.40% with 3%/3mm criteria. These two studies used the same GLAaS algorithm as EPIQA, so the results are agreeable with our work.

The gamma pass limit using EPID based dosimetry compared with other studies is shown in table 5.2

Table 5.2 The gamma pass limit using EPID based dosimetry compared with other studies

	Ezzell <i>et al</i> [22]	This study
Mean	99.40	99.29
SD	0.40	0.60
Local confidence limit (100–mean)+1.96σ	1.30(98.70)	1.88(98.12)
Number of studies	5	70

Ezzell *et al* [22] produced quantitative confidence limits as baseline expectation values for IMRT commissioning. A set of test cases was developed to assess the overall accuracy of planning and delivery of IMRT treatments. These tests were planned, delivered, measured, and analyzed by

nine facilities using a variety of IMRT planning and delivery systems. One of institutes used EPID as a QA device, the gamma pass limit was stated at 98.70%.

5.1.6 The limitation of this study

This work has several limitations. For example, dimension of the treatment field exceeded the active area of the portal imager ($x_1=20$, $x_2=20$, $y_1=15$, $y_2=15$ cm) especially side y_1 , if $y_1 > 14$ cm, some data from EPID would be loss. We suggest that the collimator should be rotated to 90 degree.

Acquisition errors may occur during the time of treatment due to malfunction of Linac or EPID but can be repeated in each arc because EPIQA calculated in a separate arc.

The calculation of dose distribution for the verification plan is taken time because the calculation is performed arc by arc. We suggest that in the process of create verification plan, the selection should be undertaken for 'place all fields into verification plan' and export RT dose in each arc by change field weight.

5.2 Conclusions

Before The EPIQA software is implemented into the clinic, the performance is validated in simple field techniques. Then EPIQA software is compared with ArcCHECK which is used routinely in the clinic in term of percent gamma pass and gamma pass limit is determined for VMAT technique.

For simple field technique, we observe that the suitable resolution for QA device should be the same as resolution of TPS to make the high percent gamma pass. EPIQA show good agreement with TPS for all of field sizes. The percent gamma pass range from 95.25 to 99.79 and 99.64 to 100 for 6 and 10 MV photon beam.

For clinical VMAT plans, EPIQA show the percent gamma pass similar values to ArcCHECK but slightly higher values. The percent gamma pass are 99.29 ± 0.63 (96.51 to 100 range) and 98.69 ± 1.14 (93.3 to 100 range) for EPIQA and ArcCHECK, respectively. However, depending on the machine time available both QA devices can be used interchangeably for routine patient-specific QA.

For studying the relationship between percent gamma pass and modulation factor, the result show poor correlation. Because VMAT technique is modulated beam by many factor, not only MLC movement but also variable dose rate and gantry speed during rotation. The MU used in VMAT is not as large as IMRT.

Based on this study, the gamma pass limits are 98% for Head, Chest, Pelvis regions and 97% for Head and Neck regions and SRS/SBRT techniques. Gamma pass limit is a useful tool for standardizing the evaluation of EPID-based VMAT QA, however, the other factors should be

considered to approve the plans. We suggest the using gamma pass limit based on this study as a tolerance limit and 95% for action limit.

Patient-specific pre-treatment verification should be kept as simple as possible because the QA efforts are proportional to the number of patients. On the other hand they should be extensive enough to be able to detect errors and problems that may occur with the specific combination of TPS, sequencer and delivery equipment.

In the future, if the DVH from EPID is constructed, more information of dose to plan target volume and organ at risk would contribute more information and accuracy than other tools.

EPIQA is an independent method of verification of the dose distribution in patient compared against dose distribution calculated by treatment planning system. EPIQA is a simple and reliable quality assurance tool for VMAT dose verification which provides the efficient results and suitable for a fast growing number of patients.

REFERENCES

1. AWUSI, K. Transit dosimetry based on water equivalent path length measured with an amorphous silicon electronic portal imaging device. Glasgow Theses Service (2011).
2. van Elmpt, W., McDermott, L., Nijsten, S., Wendling, M., Lambin, P. and Mijnheer, B. A literature review of electronic portal imaging for radiotherapy dosimetry. *Radiotherapy and Oncology* 88 (2008): 289-309.
3. Vial, P., Greer, P. B., Oliver, L. and Baldock, C. Initial evaluation of a commercial EPID modified to a novel direct-detection configuration for radiotherapy dosimetry. *Medical Physics* 35 (2008): 4362.
4. Alber, M., Broggi, S., Wagter, C. D., Eichwurz, I., Engström, P. and Fiorino, C. Guidelines for the verification of IMRT. *ESTRO booklet NO 9*. Brussels, Belgium 2008
5. Sanghangthum, T., Suriyapee, S., Srisatit, S. and Pawlicki, T. Statistical process control analysis for patient-specific IMRT and VMAT QA. *Journal of radiation research* 54 (2013): 546-52.
6. Nijsten, S. M. J. J. G. Portal dosimetry in radiotherapy. Universitaire Pers Maastricht 2009
7. Volumetric modulated radiotherapy (VMAT) [online]. 2009. Available from: <http://medicalphysicsweb.org/cws/article/opinion/39542>:
8. Mancuso, G. Evaluation of Volumetric modulated arc therapy (VMAT) patient specific quality assurance Louisiana State University; May 2011.
9. EVAN, M. D. C. Radiation Oncology Physics. Quebec Canada: McGill University Health Center; 2006.
10. AAPM. Inverse treatment planning (pdf). [online]. 2006. Available from: <http://www.aapm.org/meeting/02AM/pdf/8299-34342>:
11. ArcCHECK model 1220. Sun nuclear corporation: Melbourne: FL.
12. Buckey, C. Characterization of a Varian aS1000 EPID. *Diagnostic Imaging 2* (Spring 2010).
13. Greer, P. B. and Popescu, C. C. Dosimetric properties of an amorphous silicon electronic portal imaging device for verification of dynamic intensity modulated radiation therapy. *Medical Physics* 30 (2003): 1618.
14. Sabet, M. Investigation of a modified electronic portal imaging device for improving dosimetry in radiotherapy, University of Newcastle; January 2012.
15. Epiqa Reference Guide. EPIDOS s.r.o.: Slovak Republic; January 2012.

16. Nicolini, G., et al. The GLAaS algorithm for portal dosimetry and quality assurance of RapidArc, an intensity modulated rotational therapy. *Radiation oncology* 3 (2008): 24.
17. Low, D., Harms, W., Mutic, S., Purdy, J. and et, a. A technique for the quantitative evaluation of dose distributions. *Med Phys* (1998): 25:656–60.
18. Huang, Y. C., et al. Clinical practice and evaluation of electronic portal imaging device for VMAT quality assurance. *Medical dosimetry : official journal of the American Association of Medical Dosimetrists* 38 (2013): 35-41.
19. Varatharaj, C., Moretti, E., Ravikumar, M., Malisan, M. R., Supe, S. S. and Padovani, R. Implementation and validation of a commercial portal dosimetry software for intensity-modulated radiation therapy pre-treatment verification. *Journal of medical physics / Association of Medical Physicists of India* 35 (2010): 189-96.
20. Urso, G., et al. Epiqa: a tool for RapidArc™ Quality Assurance. A multicenter experience. Poster-Urso-Epiqa.
21. Murthy, K. Patient-specific quality assurance of RapidArc treatments: Portal prediction dosimetry compared with phantom studies. *Biomed Imaging Interv J* (2012).
22. Ezzell, G. A., et al. IMRT commissioning: Multiple institution planning and dosimetry comparisons, a report from AAPM Task Group 119. *Medical Physics* 36 (2009): 5359.
23. Gozbası, H. O. Optimization approaches for planning external beam radiotherapy: Georgia Institute of Technology; August 2010.
24. Utissarn, K. e. a. Dosemetric verification using 2D planar diode arrays and 3D cylindrical diode arrays in IMRT and VMAT: Chulalongkorn University; 2011.
25. Gaussian convolution [online]. Available from: http://www.wienkav.at/kav/kfj/91033454/physik/pd/epiqa_gauss.htm:
26. Stock M, K. B., Georg D. Interpretation and evaluation of the gamma index and the gamma index angle for the verification of IMRT hybrid plans. *Phys Med Biol* 50:399-411 (2005).
27. Fogliata, A., et al. Quality assurance of RapidArc in clinical practice using portal dosimetry. *The British journal of radiology* 84 (2011): 534-45.



APPENDIX

จุฬาลงกรณ์มหาวิทยาลัย
CHULALONGKORN UNIVERSITY

APPENDIX

Efficiency

The steps to perform the verification of VMAT plan using EPIQA and time required for their execution:

Generation of the verification plan	1 min
Calculation of dose distribution for the verification plan	5 min
Export of RT and RD DICOM files	2 min
Irradiation of the verification plan (RA field + 10x10 field) including detector setup	4 min
Export of RI DICOM files	1 min
Import of RT, RD, and RI files and evaluation in Epiqa	2 min

Total QA time per plan	15 min

VITA

Name	Chitchaya Suwanraksa
Date of Birth	Nov 12, 1981
Place of Birth	Songkhla, Thailand
Education	Faculty of Medicine Technology, Mahidol University Bachelor of Science (Radiological Technology), 2004
Address	29/15 Soi16 Klongtuey Road. T. Khohong Hat Yai Songkhla 90110
E-mail	charin_jaw@hotmail.com

ACADEMIC PUBLICATIONS

1. Suwanraksa C., Suriyapee S and Oonsiri S. Implementation and gamma pass limit of EPIQA portal dosimetry software for Volumetric modulated arc therapy pre-treatment verification in Proceedings of 13th Asia-Oceania Congress of Medical Physics & 11th South-East Asian Congress of Medical Physics, pp. 81-84. Singapore, 2013.